Appendix A: Stereoviews and Crystal Models

A.1 Stereoviews

Stereoviews of crystal structures began to be used to illustrate three-dimensional structures in 1926. Nowadays, this technique is quite commonplace, and computer programs exist (see Appendices D4 and D8.7) that prepare the two views needed for producing a three-dimensional image of a crystal or molecular structure.

Two diagrams of a given object are necessary in order to form a three-dimensional visual image. They should be approximately 63 mm apart and correspond to the views seen by the eyes in normal vision. Correct viewing of a stereoscopic diagram requires that each eye sees only the appropriate half of the complete illustration, and there are two ways in which it may be accomplished.

The simplest procedure is with a *stereoviewer*. A supplier of a stereoviewer that is relatively inexpensive is *3Dstereo.com. Inc., 1930 Village Center Circle, #3-333, Las Vegas, NV 89134, USA*. The pair of drawings is viewed directly with the stereoviewer, whereupon the three-dimensional image appears centrally between the two given diagrams.

Another procedure involves training the unaided eyes to defocus, so that each eye sees only the appropriate diagram. The eyes must be relaxed and look straight ahead. The viewing process may be aided by holding a white card edgeways between the two drawings. It may be helpful to close the eyes for a moment, then to open them wide and allow them to relax without consciously focusing on the diagram.

Finally, we give instructions whereby a simple stereoviewer can be constructed with ease. A pair of plano-convex or bi-convex lenses, each of focal length approximately 100 mm and diameter approximately 30 mm, is mounted between two opaque cards such that the centers of the lenses are approximately 63 mm apart. The card frame must be so shaped that the lenses may be brought close to the eyes. Figure A.1 illustrates the construction of the stereoviewer.

A.2 Model of a Tetragonal Crystal

A model similar to that illustrated in Fig. 1.23 can be constructed easily. This particular model has been chosen because it exhibits a four-fold inversion axis, which is one of the more difficult symmetry elements to appreciate from drawings.

M. Ladd and R. Palmer, *Structure Determination by X-ray Crystallography: Analysis by X-rays and Neutrons,* DOI 10.1007/978-1-4614-3954-7,

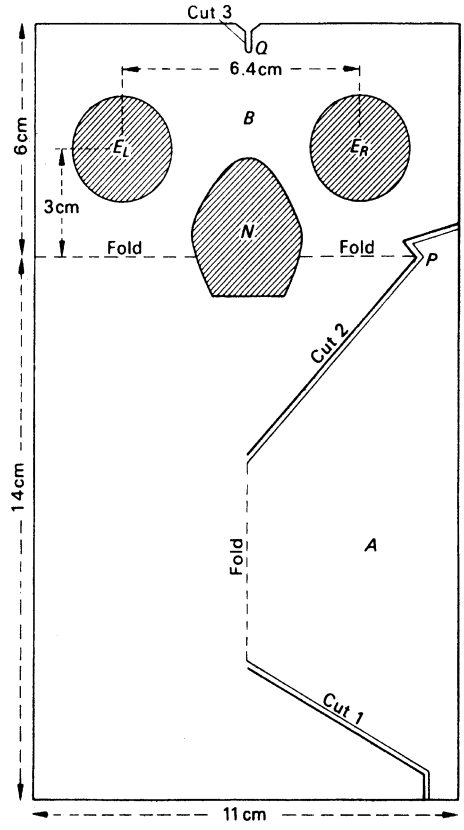

Fig. A.1 Construction of a simple stereoviewer. Cut out two pieces of card as shown and discard the *shaded portions*. Make cuts along the *double lines*. Glue the two cards together with lenses E_L and E_R in position, fold the portions *A* and *B* backward, and engage the projection *P* into the cut at *Q*. Strengthen the fold with a strip of "Sellotape." View from the side marked *B*. It may be helpful to obscure a segment on each lens of maximum depth ca. 30 % of the lens diameter, closest to the nose region

A good quality paper or thin card should be used for the model. The card should be marked out in accordance with Fig. A.2 and then cut out along the solid lines, discarding the shaded portions. Folds are made in the same sense along all dotted lines, the flaps *ADNP* and *CFLM* are glued internally, and the flap *EFHJ* is glued externally. What is the point group of the resulting model?

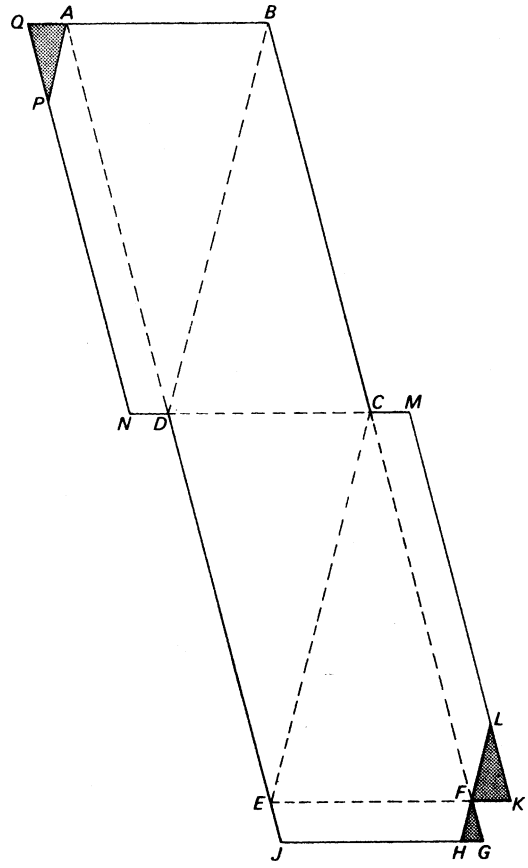

Fig. A.2 Construction of a tetragonal crystal with a $\bar{4}$ axis: $NQ = AD = BD = BC = DE = CE = CF = KM = 100$ mm; $AB = CD = EF = GJ = 50$ mm; $AP = PQ = FL = KL = 20$ mm; $AQ = DN = CM = FK = FG = FH = EJ = 10$ mm

Appendix B: Schönflies' Symmetry Notation

Theoretical chemists and spectroscopists generally use the Schönflies notation for describing point-group symmetry but, although both the crystallographic (Hermann–Mauguin) and Schönflies notations are adequate for point groups, only the Hermann–Mauguin system is satisfactory also for space groups.

The Schönflies notation uses the rotation axis and mirror plane symmetry elements that we have discussed in Sect. 1.4.2, albeit with differing notation, but introduces the alternating axis of symmetry in place of the roto-inversion axis.

B.1 Alternating Axis of Symmetry

A crystal is said to have an alternating axis of symmetry S_n of degree n, if it can be brought from one state to another indistinguishable state by the operation of rotation through $(360/n)^\circ$ about the axis and reflection across a plane normal to that axis, overall a *single* symmetry operation. It should be stressed that this plane is *not* necessarily a mirror plane in the point group.

Operations S_n are non-performable physically with models (see Sects. 1.4.1 and 1.4.2). Figure B.1 shows stereograms for S_2 and S_4; crystallographically, we recognize them as $\bar{1}$ and $\bar{4}$, respectively. The reader should consider what point groups are obtained if the plane of the diagram were a mirror plane in point groups S_2 and S_4.

B.2 Symmetry Notations

Rotation axes are symbolized by C_n in the Schönflies notation (cyclic group of degree n); n takes the meaning of R in the Hermann–Mauguin system. Mirror planes are indicated by subscripts v, d, and h; v and d refer to mirror planes containing the principal axis, and h indicates a mirror plane normal to that axis. In addition, d refers to those vertical planes that are set diagonally, between the crystallographic axes normal to the principal axis.

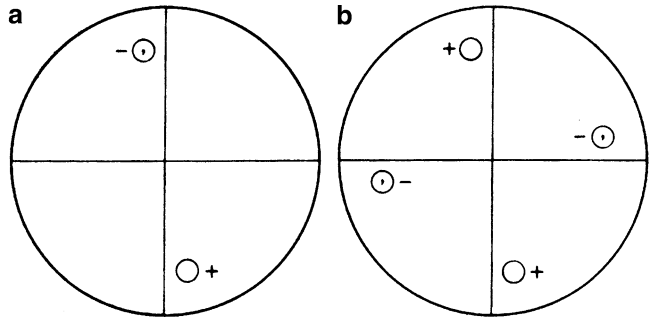

Fig. B.1 Stereograms of point groups: (**a**) S_2, (**b**) S_4

Table B.1 Schönflies and Hermann–Mauguin pointgroup symbols

Schönflies	Hermann–Mauguin[a]	Schönflies	Hermann–Mauguin[a]
C_1	1	D_4	422
C_2	2	D_6	622
C_3	3	D_{2h}	mmm
C_4	4	D_{3h}	$\bar{6}m2$
C_6	6		
C_i, S_2	$\bar{1}$	D_{4h}	$\frac{4}{m}mm$
C_s, S_1	m, $\bar{2}$		
S_6	$\bar{3}$		
S_4	$\bar{4}$	D_{6h}	$\frac{6}{m}mm$
C_{3h}, S_3	$\bar{6}$[a]		
C_{2h}	$2/m$[b]	D_{2d}	$\bar{4}2m$
C_{4h}	$4/m$[b]	D_{3d}	$\bar{3}m$
C_{6h}	$6/m$[b]	T	23
C_{2v}	$mm2$	T_h	$m\bar{3}m$
C_{3v}	$3m$	O	432
C_{4v}	$4mm$	T_d	$\bar{4}3m$
C_{6v}	$6mm$	O_h	$m\bar{3}m$
D_2	222	$C_{\infty v}$	∞
D_3	32	$D_{\infty h}$	$\infty/m(\bar{\infty})$

[a] The usual Schönflies symbol for $\bar{6}$ is C_{3h} (3/m). The reason that $3/m$ is not used in the Hermann–Mauguin system is that point groups containing the element $\bar{6}$ describe crystals that belong to the hexagonal system rather than to the trigonal system; $\bar{6}$ cannot operate on a rhombohedral lattice.

[b] R/m is an acceptable way of writing $\frac{R}{m}$, but R/mmm is not as satisfactory as $\frac{R}{m}mm$; $R/m\ mm$ is a marginally acceptable alternative.

The mirror plane symmetry *element* is denoted by σ in the Schönflies system. The symbol D_n (dihedral group of degree n) is introduced for point groups in which there are n two-fold axes in a plane normal to the principal axis of degree n. The cubic point groups are represented through the special symbols T (tetrahedral) and O (octahedral). In point group symbols, subscripts h and d are used to indicate the presence of horizontal and vertical (dihedral) mirror planes, respectively Table B.1 compares the Schönflies and Hermann–Mauguin symmetry notations.

Appendix C: Cartesian Coordinates

In calculations that lead to results in absolute measure, such as bond distance and angle calculations and location of hydrogen-atom positions, it may be desirable to convert the crystallographic fractional coordinates x, y, z, which are dimensionless, to Cartesian (orthogonal) coordinates X, Y, and Z, in Å or nm.

C.1 Cartesian to Crystallographic Transformation and Its Inverse

Instead of considering immediately the transformation $\mathbf{A} = \mathbf{M}\,\mathbf{a}$, it is simpler to consider first the inverse transformation $\mathbf{a} = \mathbf{M}^{-1}\,\mathbf{a}$, where $\mathbf{M}$ is the transformation matrix for the triplet $\mathbf{A}(A, B, C)$ to the triplet $\mathbf{a}(a, b, c)$, because the components of $\mathbf{a}$ along the Cartesian axes are direction cosines (see Web Appendix WA1).

Figure C.1 illustrates the two sets of axes. Let $\mathbf{A}$ be a unit vector along a, $\mathbf{B}$ a unit vector normal to $\mathbf{a}$, and in the a, b plane, and $\mathbf{C}$ a unit vector normal to both $\mathbf{A}$ and $\mathbf{B}$.

Then, we can write

$$\begin{bmatrix} \mathbf{a}/a \\ \mathbf{b}/b \\ \mathbf{c}/c \end{bmatrix} = \begin{bmatrix} l_1 & m_1 & n_1 \\ l_2 & m_2 & n_2 \\ l_3 & m_3 & n_3 \end{bmatrix} \begin{bmatrix} \mathbf{A} \\ \mathbf{B} \\ \mathbf{C} \end{bmatrix} \tag{C.1}$$

From the figure, we can write down some of the elements of $\mathbf{M}^{-1}$:

$$\mathbf{M}^{-1} = \begin{bmatrix} 1 & 0 & 0 \\ \cos\gamma & \sin\gamma & 0 \\ \cos\beta & m_3 & n_3 \end{bmatrix} \tag{C.2}$$

From the properties of direction cosines, we have

$$\cos\alpha = l_2 l_3 + m_2 m_3 + n_2 n_3 = \cos\beta\cos\gamma + m_3 \sin\gamma$$

so that

$$m_3 = (\cos\alpha - \cos\beta\cos\gamma)/\sin\gamma = -\cos\alpha^{*}\sin\beta \tag{C.3}$$

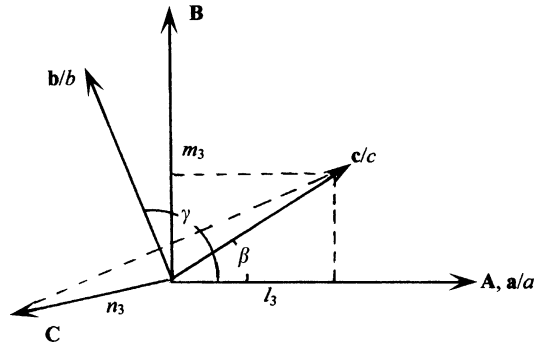

Fig. C.1 **A**, **B** and **C** are unit vectors on Cartesian (orthogonal) axes X, Y, Z, and **a**/a, **b**/b, and **c**/c are unit vectors on the conventional crystallographic axes x, y, z

Since the sums of the squares of the direction cosines is unity,

$$n_3^2 = 1 - \cos^2\beta - \sin^2\beta\cos^2\alpha^* = \sin^2\beta\sin^2\alpha^*$$

so that

$$n_3 = \sin\beta\sin\alpha^* = v/\sin\gamma \tag{C.4}$$

since[1] $V = abc \sin\alpha^* \sin\beta \sin\gamma$, and v here refers to the volume of the unit parallelepiped **a**/a, **b**/b, **c**/c, that is, $v = (1 - \cos^2\alpha - \cos^2\beta - \cos^2\gamma + 2\cos\alpha\cos\beta\cos\gamma)$. Hence, we can write the transformation in terms of the direct unit-cell parameters, multiplying the lines of the matrix by a, b, or c, as appropriate:

$$\begin{bmatrix}\mathbf{a}\\ \mathbf{b}\\ \mathbf{c}\end{bmatrix} = \begin{bmatrix} a & 0 & 0 \\ b\cos\gamma & b\sin\gamma & 0 \\ c\cos\beta & c(\cos\alpha - \cos\beta\cos\gamma)/\sin\gamma & cv/\sin\gamma \end{bmatrix} \begin{bmatrix}\mathbf{A}\\ \mathbf{B}\\ \mathbf{C}\end{bmatrix} \tag{C.5}$$

which, in matrix notation, is $\mathbf{a} = \mathbf{M}^{-1}\,\mathbf{A}$. From the transformations discussed in Sect. 2.5.5, we have $\mathbf{X} = (\mathbf{M}^{-1})^{\mathrm{T}}\mathbf{x}$, or

$$\begin{bmatrix}X\\ Y\\ Z\end{bmatrix} = \begin{bmatrix} a & b\cos\gamma & c\cos\beta \\ 0 & b\sin\gamma & c(\cos\alpha - \cos\beta\cos\gamma)/\sin\gamma \\ 0 & 0 & cv/\sin\gamma \end{bmatrix} \begin{bmatrix}x\\ y\\ z\end{bmatrix} \tag{C.6}$$

The deduction of **M**, the inverse of $\mathbf{M}^{-1}$, is straightforward for a 3×3 matrix, albeit somewhat laborious, and can be found in most elementary treatments of vectors. Thus, we have $\mathbf{A} = \mathbf{M}\,\mathbf{a}$ and $\mathbf{x} = \mathbf{M}^{\mathrm{T}}\mathbf{X}$, where

[1] Buerger MJ (1942) X-ray crystallography. Wiley, New York.

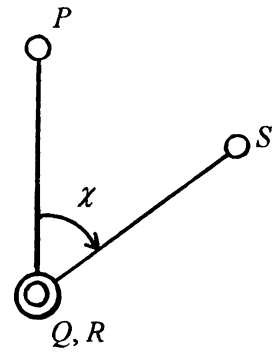

Fig. C.2 Convention for torsion angles: χ_{PQRS} is reckoned positive as shown, when the atom succession $P - Q - R - S$ is viewed along QR

$$\mathbf{M} = \begin{pmatrix} 1/a & 0 & 0 \\ -\cos\gamma/(a\sin\gamma) & 1/(b\sin\gamma) & 0 \\ (\cos\gamma\cos\alpha - \cos\beta)/(av\sin\beta) & (\cos\gamma\cos\beta - \cos\alpha)/(bv\sin\gamma) & \sin\gamma/(cv) \end{pmatrix} \quad \text{(C.7)}$$

The transformation (C.6) is employed in the program INTXYZ (see Sect. 13.6.6) for the calculation of bond lengths, bond angles, and torsion angles from crystallographic parameters. The sign of a torsion angle is governed by the convention discussed in Section 8.5.2. For the sequence of atoms, P, Q, R, S in Fig. C.2, the torsion angle χ_{PQRS} is positive if a clockwise rotation of PQ about QR, as seen along QR, brings PQ over RS.

Appendix D: Crystallographic Software

This Appendix lists software for X-ray and neutron crystallographic applications that are available to the academic community. The list is not exhaustive, and many of the packages are listed under one or other section of the Collaborative Computational Projects.[2,3] Often, the program systems are mirrored by the Engineering and Physical Sciences Research Council (EPSRC) funded CCP projects,[4] which have mirror sites in the U. S. A. and in Canada. In addition to the programs referenced here, a complete set of crystallographic programs has been promulgated elsewhere.[5]

The program systems are divided into a number of sections, and an appropriate reference has been provided for each entry, including author, e-mail address, and web site reference as appropriate.

- Single Crystal Suites
- Single Crystal Structure Solving Programs
- Single Crystal Twinning Software
- Freestanding Structure Visualization Software
- Powder Diffraction Data: Powder Indexing Suites
- Structure Solution from Powder Diffraction Data
- Software for Macromolecular Crystallography

  Data Processing; Fourier and Structure Factor Calculations; Molecular Replacement; Single and Double Isomorphous Replacement; Software for Packing and Molecular; Geometry; Software for Graphics and Model Building; Software for Molecular Graphics and Display; Software for Refinement; Software for Molecular Dynamics and Energy Minimization; Data Bases
- Bioinformatics

  Molecular Modelling Software; External Links; Useful Homepages

D.1 Single Crystal Suites

Most single crystal program suites have a large variety of functionality; WinGX is an example of a suite linking to several other programs in a seamless manner via graphical user interfaces. In most cases, programs link to multiple versions of a structure solution program, such as SHELXS-97 or SIR2008.

[2] http://www.ccp4.ac.uk.

[3] http://www.ccp14.ac.uk.

[4] http://www.epsrc.ac.uk/Pages/default.aspx.

[5] http://ww1.iucr.org/sincris-top/logiciel/lmno.html#O.

D.2 Single Crystal Structure Solution Programs

CAOS
Automated Patterson method. Spagna R et al. http://www.ic.cnr.it/caos/what.html

CRYSTALS 14.23
Watkin D. http://www.xtl.ox.ac.uk

DIRDIF 2008
Automated Patterson methods and fragment searching: Windows version ported by L. Farrugia and available via the WinGX website. http://www.chem.gla.ac.uk/~louis/software/dirdif/

OLEX2
User-friendly structure solution and refinement suite with inter alia archiving and report generation. Dolomanov OV et al (2008) J Appl Crystallogr 42:339. http://olex2.org

PATSEE
Fragment searching methods. http://www.ccp14.ac.uk/ccp/web-mirrors/patsee/egert/html/patsee.html. Windows version by Farrugia, L. and available via the WinGX website.

System S
SHELXS, DIRDIF, SIR, and CRUNCH for solution; EXOR, DIRDIF, SIR, and CRUNCH for autobuilding; SHELXL for refinement. Spek AL. http://www.ccp14.ac.uk/tutorial/platon/index.html

SIR 2008
http://www.ba.ic.cnr.it/content/il-milione-and-sir2008

SNB (*SHAKE AND BAKE*)
Direct methods. Weeks CM et al. http://www.hwi.buffalo.edu/SnB

WinGX
SHELXS, DIRDIF, SIR, and PATSEE for solution; DIRDIF phases for autobuilding; SHELX for refinement. Farrugia L. http://www.chem.gla.ac.uk/~louis/software/wingx

D.3 Single Crystal Twinning Software

TWIN 3.0
Kahlenberg V et al. http://www.ccp14.ac.uk/solution/twinning/index.html

TwinRotMac
Spek AL. http://www.ccp14.ac.uk/solution/ twinning/index.html
Windows version by Farrugia L. http://www.chem.gla.ac.uk/~louis/software/platon

D.4 Freestanding Structure Visualization Software

ORTEP-III
Burnett MN et al. http://www.chem.gla.ac.uk/~louis/software/ortep3/

D.5 Powder Diffraction Data: Powder Indexing Suites (Dedicated and Other)

Checkcell
Laugier J. http://www.ccp14.ac.uk/tutorial/lmgp/achekcelld.htm

CRYSFIRE
Shirley R. http://www.ccp14.ac.uk/tutorial/crys/ (includes the programs ITO, DICVOL, TREOR, TAUP, KOHL, LZON, LOSH, and FJZN, but is no longer under development)

DICVOL91
Louër D. http://www.ccp14.ac.uk/tutorial/crys/program/dicvol91.htm

ITO12/13
Visser JW. http://www.iucr.org/resources/commissions/crystallographic-computing/software-museum

ITO15 (*Included in FULLPROF*)
Visser J et al. http://www.ill.eu/sites/fullprof/php/programs.html

LOSH/LZON
Bergmann J et al. http://www.ccp14.ac.uk/tutorial/tutorial.htm

TAUP/Powder
Taupin D. http://www.ccp14.ac.uk/tutorial/crys/taup.htm

TREOR90 (*Included in FULLPROF*)
http://www.ill.eu/sites/fullprof/php/programsdc cc.html?pagina=Treor90

D.6 Powder Pattern Decomposition

ALLHKL
Pawley GS. http://www.ccp14.ac.uk/solution/pawley/index.html

WPPF
Hatashi S, Toraya H. http://www.icdd.com/resources/axa/vol41/V41_66.pdf

D.7 Structure Solution from Powder Diffraction Data

ESPOIR
Mileur M, Le Bail A. http://www.cristal.org/sdpd/espoir/

EXTRA (*Included in EXPO*)
http://www.ccp14.ac.uk/tutorial/expo/index.html

FULLPROF
http://www.ill.eu/sites/fullprof/

GSAS
http://www.ccp14.ac.uk/solution/gsas

RIETAN
Izumi F. http://homepage.mac.com/fujioizumi/download/download_Eng.html

SIRPOW (*Included in EXPO*)
http://www.ccp14.ac.uk/tutorial/expo/index.html

POWDER SOLVE
http://accelrys.com/resource-center/case-studies/powder-solve.html

D.8 Software for Macromolecular Crystallography

Much of the software listed in this section is fast moving, and the CCP sites[1,2] should be consulted for the latest developments.

D.8.1 Data Processing

HKL 4 (*Includes DENZO, XDISPLAY, and SCALEPACK*)
Gerwith D (2003) The HKL manual, 6th edn. http://www.hkl-xray.com/hkl_web1/hkl/manual_online.pdf

STRATEGY
Ravelli RBG et al. http://www.crystal.chem.uu.nl/distr/strategy.html

PREDICT
Noble M. http://biop.ox.ac.uk/www/distrib/predict.html

D.8.2 Fourier and Structure Factor Calculations

SFALL (Structure Factors). http://www.ccp4.ac.uk/html/sfall.html
FFT (Fast Fourier Transform). http://www.ccp4.ac.uk/html/fft.html

D.8.3 Molecular Replacement

AmoRe
Navaza J (Autostruct 2001). http://www.ccp4.ac.uk/autostruct/amore/

CNS Solve 1.1
Brünger AT et al. http://cns.csb.yale.edu/v1.1/

MOLREP
Vagin AA. alexei@ysbl.york.ac.uk

MOLPACK
Wang D et al. http://www.ccp4.ac.uk/html/molrep.html

REPLACE
http://como.bio.columbia.edu/tong/Public/Replace/replace.html

D.8.4 Schematic Structure Plots

LIGPLOT
Laskowski RA. http://www.ebi.ac.uk/thornton-srv/software/LIGPLOT/

SHELXS-86
Location of heavy-atom positions. Sheldrick GM (1994) Crystallographic computing, 3rd edn. Oxford University Press, Oxford

D.8.5 Software for Packing, Molecular Geometry, Validation and Deposition

COOT
Emsley P et al (2010) Acta Cryst D66:486. http://lmb.bioch.ox.ac.uk/coot/

PROCHECK
Laskowski RS et al. http://www.ebi.ac.uk/thornton-srv/software/PROCHECK

WHATCHECK
Hooft RWW et al. http://www.ccp4.ac.uk/dist/ccp4i/help/modules/valdep.html

D.8.6 Software for Graphics and Model Building

FRODO
Jones TA. http://www.mendeley.com/research/tek-frodo-new-version-frodo-tektronix-graphics-stations/

O
Jones TA et al. http://xray0.princeton.edu/~phil/Facility/ono.html

TURBO-FRODO
Jones TA et al. Bio-graphics. http://www.afmb.univ-mrs.fr/-TURBO-

D.8.7 Software for Molecular Graphics and Display

MERCURY
http://www.ccdc.cam.ac.uk/products/csd_system/ mercury_csd/index.php

ORTEP
Barnes CL (1997) ORTEP-3 for Windows, J Appl Cryst 30:568 [based on ORTEP-III by Johnson CK and Burnett MN.]

RASMOL
Sayle R. http://www.umass.edu/microbio/rasmol/

RASTER 3.0
Bacon DJ et al. http://skuld.bmsc.washington.edu/raster3d

SETOR
Evans SV. http://www.ncbi.nlm.nih.gov/pubmed/8347566

MOLSCRIPT 1.4
Kraulis PJ. http://www.avatar.se/molscript

BOBSCRIPT 2.4 (*Extension to MOLSCRIPT 1.4*)
Esnouf R. http://www.csb.yale.edu/userguides/graphics/bobscript/bobscript.html

D.8.8 Software for Refinement

X-PLOR 3.1
Brünger AT. http://yalepress.yale.edu/book.asp?isbn=9780300054026

CNS Solve 1.1
Brünger AT et al. http://cns.csb.yale.edu/v1.1/

RESTRAIN
Driessen HPC et al. http://scripts.iucr.org/cgi-bin/paper?gl0109

SHELXS-86
Sheldrick GM (1994) Crystallographic computing, 3rd edn. Oxford University Press, Oxford

SHELX-97 and SHELXL-97
Sheldrick GM. http://shelx.uni-ac.gwdg.de/SHELX/

REFMAC 5
http://www.ccp4.ac.uk/html/refmac5.html

D.8.9 Software for Molecular Dynamics and Energy Minimization

SYBYL-X
http://tripos.com/index.php?family=modules,SimplePage,,,&page=SYBYL-X

D.8.10 Data Bases

Protein Data Bank (PDB)
http://www.pdb.org/pdb/static.do?p=search/index.html

Basic Local Alignment Search Tool (BLAST)
http://blast.ncbi.nlm.nih.gov/Blast.cgi?PAGE= Proteins

Cambridge Crystallographic Data Centre (CCDC)
http://www.ccdc.cam.ac.uk

ReLiBase (Finds Ligands for Protein Families)
http://www.ccdc.cam.ac.uk/free_services/reliba se_free/

ChemSpider (Contains Much Chemical Information on ca. 25 Million Compounds)
http://cs.m.chemspider.com

D.8.11 Synchrotron Web Page

http://www.esrf.eu/computing/scientific/people/srio/publications/SPIE04_XOP.pdf

D.9 Bioinformatics

D.9.1 Molecular Modelling Software

The sources listed below provide software for molecular modelling. Some of them, for example, COSMOS and Sybyl are listed above. Others are readily obtained from the web sites that are given by the names, for example, $\text{Abalone}_{\text{classical}}$: http://www.sciencedirect.com/science/article/pii/S0928493110002894.

The following names may be interrogated in a similar manner:

- $\text{Abalone}_{\text{classical}}$
- $\text{ADF}_{\text{quantum}}$
- $\text{AMBER}_{\text{classical}}$
- $\text{Ascalaph Designer}_{\text{classical and quantum}}$ [http://en.wikipedia.org/wiki/Main_Page#cite_note-0]
- AutoDock
- AutoDock Vina
- BALLView
- Biskit
- $\text{BOSS}_{\text{classical}}$
- Cerius2
- $\text{CHARMM}_{\text{classical}}$
- Chimera
- Coot [http://en.wikipedia.org/wiki/Main_Pa ge#cite_note-1]
- COSMOS (software) [http://en.wikipedia.org/wiki/Main_Page#cite_note-2]
- $\text{CP2K}_{\text{quantum}}$
- $\text{CPMD}_{\text{quantum}}$
- Culgi
- $\text{Discovery Studio}_{\text{classical and quantum}}$ [http://en.wikipedia.org/wiki/Main_Page#cite_note-3]
- $\text{DOCK}_{\text{classical}}$
- $\text{Firefly}_{\text{quantum}}$
- FoldX
- $\text{GAMESS (UK)}_{\text{quantum}}$
- $\text{GAMESS (US)}_{\text{quantum}}$
- $\text{GAUSSIAN}_{\text{quantum}}$
- Ghemical
- Gorgon [http://en.wikipedia.org/wiki/Main_ Page#cite_note-4]
- $\text{GROMACS}_{\text{classical}}$
- $\text{GROMOS}_{\text{classical}}$

- InsightII$_{\text{classical and quantum}}$
- LAMMPS$_{\text{classical}}$
- Lead Finder$_{\text{classical}}$ [http://en.wikipedia.org/wiki/Main_Page#cite_note-5]
- LigandScout
- MacroModel$_{\text{classical}}$
- MADAMM [http://en.wikipedia.org/wiki/Main_Page#cite_note-6; http://en.wikipedia.org/wiki/Main_Page#cite_note-Cerqueira-7]
- MarvinSpace [http://en.wikipedia.org/wiki/Main_Page#cite_note-8]
- Materials and Processes Simulations [http://en.wikipedia.org/wiki/Main_Page#cite_note-9]
- Materials Studio$_{\text{classical and quantum}}$ [http://en.wikipedia.org/wiki/Main_Page#cite_note-10]
- MDynaMix$_{\text{classical}}$
- MMTK
- Molecular Docking Server
- Molecular Operating Environment (MOE)$_{\text{classical and quantum}}$
- MolIDE$_{\text{homology modelling}}$ [http://en.wikipedia.org/wiki/Main_Page#cite_note-11]
- Molsoft ICM [http://en.wikipedia.org/wiki/Main_Page#cite_note-12]
- MOPAC$_{\text{quantum}}$
- NAMD$_{\text{classical}}$
- NOCH
- Oscail X
- PyMOL$_{\text{visualization}}$
- Q-Chem$_{\text{quantum}}$
- ReaxFF
- ROSETTA
- SCWRL$_{\text{side-chain prediction}}$ [http://en.wikipedia.org/wiki/Main_Page#cite_note-13]
- Sirius
- Spartan (software)$_{\text{quantum}}$ [http://en.wikipedia.org/wiki/Main_Page#cite_note-14]
- StruMM3D (STR3DI32) [http://en.wikipedia.org/wiki/Main_Page#cite_note-15]
- Sybyl (software)$_{\text{classical}}$ [http://en.wikipedia.org/wiki/Main_Page#cite_note-16]
- MCCCS Towhee [http://en.wikipedia.org/wiki/Main_Page#cite_note-17]
- TURBOMOLE$_{\text{quantum}}$
- VMD$_{\text{visualization}}$
- VLifeMDS$_{\text{Integrated molecular modelling and simulation}}$
- WHAT IF [http://en.wikipedia.org/wiki/Main_Page#cite_note-18]
- xeo [http://en.wikipedia.org/wiki/Main_Page #cite_note-19]
- YASARA [http://en.wikipedia.org/wiki/Main_Page#cite_note-20]
- Zodiac (software) [http://en.wikipedia.org/wiki/Main_Page#cite_note-21]

D.9.2 External Links

These links relate to important sites on molecular modelling and molecular simulation, but are by no means exhaustive.

Center for Molecular Modelling at the National Institutes of Health (NIH) (U.S. Government Agency): http://www.bing.com/search?q=Center+for+Molecular+Modelling+at++the+National+Institutes+of+Health+%28NIH%29+%28U.S.+Government+Agency%29&src=ie9tr

Molecular Simulation, details for the Molecular Simulation journal, ISSN: 0892-7022 (print), 1029-0435 (online): http://www.bing.com/sear ch?q=Center+for+MolecularModelling+at+the+National+Institutes+of+Health+%28NIH%29+%28U.S.+Government+Agency%29&src=ie9tr

The Cheminfo Network and Community of Practice in Informatics and Modelling: http://www.bing.com/search?q=The+Cheminfo+Network+and+Community+of+Practice+in+Informatics+and+Modelling.&src=ie9tr

D.9.3 Useful Homepages

These sites relate to situations wherein extensive work on protein crystallography is being persued. Again, it is not an exhaustive list.

York Structural Biology Laboratory
http://www.york.ac.uk/chemistry/research/groups/ ysbl/

COSMOS—Computer Simulation of Molecular Structures
http://www.mybiosoftware.com/3d-molecular-model/1968

Accelrys Inc.
http://accelrys.com/
http://www.ccp4.ac.uk
http://www.ccp14.ac.uk
http://epsrc.ac.uk/Pages/default.aspx
http://ww1.iusr.org/sincris-top/logicel/Imno.html#O

Appendix E: Structure Invariants, Structure Seminvariants, Origin and Enantiomorph Specifications

E.1 Structure Invariants

As we have seen in Sect. 2.2.2, there is an infinite number of ways in which a crystal unit cell may be chosen. Conventionally, however, any crystal lattice is represented by one of the 14 Bravais lattices described in Sect. 2.2.3. For a given unit cell, the origin of the x, y, and z coordinates can be relocated for convenience, as we have seen in Sect. 2.7.7 for space group $P2_12_12_1$. The possible effects of such origin transformations were mentioned in Sect. 6.6.4, when discussing of Fourier transforms. As a general rule, the origin of a given space group is chosen with respect to its symmetry elements; for example, in centrosymmetric space groups the origin is specified on a center of symmetry. Conventions associated with the specification of the origin are fully described for all space groups in the literature. With no symmetry elements apart from the lattice translations, space group $P1$ is the exception and can accommodate an origin of coordinates in any arbitrary position. We discuss here relationships between structure factors that arise from changes in the location of the coordinate origin.

Following (3.63) we write the structure factor in the form

$$\mathrm{F}(\mathbf{h}) = \sum_j f_j \exp(\mathrm{i}2\pi\mathbf{h}\cdot\mathbf{r}_j) \tag{E.1}$$

where $\mathbf{h}$ represents a reciprocal lattice vector corresponding to reflection hkl and $\mathbf{r}_j$ is the real space vector corresponding to the point x, y, z, so that $\mathbf{h}\cdot\mathbf{r}_j = hx_j + ky_j + lz_j$. If the origin is changed to the point $\mathbf{r}_0$, then (E.1) becomes

$$\begin{aligned}\mathrm{F}(\mathbf{h})_{\mathbf{r}_0} &= \sum_j f_j \exp[\mathrm{i}2\pi\mathbf{h}\cdot(\mathbf{r}_j - \mathbf{r}_0)] \\ &= \sum_j f_j \exp(\mathrm{i}2\pi\mathbf{h}\cdot\mathbf{r}_j)\exp(-\mathrm{i}2\pi\mathbf{h}\cdot\mathbf{r}_0)\end{aligned} \tag{E.2}$$

Thus, we can write

$$\mathrm{F}(\mathbf{h})_{\mathbf{r}_0} = \mathrm{F}(\mathbf{h}) \exp(-\mathrm{i}2\pi\mathbf{h} \cdot \mathbf{r}_0) \tag{E.3}$$

so that

$$|\mathrm{F}(\mathbf{h})_{\mathbf{r}_0}| = |\mathrm{F}(\mathbf{h})| \tag{E.4}$$

and

$$\phi(\mathbf{h})_{\mathbf{r}_0} = \phi(\mathbf{h})_{\mathbf{r}} - 2\pi\mathbf{h} \cdot \mathbf{r}_0 \tag{E.5}$$

Thus, a change of origin leaves the amplitude of the structure factor unaltered, but changes the phase by $-2\pi\mathbf{h} \cdot \mathbf{r}_0$whatever the value of $\mathbf{r}_0$. The relationships (E.3)–(E.5) apply equally to the normalized structure factors E(*hkl*) that are used in direct methods of phase determination. We can illustrate (E.3)–(E.5) by a simple example.

Consider an atom at 0.3, 0.2, 0.7 in space group $P1$. For a reflection, say 213, and taking f as 1.0, we find $A'_1 = 0.8090$, $B'_1 = -0.5878$, so that $|\mathrm{F}_1| = 1$ and $\phi_1 = 324°$. We change the origin to the point 0.1, 0.1, 0.1, whereupon $A'_2 = -0.3090$, $B'_2 = 0.9511$, so that $|\mathrm{F}_2| = 1$ and $\phi_2 = 108°$. Finally, using the third term in (E.5), we find $\Delta\phi = 2\pi\mathbf{h} \cdot \mathbf{r}_0 = 360\,[2 \times (0.1) + 1 \times (0.1) + 3 \times (0.1)] = 216$, which is equal to $\phi_1 - \phi_2$. (Remember to set $\tan^{-1}(B'/A')$ in the correct quadrant according to the signs of A' and B', and to evaluate ϕ in the positive range 0–2π.)

The values of $|\mathrm{E}|$ are determined by the structure, whatever the origin, whereas the values of ϕ are determined by both the structure and the choice of origin. Thus, the values of $|\mathrm{E}|$ alone cannot determine unique values for the phases. We need a process to obtain phases from the values of $|\mathrm{E}|$ that incorporates a specification of the origin. Consider the product of three normalized structure factors in the absence of symmetry, that is, for space group $P1$. From (3.15), we can write

$$\begin{aligned}\mathrm{E}_1\mathrm{E}_2\mathrm{E}_3 = |\mathrm{E}_1||\mathrm{E}_2||\mathrm{E}_3| \exp[\mathrm{i}(\phi(\mathbf{h}_1) \\ + (\phi(\mathbf{h}_2) + (\phi(\mathbf{h}_3)]\end{aligned} \tag{E.6}$$

If the origin is moved from 0,0,0 to a point $\mathbf{r}_0$, it follows from the foregoing that (E.6) becomes

$$\mathrm{E}_1\mathrm{E}_2\mathrm{E}_3 = |\mathrm{E}_1||\mathrm{E}_2||\mathrm{E}_3| \exp[-\mathrm{i}2\pi(\mathbf{h}_1 + \mathbf{h}_2 + \mathbf{h}_3) \cdot \mathbf{r}_0] \tag{E.7}$$

Thus, the condition that the product of three structure factors be a *structure invariant* N_3, that is, a change of origin has no effect on its value in the non-centrosymmetric space group $P1$, is that

$$\mathbf{h}_1 + \mathbf{h}_2 + \mathbf{h}_3 = 0 \tag{E.8}$$

Equation (E.8) is a triplet structure invariant; it may be extended to a quartet such that the product of four structure factors is a structure invariant N_4 if

$$\mathbf{h}_1 + \mathbf{h}_2 + \mathbf{h}_3 + \mathbf{h}_4 = 0 \tag{E.9}$$

and more:

$$\mathrm{N})_n = \prod_{j=1}^{n} \mathrm{E}(\mathbf{h}_j) \tag{E.10}$$

provided that the condition

$$\sum_{j=1}^{n} \mathbf{h}_j = 0 \tag{E.11}$$

For $n = 1$, the structure factor, which is a structure invariant, is E(0) and has a phase of zero for any origin. For $n = 2$, $\mathbf{h}_1 + \mathbf{h}_2 = 0$, or $\mathbf{h}_2 = -\mathbf{h}_1$ so that $\mathrm{E}_1\mathrm{E}_2 = \mathrm{E}(\mathbf{h}_1)\mathrm{E}(-\mathbf{h}_1) = |\mathrm{E}(\mathbf{h}_1)|^2$, which is phase independent. For $n > 2$, we have (E.10) and (E.11) as already discussed. For $n = 3$ or more, we have equations such as (E.8) and (E.9).

E.2 Structure Seminvariants

Equations such as (E.8) apply also to $P\bar{1}$, because the sums of the indices, as in (E.13) below, are each zero. However, consider next a structure with symmetry $P\bar{1}$, wherein the origin is chosen, normally, on one of the eight centers of symmetry unique to the unit cell. In the presence of symmetry elements, it is always desirable to choose the origin on one of these elements, albeit such a choice may not define the origin point uniquely, such as on the twofold axis parallel to the line [0,*y*,0] in space group *P*2.

The normally permitted origins in $P\bar{1}$ are listed in Table 8.2. In general, the sign of $E(hkl)$ depends on the choice of origin except for reflection in the group **eee**, for which reflections[6]

$$(hkl) \text{ modulo}^2 \ (222) = (000) \tag{E.12}$$

Such reflections are *structure seminvariants* (semi-invariants) since their signs (phases) do not change for variation among the *permitted* origins. If three structure factors are chosen from different parity groups, other than **eee**, such that

$$h_1 + h_2 + h_3, \quad k_1 + k_2 + k_3, \quad l_1 + l_2 + l_3 \text{ modulo } (222) \tag{E.13}$$

then the product of the three structure factors is not a structure seminvariant (semi-invariant), and can be either positive or negative. An arbitrary sign can be chosen for each such structure factor in the product, and for one of the eight possible origins the choice will be true, and the origin is fixed according to that choice. Thus, for example, the reflections $10\bar{6}$, $40\bar{1}$, and $71\bar{4}$ may be chosen to specify an origin, and if we allocate a + sign arbitrarily to each, the origin is defined as 0, 0, 0. If we choose instead the reflections $10\bar{6}$, $40\bar{1}$, and $\bar{5}07$, then the origin is not specified uniquely because the determinant is less than or equal to zero. The triplet is not linearly independent (see E.14 and text):

[6] $a \equiv b$ modulo n if $a - b = kn$, where k is an integer.

$1 + 4 - 5 = 0$, $0 + 0 + 0 = 0$ and $-6 - 1 + 7 = 0$, or **oee** + **eeo** + **oeo** = **oee**, which *does* not constitute linear independence. The relation $\mathbf{h}_1 + \mathbf{h}_2 + \mathbf{h}_3 = 0$ modulo (222) has no special significance in space group $P1$.

The structure invariants and structure seminvariants have been well described in the literature for all space groups.[7–11]

E.2.1 Difference Between Structure Invariant and Structure Seminvariant

Consider two triplets $\mathrm{E}(3\bar{3}2)\mathrm{E}(012)\mathrm{E}(\bar{3}2\bar{4})$ and $\mathrm{E}(3\bar{3}2)\mathrm{E}(012)\mathrm{E}(344)$. The first product is a structure invariant because the sums $h_1 + h_2 + h_3$, $k_1 + k_2 + k_3$ and $l_1 + l_2 + l_3$ are each equal to zero. It is a structure invariant in $P1$ and $P\bar{1}$ wherever the origin point is placed in the unit cell. The second product is a structure seminvariant because the sums $h_1 + h_2 + h_3$, $k_1 + k_2 + k_3$ and $l_1 + l_2 + l_3$ are each equal to zero modulo (2), and its sign (phase) is not changed by moving to another *permitted* origin in $P\bar{1}$, but it would change if the origin were moved to a general point in the unit cell. Note that in both examples, these reflections would not serve to specify an origin because the parities sum to **eee** in each case.

E.3 Origin Specification

From the foregoing, we see that for space group $P1$, which contains no symmetry other than that of the basic translations, three reflections that form a linearly independent combination will specify the origin. The three reflections $\mathrm{E}(h_1k_1l_1)$, $\mathrm{E}(h_2k_2l_2)$, and $\mathrm{E}(h_3k_3l_3)$ will specify an origin provided that the determinant Δ satisfies the condition

$$\Delta = \begin{vmatrix} h_1 & k_1 & l_1 \\ h_2 & k_2 & l_2 \\ h_3 & k_3 & l_3 \end{vmatrix} > 0 \tag{E.14}$$

or Δ modulo (222) $= \pm 1$; the determinant is evaluated in the normal manner.

Normally, the position 0, 0, 0 is chosen for the origin in $P1$; there is no purpose in choosing any other site. The three independent phases can be given values between 0 and 2π; generally they are chosen as zero.

In any space group of symmetry greater than 1, the origin is normally chosen on that symmetry element. We have discussed the case for $P\bar{1}$ sufficiently for our purposes in Sect. 8.2.2.

E.4 Choice of Enantiomorph

In any of the 65 enantiomorphous space groups listed in Table 10.1, there exists the need to specify a molecular enantiomorph. From (E.1) we can write

[7] Hauptman H, Karle J (1953) The solution of the phase problem I, ACA monograph 3.
[8] idem. (1956) Acta Crystallogr 9:45.
[9] idem. ibid. (1959) 12:93.
[10] Karle J, Hauptman H (1961) ibid. 14:217.
[11] Lessinger L, Wondratschek H (1975) ibid. A31:382.

$$|\mathrm{E}(\mathbf{h})| = \left| \sum_j Z_j \exp[\mathrm{i}2\pi(\mathbf{h} \cdot \mathbf{r}_j)] \right| \tag{E.15}$$

If each $\mathbf{r}_j$ is replaced by its inverse, the right-hand side of (E.15) and, hence, $|\mathrm{E}(\mathbf{h})|$ remain unchanged. The $|\mathrm{E}|$ values relate to both a structure and its inverse, or roto-reflection, through a point. If this point is the origin 0, 0, 0, then the structure factors are $\mathrm{E}(\mathbf{h})$ and its conjugate $\mathrm{E}^*(\mathbf{h})$ and its phases are $\phi(\mathbf{h})$ and $-\phi(\mathbf{h})$. Thus, the two values for a structure invariant differ only in sign.

If a structure invariant phase is 0 or π, then it has the same value for both enantiomorphs. If a structure invariant is enantiomorph-sensitive, then its value differs significantly from 0 or π, and its value may be specified arbitrarily within this range, generally a value of $\pi/2$, $\pi/4$, or $3\pi/4$. Of course, the structure determined may not correspond to the true chemical configuration and that problem must be addressed (see Sect. 7.6.1). The selection of an enantiomorph has been discussed in a practical manner through the structure analysis in Sect. 8.2.10.

Tutorial Solutions

Solutions 1

1.1. Extend CA to cut the x' axis in H. All angles in the figure are easily calculated ($OA = OC = x$). Evaluate OP, or a' (1.623x), and OH (2.732x). Express OH, the required intercept on the x' axis, as a fraction of a' (1.683). The intercept along b' (and b) remains unaltered, so that the fractional intercepts of the line CA are 1.683 and 1/2 along x' and y respectively. Hence, CA has the Miller indices (0.5941, 2), or (1, 3.366), referred to the oblique axes.

1.2. (a) $h = a/(a/2) = 2$, $k = b/(-b/2) = \bar{2}$, $l = c/\infty = 0$; hence $(2\,\bar{2}\,0)$. Similarly,
(b) (164) (c) $(0\,0\,\bar{1})$ (d) $(3\,\bar{3}\,4)$ (e) $(0\,\bar{4}\,3)$ (f) $(\bar{4}\,2\,\bar{3})$

1.3. Use (1.6), (1.7), and (1.8). More simply, set down the planes twice in each of the two rows, ignore the first and final indices in each row, and then cross-multiply, similarly to the evaluation of a determinant.

1	2	3	1	2	3
	×	×	×		
0	$\bar{1}$	1	0	$\bar{1}$	0

Hence, $U = 2 - (-3) = 5$, $V = 0 - 1 = -1$, $W = -1 - 0 = -1$ so that the zone symbol is $[5\,\bar{1}\,\bar{1}]$. If we had written the planes down in the reverse order, we would have obtained $[\bar{5}\,1\,1]$. (What is the interpretation of this result?) Similarly:
(b) $[3\,\bar{5}\,2]$ (c) $[\bar{1}\,\bar{1}\,\bar{1}]$ (d) [110]

1.4. Use (1.9) or, more simply, set down the procedure as in Solution 1.3, but with zone symbols, which leads to $(\bar{5}\,\bar{2}\,3)$. This plane and $(5\,2\,\bar{3})$ are parallel; $[UVW]$ and $[\overline{U}\,\overline{V}\,\overline{W}]$ are coincident.

1.5. Formally, one could write 422, $4\,2\,\bar{2}$, $4\,\bar{2}\,2$, $4\,\bar{2}\,\bar{2}$, $\bar{4}\,2\,2$, $\bar{4}\,2\,\bar{2}$, $\bar{4}\,\bar{2}\,2$, $\bar{4}\,\bar{2}\,\bar{2}$. However, the interaction of two inversion axes leads to an intersecting *pure* rotation axis, so that all symbols with one or three inversion axes are invalid. Now $\bar{4}\,2\,\bar{2}$ and $\bar{4}\,\bar{2}\,2$ are equivalent under rotation of the x and y axes in the x, y plane by 45 deg, so that there remain 422, $4\,\bar{2}\,\bar{2}$, and $\bar{4}\,2\,\bar{2}$ as unique point groups. Their standard symbols are 422, 4mm, and $\bar{4}\,2\,m$, respectively. Note that if we do postulate a group with the symbol $4\,2\,\bar{2}$, for example, it is straightforward to show, with the aid of a stereogram, that it is equivalent to, and a non-standard description of $\frac{4}{m}mm$.

1.6. (a) mmm (b) $2/m$ (c) 1

1.7. Refer to Fig. S1.1 (a) mmm; $\mathbf{m\,m\,m} \equiv \bar{\mathbf{1}}$ (b) $2/m$; $\mathbf{2\,m} \equiv \bar{\mathbf{1}}$

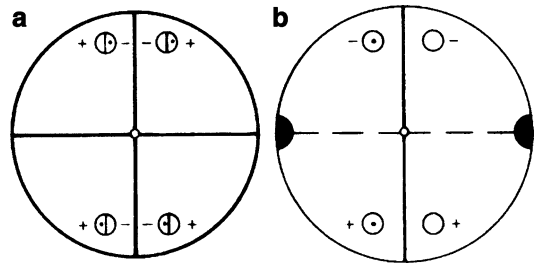

Fig. S2.1

1.8.

	{010}	$\{\bar{1}10\}$	$\{11\bar{3}\}$
$2/m$	2	4	4
$\bar{4}2m$	4	4	8
$m\bar{3}$	6	12	24

1.9. (a) 1; (b) *m*; (c) 2; (d) *m*; (e) 1; (f) 2; (g) 6; (h) 6*mm*; (i) 3; (j) 2*mm*. (Did you remember to use the Laue group for each example?)

1.10. (a) From a thin card, cut out four but identical quadrilaterals; when fitted together, they make a (plane) figure of symmetry 2. (b) *m*. (A beer "jug" has the same symmetry.) (c) a, ∞/m; b, 3; $\frac{4}{m}mm$; d, $\overline{10}2m$; e, $\frac{6}{m}mm$; f, *m*.

1.11.

(a)	$\bar{6}m2$	D_{3h}
(b)	$\frac{4}{m}mm$	D_{4h}
(c)	$m\bar{3}m$	O_h
(d)	$\bar{4}3m$	T_d
(e)	$3m$	C_{3v}
(f)	1	C_1
(g)	$\frac{6}{m}mm$	D_{6h}
(h)	$mm2$	C_{2v}
(i)	mmm	D_{2h}
(j)	$mm2$	C_{2v}
(k)	2	C_2
(l)	3	C_3
(m)	$\bar{1}$	C_i
(n)	$\bar{3}$	S_6
(o)	$\bar{4}$	S_4
(p)	m	C_s
(q)	$\bar{6}$	C_{3h}
(r)	$2/m$	C_{2h}
(s)	222	D_2
(t)	422	D_4
(u)	$4mm$	C_{4v}
(v)	$\bar{4}2m$	D_{2d}

1.12. Remember first to project the general form of the point group on to a plane of the given form, and then relate the projected symmetry to one of the two-dimensional point groups. In some cases, you will have more than one set of representative points in two dimensions.
(a) 2 (b) m (c) 1 (d) m (e) 1 (f) 1 (g) 3 (h)3m (i) 3 (j) 2mm

1.13. (10), (01), $(\bar{1}\,0)$, $(0\,\bar{1})$. They are the same for the parallelogram, provided that the axes are chosen parallel to the sides of the figure.

1.14. Refer to Fig. S1.2, and from the definition of Miller indices: $OA = a/h$; $OB = b/k$. Let the plane $(hkil)$ intercept the u axis at p; draw DE parallel to AO. Since OD bisects $<AOB$, $AOD = 60$ deg, so that ΔODE is equilateral; hence $OD = DE = OE = p$. Triangles EBD and OBA are similar; hence $EB/DE = OB/OA = (b/k)/(a/h)$. Now $EB = b/k - p$, and from the above, it follows that $p = ab/(ak + bh)$. Since $a = b = u$, from the symmetry, $u/p = h + k$. We write u/p as $-i$, since p lies on the negative side of the u axis ($OD = -u/p$), so that

$$i = -(h + k)$$

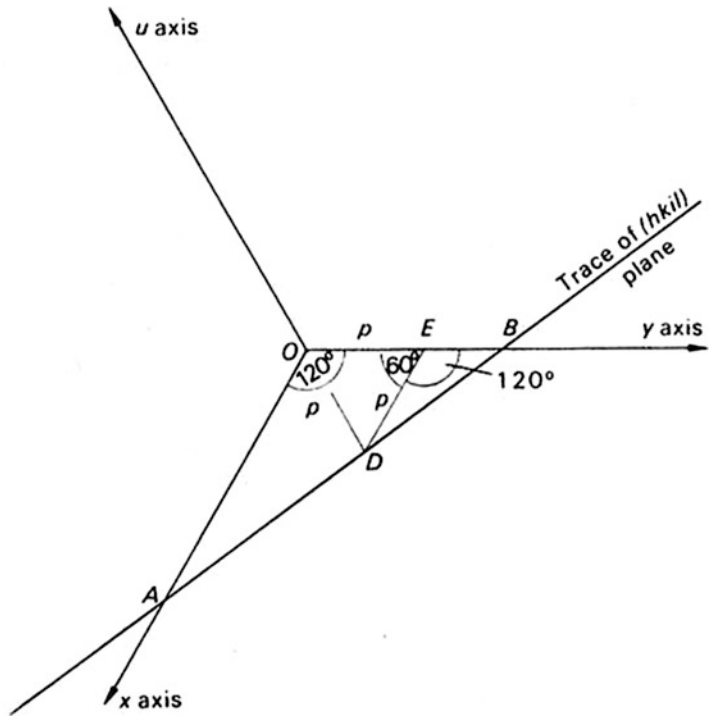

Fig. S1.2

1.15. Refer to Chap. 1, Fig. P1.6; the points $ACGE$ mark out one of the diagonal m planes of the cube. From the symmetry of the cube, the currents through the resistors have the values as shown. Hence, any path through the cube from A to G has a resistance of 5/6 Ω.

Solutions 2

2.1. The translations, equal to the lengths of the two sides of any parallelogram unit, repeat the molecule ad infinitum in the two dimensions shown. A two-fold rotation point placed at any corner of a parallelogram is, itself, repeated by the same translations (see Fig. P2.1).
(i) The two-fold rotation points lie at each corner, half-way along each edge and at the geometrical center of each parallelogram unit.
(ii) There are four unique two-fold points per parallelogram unit: one at a corner, one at the center of each of two non-collinear edges, and one at the geometrical center.

2.2.

	(i)	(ii)
(a)	4*mm*	6*mm*
(b)	Square	Hexagonal

(c) (i) If unit cell is centered, then another square can be drawn to form a conventional unit cell of half the area of the centered unit cell.
(ii) If unit cell is centered it is no longer hexagonal; each point is degraded to the 2*mm* symmetry of the rectangular system, and may be described by a conventional *p* unit cell. The transformation equations in each example are:

$$\mathbf{a}' = \mathbf{a}/\mathbf{2} + \mathbf{b}/\mathbf{2}; \quad \mathbf{b}' = -\mathbf{a}/\mathbf{2} + \mathbf{b}/\mathbf{2}$$

Note. A regular hexagon of "lattice" points with another point placed at its center is not a centered hexagonal unit cell: it represents three adjacent *p* hexagonal unit cells in different relative orientations. (Without the point at the center, the hexagon of points is not even a lattice.)

2.3. A *C* unit cell may be obtained by the transformations:

$$\mathbf{a}_C = \mathbf{a}_F; \quad \mathbf{b}_C = \mathbf{b}_F; \quad \mathbf{c}_C = -\mathbf{a}_F/2 + \mathbf{c}_F/2.$$

The new *c* dimension is obtained from evaluating the dot product:

$$(-\mathbf{a}/2 + \mathbf{c}/2) \cdot (-\mathbf{a}/2 + \mathbf{c}/\mathbf{2})$$

to give c' 5.7627 Å; *a* and *b* are unchanged. The angle β' in the transformed unit cell is obtained by evaluating

$$\cos\beta' = \mathbf{a} \cdot (-\mathbf{a}/2 + \mathbf{c}/2)/a'c' = (-a + c\cos\beta)/(2c')$$

so that $\beta' = 139.29°$.
$V_C(C\,\text{cell})/V_F(F\,\text{cell}) = \frac{1}{2}$. (Count the number of unique lattice points in each cell: each lattice point is associated with a unique portion of the volume.)

2.4. (a) The symmetry is no longer tetragonal, although the lattice is true: it is now orthorhombic.
(b) The tetragonal symmetry is apparently restored, but the lattice is no longer true: the lattice points are not all in the same environment in the same orientation.
(c) A tetragonal *F* unit cell is formed and represents a true tetragonal lattice.

However, tetragonal F is equivalent to tetragonal I (of smaller volume) under the transformation

$$\mathbf{a}_I = \mathbf{a}_F/2 + \mathbf{b}_F/2; \quad \mathbf{b}_I = -\mathbf{a}_F/2 + \mathbf{b}_F/2; \quad \mathbf{c}'_I = \mathbf{c}_F$$

2.5. F unit cell: $r^2_{[31\bar{2}]}/\text{Å}^2 = \mathbf{r}_{[31\bar{2}]} \cdot \mathbf{r}_{[31\bar{2}]} = 3^2a^2 + 1^2b^2 + 2^2c^2 + 2 \cdot 3 \cdot (-2) \times 6 \times 8 \times \cos 110$, so that r = 28.64 Å. To obtain the value in the C unit cell, we could repeat this calculation with the dimensions of the C unit cell, leading to 28.64 Å. Alternatively, we could use the transformation matrix to obtain the F equivalent of $[31\bar{2}]c$, and then use the original F cell dimensions on it. The matrix for this F cell in terms of the C is:

$$\mathbf{S} = \begin{bmatrix} 1 & 0 & 0 \\ 0 & 1 & 0 \\ 1 & 0 & 2 \end{bmatrix} \quad \text{so that} \quad (\mathbf{S}^{-1})^T = \begin{bmatrix} 1 & 0 & -\frac{1}{2} \\ 0 & 1 & 0 \\ 0 & 0 & \frac{1}{2} \end{bmatrix}$$

Then, $[UVW]_F = (\mathbf{S}^{-1})^T \cdot [UVW]_C = [41\bar{1}]_F$, so that $r_{[41\bar{1}]F} = 28.64\,\text{Å}$.

2.6. It is not an eighth crystal system because the symmetry at each lattice point is $\bar{1}$. It is a special case of the triclinic system in which the γ angle is 90°.

2.7. (a) Plane group $c2mm$ is shown in Fig. S2.1, with the coordinates listed below it.

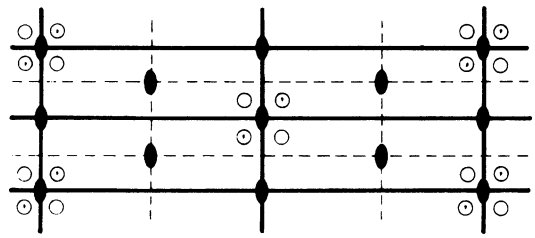

Fig. S2.1

			Origin on $2mm$				
			$(0,0;\frac{1}{2},\frac{1}{2})+$				Limiting conditions
8	(f)	1	$x,y;$	$x,\bar{y};$	$\bar{x},y;$	$\bar{x},\bar{y}$	hk: $h+k=2n$
4	(e)	m	$0,y;$	$0,\bar{y};$			—
4	(d)	m	$x,0;$	$\bar{x},0$			—
4	(c)	2	$\frac{1}{4},\frac{1}{4};$	$\frac{1}{4},\frac{3}{4}$			As above +
							hk: $h=2n, (k=2n)$
2	(b)	$2mm$	$0,\frac{1}{2}$				—
2	(a)	$2mm$	0,0				—

(b) Plane group $p2mg$ is shown in Fig. S2.2; this diagram also shows the minimum number of motifs p, V, and Z.

Note that if the symmetry elements are arranged with 2 at the intersection of m and g, they do not form a group. Attempts to draw such an arrangement lead to continued halving of the repeat distance parallel to the g line.

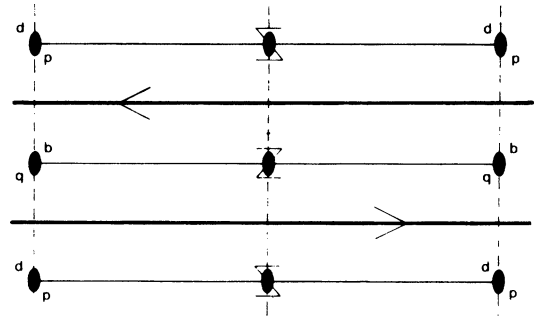

Fig. S2.2

2.8. (a)

			Origin on $\bar{1}$	Limiting conditions
4	(e)	1	$x, y, z;\ x, \frac{1}{2}-y, \frac{1}{2}+z$	hkl: None
			$\bar{x}, \bar{y}, \bar{z};\ \bar{x}, \frac{1}{2}+y, \frac{1}{2}-z$	$h0l: l = 2n$
				$0k0: k = 2n$
2	(d)	$\bar{1}$	$\frac{1}{2}, 0, \frac{1}{2};\ \frac{1}{2}, \frac{1}{2}, 0$	As above + $hkl: k + l = 2n$
2	(c)	$\bar{1}$	$0, 0, \frac{1}{2};\ 0, \frac{1}{2}, 0$	
2	(b)	$\bar{1}$	$\frac{1}{2}, 0, 0;\ \frac{1}{2}, \frac{1}{2}, \frac{1}{2}$	
2	(a)	$\bar{1}$	$0, 0, 0;\ 0, \frac{1}{2}, \frac{1}{2}$	
(100) $p2gg : b' = b, c' = c$			(010) $p2 : a' = a, c' = c/2$	(001) $p2gm : a' = a, b' = b$

Space group $P2_1/c$ is shown in Fig. S2.3, on the (010) plane.

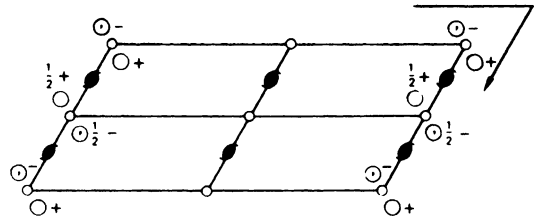

Fig. S2.3

(b) Figure S2.4 shows the molecular formula of biphenyl, excluding the hydrogen atoms. The two molecules in the unit cell lie on any set of special positions, Wyckoff (a)–(d), with the center of the C(1)–C(1)′ bond on $\bar{1}$. Hence, the molecule is centrosymmetric and planar. The planarity imposes a conjugation on the molecule, including the C(1)–C(1)′ bond. (This result is supported by the bond lengths C(1)–C(1)′ $\approx$ 1.49 Å and C_{arom}–$C_{arom} \approx$ 1.40 Å. In the free-molecule state, the rings rotate about the C(1)–C(1)′ bond to the energetically favorable conformation with the ring planes at approximately 45° to each other).

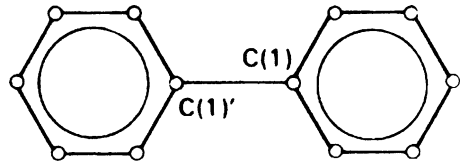

Fig. S2.4

2.9. Each pair of positions forms two vectors, between the origin and the points: $\pm\{(x_2 - x_1), (y_2 - y_1), (z_2 - z_1)\}$. Thus, there is a single vector at each of the positions:

$$2x, 2y, 2z;\ 2\bar{x}, 2\bar{y}, 2\bar{z};\ 2x, 2\bar{y}, 2z;\ 2\bar{x}, 2y, 2\bar{z}$$

and two superimposed vectors at each of the positions:

$$2x, 1/2, 1/2 + 2z;\ 0, 1/2 + 2y, 1/2; 2\bar{x}, 1/2, 1/2 - 2z; 0, 1/2 - 2y, 1/2$$

Note: $-(2x, 1/2, 1/2 + 2z) \equiv 2\bar{x}, 1/2, 1/2 - 2z$

2.10.

$$\begin{array}{ccc} x, y, z & \xrightarrow{\quad b \quad} & 2p - x, \tfrac{1}{2} + y, z \\ \Big| & & \Big| \\ \bar{1} & & a \\ \downarrow & & \Big| \\ \bar{x}, \bar{y}, \bar{z} & & \downarrow \\ 2p - x, 2q - y, 2r - z & \xleftarrow{\quad n \quad} & \tfrac{1}{2} + 2p - x, 2q - \tfrac{1}{2} - y, z \end{array}$$

Since $\bar{x}, \bar{y}, \bar{z}$ and $2p - x$, $2q - y$, $2r - z$ are one and the same point, $p = q = r = 0$, so that the three symmetry planes intersect in a center of symmetry at the origin.

Otherwise, by applying the half-translation rule, $T = a/2 + b/2 + a/2 + b/2 = 0$. Hence, the center of symmetry lies at the intersection of the three symmetry planes.

2.11. Figure S2.5 shows space group *Pbam*.

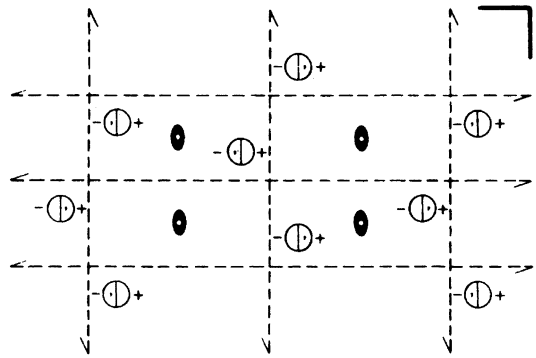

Fig. S2.5

Coordinates of general equivalent positions

$x, y, z; \quad 1/2 - x, 1/2 - y, z; \quad 1/2 + x, \bar{y}, z; \quad \bar{x}, 1/2 + y, z;$

$x, y, \bar{z}; \quad 1/2 - x, 1/2 - y, \bar{z}; \quad 1/2 + x, \bar{y}, \bar{z}; \quad \bar{x}, 1/2 + y, \bar{z}$

Coordinates of centers of symmetry

$1/4, 1/4, 0; \quad 1/4, 3/4, 0; \quad 3/4, 1/4, 0; \quad 3/4, 3/4, 0;$

$1/4, 1/4, 1/2; \quad 1/4, 3/4, 1/2; \quad 3/4, 1/4, 1/2; \quad 3/4, 3/4, 1/2$

Change of origin to $\frac{1}{4}, \frac{1}{4}, 0$:

(i) Subtract $\frac{1}{4}, \frac{1}{4}, 0$ from the above set of coordinates of general equivalent positions.

(ii) Let $x_0 = x - 1/4$, $y_0 = y - 1/4$, and $z_0 = z$.

(iii) After making all substitutions, drop the subscript, and rearrange to give:

$$\pm \{x, y, z; \quad \bar{x}, \bar{y}, z; \quad 1/2 + x, 1/2 - y, z; \quad 1/2 - x, 1/2 + y, z\}$$

This result may be confirmed by redrawing the space group with the origin on $\bar{1}$.

2.12. Figure S2.6 shows two adjacent unit cells of space group *Pn* on the (010) plane. In the transformation to *Pc*, only the *c* spacing is changed:

$$\mathbf{c}_{P_c} = -\mathbf{a}_{P_n} + \mathbf{c}_{P_n}$$

Hence, $Pn \equiv Pc$. By interchanging the labels of the *x* and *z* axes, which are not constrained by the two-fold symmetry, we see that $Pc \equiv Pa$. Note that it is necessary to invert the sign on **b**, so as to preserve a right-handed set of axes. The translation *a*/2 in the *C* unit cell in *Cm* means that $Ca \equiv Cm$. Since there is no half-translation along *c* in *Cm, Cm* is not equivalent to *Cc*, although *Cc* is equivalent to *Cn*. If the *x* and *z* axes in *Cc* are interchanged, with due attention to **b**, the symbol becomes *Aa*. (The *standard* symbols among these groups are *Pc, Cm*, and *Cc*.)

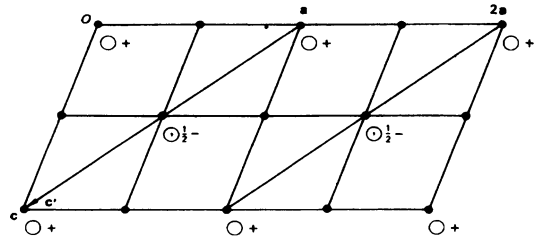

Fig. S2.6

2.13. *P*2/*c*

(a) 2/*m*; monoclinic.

(b) Primitive unit cell; *c*-glide plane $\perp$ *b*; two-fold axis $\parallel$ *b*.

(c) *h*0*l*: $l = 2n$.

(d) 12/*m*1 *P* . *c*.

$Pca2_1$
(a) *mm*2; orthorhombic.
(b) Primitive unit cell; *c*-glide plane ⊥ *a; a*-glide plane ⊥ *b*; 2_1 axis || i*c*.
(c) 0*kl: l* = 2*n; h*0*l: h* = 2*n*.
(d) *mmm P c a* .

Cmcm
(a) *mmm*; orthorhombic.
(b) *C*-face centered unit cell; *m* plane ⊥ *a; c*-glide plane ⊥ *b; m* plane ⊥ *c*.
(c) *hkl: h* + *k* = 2*n; h*0*l* :*l* = 2*n*.
(d) *mmm C* . *c* .

$P\bar{4}2_1c$
(a) $\bar{4}2m$; tetragonal.
(b) Primitive unit cell; $\bar{4}$ axis || *c*; 2_1 axes || *a* and *b; c*-glide planes ⊥ [110] and $[1\bar{1}0]$.
(c) *hhl: l* = 2*n; h*00: *h* = 2*n*.
(d) $\frac{4}{m}mm\ P\ .\ 2_1\ c$

$P6_122$
(a) 622; hexagonal.
(b) Primitive unit cell; 6_1 axis || *c*; two-fold axes || *a, b*, and *u*; two-fold axes 30° to *a, b*, and *u*, and in the (0001) plane.
(c) 000 *l*: *l* = 6*n* (Similarly for $P6_522$).
(d) $\frac{6}{m}mm$ P6_1 ...

$Pa\bar{3}$
(a) $m\bar{3}$; cubic.
(b) Primitive unit cell; *a*-glide plane ⊥ *b* (equivalent statements are *b*-glide plane ⊥ *c, c*-glide plane ⊥ *a*); three-fold axes || [111], $[1\bar{1}1]$, $[\bar{1}11]$, and $[\bar{1}\bar{1}1]$.
(c) 0*kl: k* = 2*n*; (equivalent statements are *h*0*l: l* = 2*n; hk*0: *h* = 2*n*.)
(d) $m\bar{3}\ Pa$.

2.14. Plane group *p*2; the unit cell repeat along *b* is halved, and γ has the particular value of 90°. Note that, because of the *contents* of the unit cell, it cannot belong to the rectangular two-dimensional system.

2.15. (a) Refer to Fig. 2.24, number 10, for a cubic *P* unit cell (vectors **a**, **b**, and **c**).
(b) Tetragonal *P*
$\mathbf{a}_P = \mathbf{b}/2 + \mathbf{c}/2$
$\mathbf{b}_P = -\mathbf{b}/2 + \mathbf{c}/2$
$\mathbf{c}_P = \mathbf{a}$
(c) Monoclinic *C*
$\mathbf{a}_C = \mathbf{c}$
$\mathbf{b}_C = -\mathbf{b}$
$\mathbf{c}_C = \mathbf{a}$
(d) Triclinic *P*
$\mathbf{a}_T = \mathbf{a}$
$\mathbf{b}_T = \mathbf{b}/2 + \mathbf{c}/2$
$\mathbf{c}_T = -\mathbf{b}/2 + \mathbf{c}/2$

2.16.

$$\underset{\bar{4}\ along\ z}{\begin{bmatrix} 0 & 1 & 0 \\ \bar{1} & 0 & 0 \\ 0 & 0 & \bar{1} \end{bmatrix}} \underset{m \perp b}{\begin{bmatrix} 1 & 0 & 0 \\ 0 & \bar{1} & 0 \\ 0 & 0 & 1 \end{bmatrix}}$$
$$\mathbf{R}_1 \qquad\qquad \mathbf{R}_2$$

$\mathbf{R_2R_1h} = \mathbf{h}'$. Forming first $\mathbf{R}_3 = \mathbf{R}_2\mathbf{R}_1$, remembering the order of multiplication, we then evaluate

$$\underset{\mathbf{R}_3}{\begin{bmatrix} 0 & 1 & 0 \\ 1 & 0 & 0 \\ 0 & 0 & \bar{1} \end{bmatrix}} \underset{\mathbf{h}}{\begin{bmatrix} h \\ k \\ l \end{bmatrix}} = \underset{\mathbf{h}'}{\begin{bmatrix} k \\ h \\ \bar{l} \end{bmatrix}}$$

that is, $\mathbf{R}_3\mathbf{h} = \mathbf{h}'$, so that $\mathbf{h}' = kh\bar{l}$; $\mathbf{R}_3$ represents a two-fold rotation axis along [110].

2.17. The matrices are multiplied in the usual way, and the components of the translation vectors are added, resulting in

$$\begin{bmatrix} \bar{1} & 0 & 0 \\ 0 & \bar{1} & 0 \\ 0 & 0 & 1 \end{bmatrix} + \begin{bmatrix} 1/2 \\ 1/2 \\ 1/2 \end{bmatrix}$$

which corresponds to a 2_1 axis along $[1/4,\ 1/4,\ z]$. The space group symbol is $Pna2_1$.

2.18. (a) We can see from the hexagonal stereograms (Fig. 1.32) that $\mathbf{2}\,\mathbf{3}^2 \equiv \mathbf{6}$. Hence the matrix for 6_3 about $[0, 0, z]$ is

$$\begin{bmatrix} 1 & \bar{1} & 0 \\ 1 & 0 & 1 \\ 0 & 0 & 1 \end{bmatrix} + \begin{bmatrix} 0 \\ 0 \\ 1/2 \end{bmatrix}$$

and that for the c- glide is

$$\begin{bmatrix} 0 & \bar{1} & 0 \\ \bar{1} & 0 & 0 \\ 0 & 0 & 1 \end{bmatrix} + \begin{bmatrix} 0 \\ 0 \\ 1/2 \end{bmatrix}$$

(b) Since the sum of the translation vectors of 6_3 and c is zero, the symbol $*$ represents an m plane; the point-group symbol is $6mm$ and the space-group symbol is $P6_3cm$.

(c) The matrix for the m plane in this space group is given by (remember to multiply the matrices and add the translation vectors)

$$\underset{6_3}{\begin{bmatrix} 0 & \bar{1} & 0 \\ \bar{1} & 0 & 0 \\ 0 & 0 & 1 \end{bmatrix}} + \begin{bmatrix} 0 \\ 0 \\ 1/2 \end{bmatrix} \quad \underset{c}{\begin{bmatrix} 1 & \bar{1} & 0 \\ 1 & 0 & 0 \\ 0 & 0 & 1 \end{bmatrix}} + \begin{bmatrix} 0 \\ 0 \\ 1/2 \end{bmatrix} = \underset{m}{\begin{bmatrix} \bar{1} & 0 & 0 \\ \bar{1} & 1 & 0 \\ 0 & 0 & 1 \end{bmatrix}} + \begin{bmatrix} 0 \\ 0 \\ 0 \end{bmatrix}$$

(d) Refer to Fig. S2.7; not all symmetry symbols are entirely standard (red = c glide; m = mirror plane). The general equivalent positions are:

$$12 \quad d \quad 1 \quad x,y,z;\, x-y,x,1/2+z;\, \bar{y},x-y,z;\ \bar{x},\bar{y},1/2+z;\, y-x,\bar{x},z;\, y,y-x,1/2+z;$$
$$\bar{y},\bar{x},1/2+z;\, \bar{x},y-x,z;\, y-x,y,1/2+z;\, y,x,z;\ x,x-y,1/2+z;\, x-y,\bar{y},z.$$

There are three sets of special equivalent positions:

$$6 \quad c \quad m \quad x,0,z;\, x,x,1/2+z;\, 0,x,z;\, \bar{x},0,1/2+z;\ \bar{x},\bar{x},z;\, 0,\bar{x},1/2+z$$
$$4 \quad b \quad 3 \quad 1/3,2/3,z;\, 2/3,1/3,z;\, 1/3,2/3,1/2+z;\, 2/3,1/3,1/2+z$$
$$2 \quad a \quad 3m \quad 0,0,z;\ 0,0,1/2+z$$

Wyckoff site	Limiting conditions	
d	$hkil$	none
	$hh2\bar{h}l$	none
	$h\bar{h}0l$	none
c	as above	
b	as above + $hkil$: $l = 2n$	
a	as for site b	

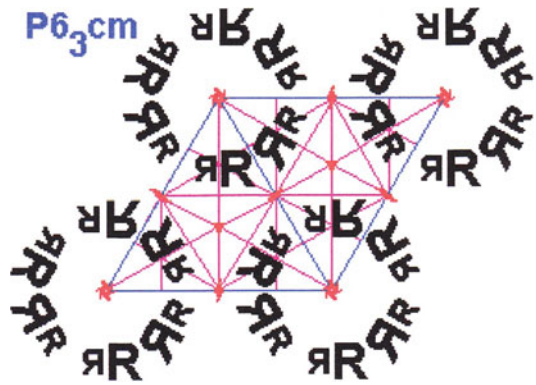

Fig. S2.7

[Courtesy Professor Steven Dutch, University of Wisconsin-Green Bay]

2.19. From Chap. 2, Fig. 2.11, it follows that

$$\mathbf{a}_R = 2\mathbf{a}_H/3 + \mathbf{b}_H/3 + \mathbf{c}_H/3$$
$$\mathbf{b}_R = -\mathbf{a}_H/3 + \mathbf{b}_H/3 + \mathbf{c}_H/3$$
$$\mathbf{c}_R = -\mathbf{a}_H/3 - 2\mathbf{b}_H/3 + \mathbf{c}_H/3$$

Following Sect. 2.2.3, we have $\mathbf{a}_R \cdot \mathbf{a}_R = (2\mathbf{a}_H/3 + \mathbf{b}_H/3 + \mathbf{c}_H/3)\cdot(2\mathbf{a}_H/3 + \mathbf{b}_H/3 + \mathbf{c}_H/3) = 3a^2/9 + c^2/9 = 12\,\text{Å}^2$, so that $a_R = 3.464$ Å. Similarly, $\cos\alpha_{\mathbf{R}} = (2\mathbf{a}_H/3 + \mathbf{b}_H/3 + \mathbf{c}_H/\mathbf{3})\cdot(-\mathbf{a}_H/3 + \mathbf{b}_H/3 + \mathbf{c}_H/\mathbf{3})/a_R^2$, so that $\alpha_{\mathrm{R}} = 51.32°$. (Remember that $a = b = c$ and $\alpha = \beta = \gamma$ in a rhombohedral unit cell.)

2.20. The transformation matrix S for $R_{\text{hex}} \rightarrow R_{\text{obv}}$ is given, from the solution to Problem 2.19, by

$$\mathbf{S} = \begin{bmatrix} 2/3 & 1/3 & 1/3 \\ -1/3 & 1/3 & 1/3 \\ -1/3 & -2/3 & 1/3 \end{bmatrix}$$

and its inverse is

$$\mathbf{S}^{-1} = \begin{bmatrix} 1 & \bar{1} & 0 \\ 0 & 1 & \bar{1} \\ 1 & 1 & 1 \end{bmatrix}$$

so that the transpose becomes

$$(\mathbf{S}^{-1})^T = \begin{bmatrix} 1 & 0 & 1 \\ \bar{1} & 1 & 1 \\ 0 & \bar{1} & 1 \end{bmatrix}$$

Hence $(13*4)_{\text{hex}}$ is transformed to $(32\bar{1})_{obv}$, and $[1\bar{2}*3]_{hex}$ to $[405]_{\text{obv}}$.

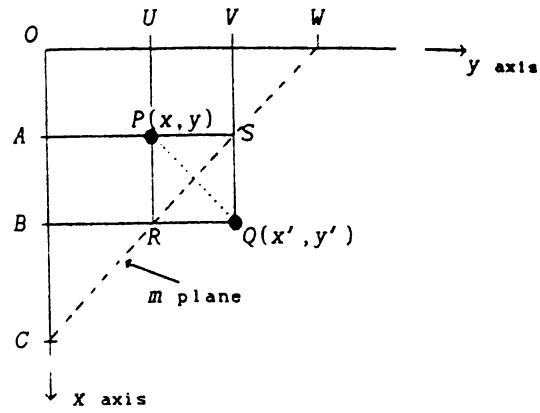

Fig. S2.8

2.21. Figure S2.8 illustrates the reflection of x, y, z across the plane (qqz), where $OC = OW = q$, so that $OCW = 45°$ Q is the point $q - x, q - y, z$, and the remainder of the diagram is self-explanatory.

As an alternative procedure, we know that in point group $4mm$, $4\mathbf{m}_y = \mathbf{m}_{diag}$. Hence, x, y is transformed to $\bar{y}, \bar{x}$ by the operation $\mathbf{m}_{diag}$. If we now move the origin to the point $-q, -q$, it follows that $\bar{y}, \bar{x}$ then becomes $q - y, q - x$.

2.22.

Diffraction symbol					Point group		
					2	m	$2/m$
$12/m1$	P	.	.	.	$P2$	Pm	$P2/m$
$12/m1$	P	.	c	.	Pc	$P2/c$	
$12/m1$	P	.	2_1	.	$P2_1$		$P2_1/m$
$12/m1$	P	.	$2_1/c$	.			$P2_1/c$
$12/m1$	C	.	.	.	$C2$	Cm	$C2/m$
$12/m1$	C	.	c	.		Cc	$C2/c$

2.23. (a) From the matrix $\begin{bmatrix} 1/2 & 0 & 0 \\ 0 & 1 & 0 \\ 0 & 0 & 1 \end{bmatrix}$, (210) becomes (110) and may be confirmed by drawing to scale.

(b) From the matrix $\begin{bmatrix} 1 & 0 & 0 \\ 0 & 1/2 & 0 \\ 0 & 0 & 1 \end{bmatrix}$, (210) becomes (410), after clearing the fraction.

By drawing to scale, we see that the original (210) plane is now the second plane from the origin in the (410) family of planes; $d(410)_{new} = d(210)_{old}/2$ under the given transformation. In each case, the Miller index corresponding to the unit cell halving is also halved.

2.24. In $Cmm2$, the polar (two-fold) axis is normal to the centered plane, but parallel to it in $Amm2$. $Cmmm$ and $Ammm$ are equivalent by interchange of axes, so that they are not two distinct arrangements of points.

2.25. (a) $a' = 4.850$, $b' = 6.150$, $c' = 7.963$ Å

(b) (12,12,7)

The following matrix may be helpful

$$(\mathbf{M}^{-1})^T = \begin{bmatrix} 1/2 & \overline{1/4} & 1/2 \\ 1/2 & 0 & \overline{1} \\ 0 & 1 & 2 \end{bmatrix}$$

(c) $[3\overline{3}8]$

(d) 0.09486, 0.008930, 0.3120 $Å^{-1}$

(e) $x' = -0.2192$, $y' = 0.6745$, $z' = -0.5645$

Solutions 3

3.1. $d\lambda/Å = 0.0243\ (1 - \cos 45) = 0.00712$. Energy/J $= hc/(1 + 0.00712) = 1.97 \times 10^{-15}$.

3.2. Set an origin at the center of a line joining the two scattering centers; then the coordinates are $\pm\lambda$. The amplitude of the separated points $A_\lambda = 2\ \cos(2\pi \times \lambda \times 2\lambda^{-1} \sin\theta \times \cos\theta) =$

$2\ \cos(2\pi \sin 2\theta)$, the angle between **r** and **S** being θ. For the two centers at one point ($r = 0$) the amplitude $A_p = 2$. Hence:

2θ	Ratio A_λ/A_p	Intensity
0	1	1
30, 150	−1	1
60, 120	0.666	0.444
90	1	1
180	1	1

3.3. We proved in the text that $f_{1s} = c_1^4/(c_1^4 + \pi^2 S^2)^2$, where c_1=(4−0.3)/0.529 = 6.994 Å^{-1} and $S = 2(\sin\theta)/\lambda$. For the 2s contribution, the integral $\int_0^\infty x^3 \exp(-ax)\sin bx\,dx$ evaluates to $4(a^3b - ab^3)/(a^2 + b^2)^4$, so that f_{2s}, becomes $[2\pi c_2^5/(96\pi S)] \times 3 \times 16\pi S c_2[c_2^2 - (2\pi S)^2]/[c_2 + 4\pi^2 S^2]^4 = c_2^6[c_2^2 - 4\pi^2 S^2)/(c_2^2 + 4\pi^2 S^2)^4$, where c_2 = (4 − 2.05)/0.529 = 3.685 Å^{-1}. Hence:

	Scattering formula			Exponential formula
$\sin\theta/\lambda Z$	f_{1s}	f_{2s}	$(2f_{1s} + 2f_{2s})$	f
0.0	1.000	1.000	4.000	4.002
0.2	0.938	0.116	2.108	2.060
0.5	0.692	−0.0082	1.368	1.360

3.4. Photon energy = $h\nu = hc/\lambda = hc/(hc/eV) = 1.6021 \times 10^{-19} \times 30000 = 4.806 \times 10^{-15}$ J.

3.5. $M_r(C_6H_6) = 78.11$. $M_r(C)/M_r(C_6H_6) = 0.154$; $M_r(H)/M_r(C_6H_6) = 0.0129$. Hence, $\mu = 1124\ [0.154 \times 0.46 \times 6) + (0.0129 \times 0.04 \times 6)] = 481.2\ m^{-1}$, so that the transmittance (I/I_0) is $\exp(-481.2 \times 1 \times 10^{-3}) = 0.618$, or 61.8 %.

3.6. It is necessary to note carefully the changes in sign of both $A(hkl)$ and $B(hkl)$. Thus, the following diagram is helpful, together with the changes in sign of the argument of the trigonometric functions. For example, if both A and B change sign, ϕ is not unaltered by canceling the signs, but becomes $\pi + \phi$

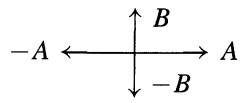

$$\sin(-\theta) = -\sin(\theta)$$
$$\cos(-\theta) = \cos(\theta)$$
$$\tan(-\theta) = -\tan(\theta)$$

$P2_1$: Use (3.80)–(3.83) for k even and k odd

$$k = 2n: \quad \phi(hkl) = -\phi(\bar{h}\,\bar{k}\,\bar{l}) = -\phi(h\,\bar{k}\,l) = \phi(\bar{h}\,k\,\bar{l}) \neq \phi(\bar{h}kl)$$
$$\phi(\bar{h}kl) = -\phi(h\,\bar{k}\,\bar{l}) = \phi(hk\bar{l}) = -\phi(\bar{h}\,\bar{k}\,l)$$
$$k = 2n+1: \quad \phi(hkl) = -\phi(\bar{h}\,\bar{k}\,\bar{l}) = \pi - \phi(h\bar{k}l) = \pi + \phi(\bar{h}\,k\,\bar{l}) \neq \phi(\bar{h}\,k\,l)$$
$$\phi(\bar{h}kl) = -\phi(h\,\bar{k}\,\bar{l}) = \pi + \phi(hk\,\bar{l}) = \pi - \phi(\bar{h}\,\bar{k}\,l)$$

*Pma*2: Use (3.94) and (3.95) for h even and odd

$$\begin{aligned} h \text{ even}: \quad & \phi(hkl) = -\phi(\bar{h}\,\bar{k}\,\bar{l}) = \phi(\bar{h}\,k\,l) = \phi(h\,\bar{k}\,l) = -\phi(h\,k\,\bar{l}) = -\phi(h\,\bar{k}\,\bar{l}) \\ & = -\phi(\bar{h}\,k\,\bar{l}) = \phi(\bar{h}\,\bar{k}\,l) \\ h \text{ odd}: \quad & \phi(hkl) = -\phi(\bar{h}\,\bar{k}\,\bar{l}) = \pi + \phi(\bar{h}\,k\,l) = \pi + \phi(h\,\bar{k}\,l) = -\phi(h\,k\,\bar{l}) \\ & = \pi - \phi(h\,\bar{k}\,\bar{l}) = \pi - \phi(\bar{h}\,k\,\bar{l}) = \phi(\bar{h}\,\bar{k}\,l) \end{aligned}$$

3.7. From the equations developed in Sects. 3.4 and 3.4.1, but taking the reciprocal space constant κ as the X-ray wavelength of 1.5418 Å, we find:
$a^* = 0.30314$, $b^* = 0.23115$, $c^* = 0.14096$, $\alpha^* = 60.182$, $\beta^* = 55.878$, $\gamma^* = 47.591°$. $V = 618.916$ Å^3; $V^* = 5.9218 \times 10^{-3}$. The reciprocal unit-cell lengths are dimensionless here, and V^* may be calculated as λ^3/V.

3.8. If $\mathbf{r}_1$ and $\mathbf{r}_2$ are the distances of the two atoms from the origin, then we use $\mathbf{r}_1 = x_1\mathbf{a} + y_1\mathbf{b} + z_1\mathbf{c}$ and $\mathbf{r}_2 = x_2\mathbf{a} + y_2\mathbf{b} + z_2\mathbf{c}$. Then $r_1 = (\mathbf{r}_1 \cdot \mathbf{r}_1)^{1/2}$ (not forgetting the cross-products), and similarly for r_2. The angle θ at the origin is given by $\cos\theta = \mathbf{r}_1 \cdot \mathbf{r}_2/(r_1\ r_2)$. Thus, the two distances are 2.986 and 4.310 Å, and $\theta = 45.58°$.

3.9. The resultant $\mathbf{R}$ is obtained in terms of the amplitude $|R|$ and phase ϕ from $|R| = [(\Sigma_j A\cos\phi_j)^2 + (\Sigma_j B\sin\phi_j)^2]^{1/2} = [(-21.763)^2 + (-22.070)^2]^{1/2} = 31.00$, and $\phi = \tan^{-1}[(-22.070)/(-21.763)] = 45.40°$, but because both the numerator and denominator are negative the phase angle lies in the third quadrant, and 180° must be added to give $\phi = 225.40°$.

3.10. A-centering implies pairs of positions x, y, z and $x, \frac{1}{2}+y, \frac{1}{2}+z$. Hence, we write

$$F(hkl) = \sum_{j=1}^{n/2} f_j\{\exp[\mathrm{i}2\pi(hx_j + ky_j + lz_j)] + \exp[\mathrm{i}2\pi(hx_j + ky_j + lz_j + k/2 + l/2)]\}$$

The terms within the braces { } may be expressed as $\exp[\mathrm{i}2\pi(hx_j + ky_j + lz_j)]\{1 + \exp[\mathrm{i}2\pi(k/2 + l/2)]\}$ which is 2 for $(k + l)$ even, and zero for $(k + l)$ odd ($\mathrm{e}^{\mathrm{i}n\pi} = 1/0$ for n even/odd). Hence, the limiting condition is *hkl:* $k + l = 2n$.

3.11. The coordinates show that the structure is centrosymmetric. Hence, $F(hk0) = A(hk0) = 2[g_P\cos 2\pi(hx_P + ky_P) + g_Q\cos 2\pi(hx_Q + ky_Q)]$

hk	*A*(*hk*)	*hk*	*A*(*hk*)	*hk*	*A*(*hk*)	*hk*	*A*(*hk*)
5 0	$2(-g_P + g_Q)$	0 5	$2(g_P - g_Q)$	5 5	$2(-g_P - g_Q)$	5 10	$2(-g_P + g_Q)$

For $g_P = 2g_Q$, ϕ (0 5) = 0, ϕ (5 0) = ϕ (5 5) = ϕ (5 10) = π.

3.12. $F(hk0) = 4g_U\cos 2\pi[ky_U + (h + k)/4]\cos 2\pi(h + k)/4$ which, because $(h + k)$ is even in the data, reduces to $F(hk0) = 4g_U\cos 2\pi\, ky_U$.

*hk*0	$\lvert F(hk0)_{y=0.10}\rvert$	$\lvert F(hk0)_{y=0.15}\rvert$
020	86.5	86.5
110	258.9	188.1

Hence, 0.10 is the better value for y_U in terms of the two reflections given.

3.13. The shortest U–U distance d_{U-U} is from 0, y, $\frac{1}{4}$ *to* 0, $\bar{y}$, $\frac{3}{4}$, so that $d_{U-U} = [(0.20b)^2 + (0.5\ c)^2]^{1/2} = 2.76$ Å.

3.14. (a) $P2_1$, $P2_1/m$; (b) *Pa, P*2/*a*; (c) *Cc, C*2/*c*; (d) *P*2, *Pm, P*2/*m*.

3.15. (a) $P2_12_12$; (b) *Pbm*2, *Pbmm*; (c) *Ibm*2, *Ibmm*. Note that *Ibm*2, for example, might have been named $Icm2_1$: normally, where more than one symmetry element lies in a given orientation, the rules of precedence in naming is $m > a > b > c > n > d$ and $2 > 2_1$. In a few cases the rules may be ignored. For example, *I*4*cm* could be named *I*4*bm*, but with the origin on 4, the *c*-glides pass through the origin, and the former symbol is preferred.

Writing example (c) with the redundancies indicated, we have

hkl: $h + k + l = 2n$
0*kl*: $k = 2n$, $(l = 2n)$ or $l = 2n$, $(k = 2n)$
*h*0*l*: $(h + l = 2n)$
*hk*0: $(h + k = 2n)$
*h*00: $(h = 2n)$
0*k*0: $(k = 2n)$
00*l*: $(l = 2n)$

3.16. (a)

(i) *h*0*l*: $h = 2n$; 0*k*0: $k = 2n$.
(ii) *h*0*l*: $l = 2n$
(iii) *hkl*: $h + k = 2n$
(iv) *h*00: $h = 2n$
(v) 0*kl*: $l = 2n$; *h*0*l* : $l = 2n$
(vi) *hkl* : $h + k + l = 2n$; *h*0*l*: $h = 2n$

Other space groups with the same conditions: (i) None; (ii) *P*2/*c*; (iii) *C*2, *C*2/*m*; (iv) None; (v) *Pccm*; (vi) *Ima*2 (*I*2*am*)

(b) *hkl*: None
*h*0*l*: $h + l = 2n$
0*k*0: $k = 2n$

(c) *C*2/*c*; *C*222

3.17. (a) In the given setting x' and **a** are normal to a *c*-glide, y' and $\bar{\mathbf{c}}$ are normal to an *a*-glide, and z' and **b** are normal to a *b*-glide. In the standard setting, x is along x' and the plane normal to has its glide in the new y direction, so that it is a *b*-glide; y is along z' and the plane normal to it is a glide now in the direction of z, a *c* glide; z is along $-y'$ and the plane normal to it is now an *a*-glide. Thus, the symbol in the standard setting is *Pbca*.

(b) In *Pmna* the symmetry leads to translations of $(c + a)/2$ and $a/2$, overall $c/2$, and in *Pnma* the translations arising are $a/2$, $b/2$, and $c/2$. Hence, the full symbol for *Pmna* is $P\frac{2}{m}\frac{2}{n}\frac{2_1}{a}$, whereas that for *Pnma* is $P\frac{2_1}{n}\frac{2_1}{m}\frac{2_1}{a}$.

3.18. $\mu R = 2.00$, so that $A = 10.0$. Hence, $|\mathrm{F}(hkl)|^2 = I \times Lp^{-1} \times A = 56.3 \times 0.625 \times 1.1547 \times 10.0 = 406.3$.

3.19. (*a*) C_{6h} (*b*) $\frac{6}{m}11$; $P\frac{6_3}{m}11$ (c) Hexagonal/Trigonal (d) Hexagonal (e) Hexagonal (f) *P*.

3.20. In this example, we need the *A* and *B* terms of the geometrical structure factor. From the coordinates of the general equivalent position, we have

$$
\begin{aligned}
A = {} & \cos 2\pi(hx + ky + lz) + \cos 2\pi(-hx - ky + lz) + \cos 2\pi(-hy + kx + lz) + \cos 2\pi(hy - kx + lz) \\
& + \cos 2\pi\left(hx - ky + lz + \frac{h+k+l}{2}\right) + \cos 2\pi\left(-hx + ky + lz + \frac{h+k+l}{2}\right) \\
& + \cos 2\pi\left(hy + kx + lz + \frac{h+k+l}{2}\right) + \cos 2\pi\left(-hy - kx + lz + \frac{h+k+l}{2}\right)
\end{aligned}
$$

Combining the terms appropriately:

$$A/2 = \cos 2\pi lz\{\cos 2\pi(hx + ky) + \cos 2\pi(-hy + kx)\} + \cos 2\pi\left(lz + \frac{h+k+l}{2}\right)\cos 2\pi(hx - ky) + \cos 2\pi\left(lz + \frac{h+k+l}{2}\right)\cos 2\pi(hy + kx)$$

The expansion of $\cos 2\pi\left(lz + \frac{h+k+l}{2}\right)$ shows that we need to consider the cases of $h + k + l$ even and odd, and recalling that $\cos P \pm \cos Q = \cos P \cos Q \mp \sin P \sin Q$, we find the following:

$\underline{h + k + l = 2n}$

$$A = 4\cos 2\pi lz(\cos 2\pi hx \cos 2\pi ky - \sin 2\pi hy \sin 2\pi kx)$$

Similarly

$$B = 4\sin 2\pi lz(\cos 2\pi hx \cos 2\pi ky - \sin 2\pi hy \sin 2\pi kx)$$

From the equations for $|F(hkl)|$ and $\phi(hkl)$, we find $\underline{h + k + l = 2n + 1}$.
Proceeding in a similar manner, we now find

$$A = 4\cos 2\pi lz(-\sin 2\pi hx \sin 2\pi ky + \sin 2\pi hy \sin 2\pi kx)$$

and

$$B = -4\sin 2\pi lz(-\sin 2\pi hx \sin 2\pi ky + \sin 2\pi hy \sin 2\pi kx)$$

It is clear now that for $h + k + l$ odd, $A = B = 0$ if $h = 0$, or $k = 0$, or $h = \pm k$. Hence, the limiting conditions: $0kl$: $k + l = 2n$[12] ($h0l$: $h + l = 2n$), and hhl: $l = 2n$. The first of these conditions corresponds to an n-glide $\perp a$, (b) while the second indicates a c-glide $\perp$<110>, consistent with space group $P4nc$.

Solutions 4

4.1. For the given reflection, $(\sin\theta)/\lambda = 0.30$, for which $f_C = 2.494$. Hence, $\exp[-B(\sin^2\theta)/\lambda^2] = 0.5423$, so that $f_{C,27.55^\circ} = 1.352$, which is 54.2 % of what its value would be at rest. The root mean square displacement is $[6.8/(8\pi^2)]^{1/2} = 0.29$ Å. Since vibrational energy is proportional to kT, where k is the Boltzmann constant, a reduced temperature factor with concomitant enhanced scattering would be achieved by conducting the experiment at a low temperature.

4.2. For NaCl, $d_{111} = a/\sqrt{3} = 2.2487$ Å, so that $(\sin\theta_{111})/\lambda = 0.1539$ Å^{-1} and $(\sin\theta_{222})/\lambda = 0.3078$ Å^{-1}. Similarly, for KCl, $(\sin\theta_{111})/\lambda = 0.1379$ Å^{-1} and $(\sin\theta_{222})/\lambda = 0.1379$ Å^{-1}.

[12] [$h + k + l = 2n + 1 \rightarrow k + l = 2n + 1$ for $h = 0$].

Using the structure factor equation for the NaCl structure type, we have $F(111) = 4[f_{Na^+/K^+} + f_{Cl^-}\cos(3\pi)] = 4[f_{Na^+/K^+} - f_{Cl^-}]$, whereas $F(222) = 4[f_{Na^+/K^+} + f_{Cl^-}]$. Thus, we obtain the following results:

	111		222	
	NaCl	KCl	NaCl	KCl
(sin θ)/λ	0.1539	0.1379	0.3078	0.2759
f_+	8.979	15.652	6.777	11.576
f_-	13.593	14.207	9.387	9.997
F	−18.46	1.445	64.66	86.29

Remembering that we measure $|F|^2$, it is clear that |F(111)| for KCl is relatively vanishingly small.

4.3. $\overline{F} = (2/\pi\Sigma)^{1/2}\int_0^\infty F\exp(-F^2/2\Sigma)\mathrm{d}F$. Let $F^2/2\Sigma = t$, so that $\mathrm{d}F = (\Sigma/2t)^{1/2}\mathrm{d}t$. Then, $\overline{F} = (2\Sigma/\pi)^{1/2}\int_0^\infty t^0\exp(-t)\mathrm{d}t$. Since $t^0 = t^{(1-1)}$, the integral (see Web Appendix WA7) is Γ(1) = 1, Hence, $\overline{F} = (2\Sigma/\pi)^{1/2}$.

Making the above substitution again, we have $\overline{F^2} = (2\Sigma/\pi)^{1/2}\int_0^\infty t^{1/2}\exp(-t)dt = (2\Sigma/\pi^{1/2})$ $^1/_2\,\Gamma(^1/_2) = \Sigma$.

Thus, $M_c = (2\Sigma/\pi)/\Sigma = 2/\pi = 0.637$.

4.4. $\overline{E^3} = (2/\pi)^{1/2}\int_0^\infty E^3\exp(-E^2/2)\mathrm{d}E$. *Let* $E^2/2 = t$, so that $\mathrm{d}E = (2t)^{-1/2}\mathrm{d}t$. Then, $\overline{E^3} = (8/\pi)^{1/2}\int_0^\infty t\exp(-t)\,\mathrm{d}t = (8/\pi)\,\frac{1}{2}\Gamma(2) = 1.596$.

4.5.

$$\overline{|E^2-1|} = 2\int_0^\infty |E^2-1|\,E\exp(-E^2)\,\mathrm{d}E$$

By making the substitution $E^2 = t$, we have

$$\begin{aligned}\overline{|E^2-1|} &= \int_0^1 (1-t)\exp(-t)\,\mathrm{d}t + \int_1^\infty (t-1)\exp(-t)\mathrm{d}t\\ &= (-e^{-t}|_0^1 + (te^{-t}|_0^1 + (e^{-t}|_0^1 - (te^{-t}|_1^\infty - (e^{-t}|_1^\infty + (e^{-t}|_1^\infty\\ &= 2/e = 0.736\end{aligned}$$

4.6. The statistically distinguishable features of classes 2, *m* and 2/*m* are summarized as follows:

	*P*2	*Pm*	*P*2/*m*
hkl	1A	1A	1C
*h*0*l*	1C	2A	2C
0*k*0	2A	1C	2C

When finding the average intensities, do not mix the *h*0*l* and 0*k*0 reflections either with themselves or with the *hkl* reflections until the space-group ambiguity has been resolved. Instead get them from some other zone, excluding any terms it contains that lie in [*h*0*l*] or [0*k*0] zones, and check the distribution of this chosen zone. If it is centric, the space group is *P*2/*m*. To distinguish between the other two space group, examine the distribution in the [*h*0*l*] zone. Generally there will be insufficient 0*k*0 reflections alone to give reliable results.

4.7. (a) *mmmPc* - - leaves the following space groups unresolved:

$Pcm2_1$	2/2; 2/2; 4(1)
*Pc*2*m*	2/2; 4/(1); 2/2
Pcmm	(4/2; 4/2; 4/2)

The numbers are the multiples for the principal rows and zones (see Table 4.2). Parentheses indicate centric zones or the complete weighted reciprocal lattice. One would examine the distribution in both the [$h0l$] and [$0k0$] zones. Alternatively, an examination of the [$0k0$] zone, excluding the $h0l$ and $0k0$ data, could be considered. A centric distribution would identify $Pccm$. The other two could be separated by reference to zones, but distinction may be difficult at this stage.

(b) *mmmC* - - - leaves the following space groups unresolved:

$Cmm2$	2/2; 2/2; 4(1)
$Cm2m$	2/2; 4/(1); 2/2
$C222$	2/(1); 2/(1) 2/(1)
$Cmmm$	(4/2; 4/2; 4/2)

Again, parentheses indicate centric zones or the complete weighted reciprocal lattice. All principal zones must be examined in order to resolve the ambiguities here.

Solutions 5

5.1. (a) The crystal system is tetragonal, and the Laue group is $\frac{4}{m}mm$; the optic axis lies along the needle axis (z) of the crystal.
(b) The section is in extinction for any rotation in the x,y plane, normal to the needle axis; the section is optically isotropic.
(c) For a general oscillation photograph with the X-ray beam normal to z, the symmetry is m. For a symmetrical oscillation photograph with the beam along a, b or any direction in the form $\langle 110 \rangle$ at the mid-point of the oscillation, the symmetry is $2mm$.

5.2. (a) The crystal system is orthorhombic.
(b) Suitable axes may be taken parallel to three non-coplanar edges of the brick.
(c) Symmetry m.
(d) Symmetry $2mm$, with the m lines horizontal and vertical.

5.3. (a) Monoclinic, or possibly orthorhombic.
(b) If monoclinic, p is parallel to the y axis. If orthorhombic, p is parallel to one of x, y, or z.
(c) (i) Mount the crystal perpendicular to p, about either q or r, and take a Laue photograph with the X-ray beam parallel to p. If the crystal is monoclinic, symmetry 2 would be observed. If orthorhombic, the symmetry would be $2mm$, with the m lines in positions on the film that define the directions of the crystallographic axes normal to p. If the crystal is rotated such that the X-rays travel through the crystal perpendicular to p, a vertical m line would appear on the Laue photograph of either a monoclinic or an orthorhombic crystal. (ii) Use the same crystal mounting as in (i), but take a symmetrical oscillation photograph with the X-ray beam parallel or perpendicular to p at the mid-point of the oscillation. The rest of the answer is as in (i).

5.4. Refer to Fig. S5.1. Let $h_{\max}$ represent the maximum value sought. Since we are concerned with a large d^* value, we take $\lambda \approx 0.2$ Å, the minimum value in the white radiation. Now $d^* = ha^* = (2/\lambda) \sin \theta$ and since, from the diagram, θ is the angle subtended at the circumference by d^*, $\theta = 20°$, so that $h_{\max}$ is the integral part of $2/(0.2\lambda) \sin 20$, which is 17. The X-coordinate on the film is 60 tan 40 = 50.35 mm. The half-width of the film is 62.5 mm, so the 17,00 reflection will be recorded on the film.

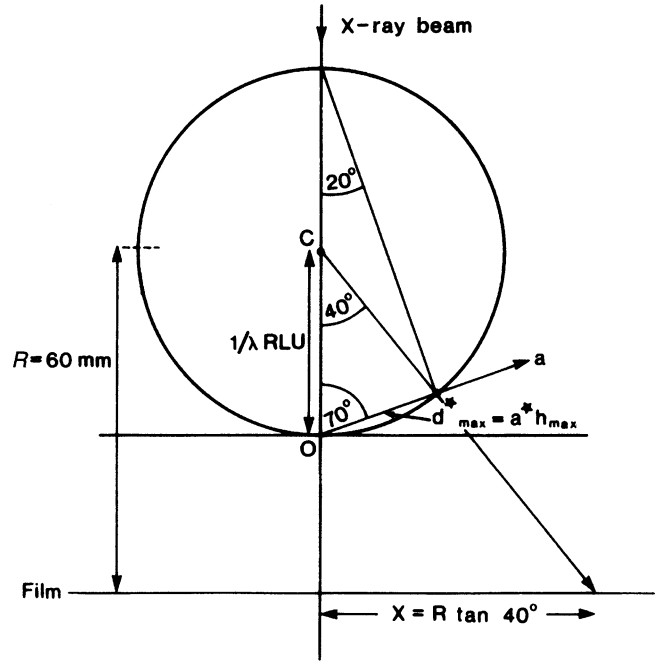

Fig. S5.1

5.5. For the first film, we can write $I(hkl) + I(2h, 2k, 2l) = 300$, and for the second film, after absorption, we have $0.35I(hkl) + 0.65I(2h, 2k, 2l) = 130$. Solving these equations gives $I(hkl) = 216.7$ and $I(2h, 2k, 2l) = 83.3$.

5.6. (a) For symmetry $2mm$ in Laue group $m\bar{3}m$, the X-ray beam must be traveling along a <110> direction (Table 1.6); we will choose [110], so that a and b lie in the horizontal plane; c is then the vertical direction.

(b) We can use Fig. 5.17, changing the sign of $-a^*$, and with $\phi = 45°$ because XO is [110] for the present problem. For an inner spot, it follows readily that $2\theta = \tan^{-1}(43.5/60.0)$, so that $2\theta = 35.94°$, and $\varepsilon = 27.03°$ (Chap. 5, Fig. 5.17).

(c) Now, $\tan 27.03 = 0.5102 = h/k$, since $a = b$. In the given orientation, the reflections on the horizontal line are $hk0$ and, since the unit cell is F, h and k must be both even, with $k = 2h$, from above. Possible reflections are, therefore, 240, 480, 612,0, . . . It is straightforward to show that $\lambda = 2a \sin \theta/\sqrt{N}$, where $N = h^2 + k^2$.

For 240, $\lambda = 0.746$ Å, for 480, $\lambda = 0.373$ Å, which is unreasonably small in crystallographic work. We note from the orientation of the a and b axes (a^* and b^*) that one of h and k must be negative; we can choose k. For an outer spot, we find in a similar manner that $\tan \varepsilon = 0.3418$, so that $k = 3h$. Reasonable indices correspond to $h = 2$ and $k = 6$, again with one index negative; here, $\lambda = 0.753$ Å. To summarize:

The X-ray beam is along [110]. For the inner spots: $\theta = 17.97°$; $2\bar{4}0$ and $4\bar{2}0$; $\lambda = 0.746$ Å. For the outer spots: $\theta = 26.13°$; $2\bar{6}0$ and $6\bar{2}0$; $\lambda = 0.753$ Å.

5.7. Since the crystal is uniaxial, it must be hexagonal, tetragonal, or trigonal. The Laue symmetry along axis 1 indicates that the crystal is trigonal, referred to hexagonal axes, and that axis 1 is therefore c. Following Chap. 5, Sect. 5.4.3, we find for the repeat distances along the three axes:

Axis	1	2	3
Repeat/Å	15.65	8.264	4.772

The smallest repeat distance corresponds to the unit-cell dimension a, direction $[10\bar{1}0]$, Laue symmetry 2 (Chap. 1, Fig. 1.36 and Table 1.6). Axis 2 must be a direction in the x, y plane, and it is straightforward to show that it is the repeat distance along $[12\bar{3}0]$, Laue symmetry m. Thus, we have: $a = b = 4.772$, $c = 15.65$ Å; $\alpha = \beta = 90°$, $\gamma = 120°$; the Laue group is $\bar{3}m$.

5.8. Applying the Bragg equation, $\lambda = 2d \sin\theta$, where $d = 6.696/2$ Å. Thus, (a) θ_{0002} (Cu) = 13.31°, and (b) θ_{0002} (Mo) = 6.093°.

5.9. (a) The data indicate a pseudo-monoclinic unit cell with γ unique. Following Chap. 2, Sect. 2.5, we find $a = b = 6.418$, $c = 3.863$ Å. It would appear that the c dimension is true, and that the ab plane is centered. It is straightforward to show that a and b are the half-diagonals of a rectangle with sides $\mathbf{a}' = \mathbf{a} - \mathbf{b}$ and $\mathbf{b}' = \mathbf{a} + \mathbf{b}$. Thus, the orthorhombic unit cell has the dimensions $a = 3.062$, $b = 12.465$, and $c = 3.863$ Å. The transformation can be written as $\mathbf{a}_{\text{true}} = \mathbf{M}\mathbf{a}_{\text{diff}}$, where

$$\mathbf{M} = \begin{bmatrix} 1 & -1 & 0 \\ 1 & 1 & 0 \\ 0 & 0 & 1 \end{bmatrix}$$

(b) The reciprocal cell is transformed according to $\mathbf{a}^*_{\text{true}} = (\mathbf{M}^{-1})^{\text{T}}\mathbf{a}^*_{\text{diff}}$. The transpose of the inverse matrix is

$$\begin{bmatrix} 1/2 & -1/2 & 0 \\ 1/2 & 1/2 & 0 \\ 0 & 0 & 1 \end{bmatrix}$$

Hence, $a^* = 0.2321$, $b^* = 0.05702$, $c^* = 0.1840$. These values may be confirmed by dividing the "true" values, for the orthorhombic cell, into the wavelength.

5.10. (a) Refer to Sect. 5.2.4: $\tan 2\theta_{\max} = r/R$, where r is the radius of the plate, 172.5 mm. $2d_{\min} \sin\theta_{\max} = 1.05/\quad(2 \times 1.0) = 0.525$, and $\theta_{\max} = 63.336°$. Hence, $R = 172.5/\tan 63.336$, or 86.6 mm.

(b) The whole image would shrink but would still contain the same amount of data, and the spots would become closer together.

(c) Some of the pattern would be lost because the angle subtended at the edge of the plate would become less: the spots would then be further apart.

5.11. (a) A 5, B 1, C 0.1 mm

(b) A 450, B 250, C 80 mm

(c) A 12, B 60, C 300 s

Solutions 6

6.1. $\int_{-c/2}^{c/2} \sin(2\pi m x/c)\cos(2\pi n x/c)\mathrm{d}x = \int_{-c/2}^{c/2} \{\frac{1}{2}\sin[2\pi(m+n)x/c] + \frac{1}{2}\sin[2\pi(m-n)x/c]\}\mathrm{d}x$ using identities from Web Appendix WA5. Integration leads to $-[c/2\pi(m+n)]\cos[2\pi(m+n)x/c]\ |_{-c/2}^{c/2} - [c/2\pi(m-n)]\ \cos[2\pi(m-n)x/c]|_{-c/2}^{c/2}$. Since m and n are integers the integral is zero for $m \neq n$. For $m = n$, the original integral becomes $\int_{-c/2}^{c/2} \frac{1}{2}\sin(4\pi m x/c)\,\mathrm{d}x$, which is also zero.

6.2. A plot of $\rho(x)$ as a function of x (in 40ths) shows peaks at 0, 20, and 40 for Mg (as expected), and at *ca* 8.25, 11.75, 28.25, and 31.75, for the 4F atoms per repeat unit a; thus, x_F is $\pm(0.206; 0.706)$. Only the function to $a/4$ need be calculated, since there is m symmetry across the points $\frac{1}{4}(10/40)$, $\frac{1}{2}(20/40)$ and $\frac{3}{4}(30/40)$.

(a) The first three terms alone are insufficient to resolve clearly the pairs of fluorine peaks that are closest in projection.

(b) Changing the sign of the 600 reflection results in single peaks for fluorine at 10/40 and 30/40. The error in sign (phase) is clearly the more serious fault.

6.3. $G(S) = \int_{-p}^{p} a \exp\,(\mathrm{i}2\pi Sx)\,\mathrm{d}x = a\int_{-p}^{p}\cos\,(2\pi Sx) + \mathrm{i}a\int_{-p}^{p}\sin(2\pi Sx)\,\mathrm{d}x$. The second integral is zero, because the integrand is an odd function. Hence,

$$G(S) = a\,(2\pi\,S)\,\sin(2\pi Sx)|_{-p}^{p} = 2ap\,\sin(2\pi Sp)/2\pi Sp)$$

and we retain the parameters which would obviously cancel, so as to preserve the characteristic sin $(ax)/(ax)$ form. To obtain the original function, we evaluate

$$f(x) = (a/\pi)\int_{-\infty}^{\infty}(1/S)\sin(2\pi Sp)\exp(-\mathrm{i}2\pi xS)\,\mathrm{d}S = (a/\pi)\int_{-\infty}^{\infty}(1/S)\sin(2\pi Sp)\cos(2\pi xS)\,\mathrm{d}S$$

where the sine term from the expanded integrand is zero as before. Using results from Web Appendix WA5, the integral becomes

$$(a/2\pi)\left\{\int_{-\infty}^{\infty}(1/S)\sin(2\pi S(p+x)]\,\mathrm{d}S + \int_{-\infty}^{\infty}(1/S)\sin(2\pi S(p-x)]\right\}\mathrm{d}S$$
$$a(p-x)\int_{-\infty}^{\infty}\sin[2\pi S(p-x)]/[2\pi(p-x)]\,\mathrm{d}S.$$

From Web Appendix WA9, $\int_{-\infty}^{\infty}(\sin y/y)\,\mathrm{d}y = \pi$; hence, we derive

$$f(x) = (a/2)(p+x)/|p+x| + (a/2)(p-x)/|p-x|.$$

It is clear from this result that $f(x) = a$ for $|\,x\,| < p$, $f(x) = a/2$ for $x = \pm p$, and $f(x) = 0$ for $|\,x\,| = 0$, which correspond to the starting conditions.

6.4.

$$\begin{aligned} G(f) &= A\int_{-\infty}^{\infty}\cos(2\pi f_0 t)\exp(-\mathrm{i}2\pi ft)\,\mathrm{d}t \\ &= (A/2)\int_{-\infty}^{\infty}\{[\exp(\mathrm{i}2\pi f_0 t) + \exp(-\mathrm{i}2\pi ft)]\exp(-\mathrm{i}2\pi ft)\}\,\mathrm{d}t \\ &= (A/2)\int_{-\infty}^{\infty}\{\exp[-\mathrm{i}2\pi(f-f_0)t] + \exp[-\mathrm{i}2\pi(f+f_0)t]\}\,\mathrm{d}t \\ &= (A/2)\delta(f+f_0) + (A/2)\delta(f-f_0). \end{aligned}$$

In the inversion, the δ-function repeats the function at $f = f_0$. Thus,

$$\begin{aligned} f(t) &= (A/2)\int_{-\infty}^{\infty}[\delta(f+f_0) + \delta(f-f_0)]\exp(\mathrm{i}2\pi ft)\,\mathrm{d}f = (A/2)[\exp(\mathrm{i}2\pi f_0 t) + \exp(-\mathrm{i}2\pi f_0 t)] \\ &= A\cos(2\pi f_0 t). \end{aligned}$$

6.5. The molecules have the displacements $\mathbf{p}$ and $-\mathbf{p}$ from the origin. Hence, the total transform $G_T(\mathbf{S})$ is given by

$$G_T(\mathbf{S}) = G_0(\mathbf{S})\exp(i2\pi\,\mathbf{p}\cdot\mathbf{S}) + G_0^*(\mathbf{S})\exp(-i2\pi\,\mathbf{p}\cdot\mathbf{S})$$

Using results from Sect. 3.2.3, we can write $G_0(\mathbf{S}) = |G_0|\exp(i\phi)$, and $G_0^*(\mathbf{S}) = |\mathbf{G_0}|\exp(-\phi)$, where ϕ is a phase angle. Hence,

$$G_T(\mathbf{S}) = |G_0|\{\exp(i2\pi\mathbf{p}\cdot\mathbf{S}+\phi) + \exp(-i2\pi\mathbf{p}\cdot\mathbf{S}-\phi) = 2|G_0|\cos(2\pi\mathbf{p}\cdot\mathbf{S}+\phi)$$

As discussed in Sect. 6.6.3, the maximum value of the transform is $2|G_0|$, at those points where $\cos(2\pi\mathbf{p}\cdot\mathbf{S} + \phi)$ is equal to unity. In this example, however, such points do not lie in planes and, consequently, the fringe systems are curved rather than planar.

6.6. The atoms related by the screw axis would have the fractional coordinates x, y, z and $\bar{x}, \frac{1}{2}+y, \frac{1}{2}-z$. From (6.50), we have

$$G(\mathbf{S}) = \sum_{j=1}^{n/2} f_j\{\exp[i2\pi(hx_j + ky_j + lz_j)] + \exp[i2\pi(-hx_j + ky_j - lz_j + k/2 + l/2)]\}$$

where the summation is over $n/2$ atoms in the unit cell not related by the 2_1 symmetry. Hence,

$$G(\mathbf{S}) = \sum_{j=1}^{n/2} f_j\{\exp[i2\pi ky_j\{\exp[i2\pi(hx_j + lz_j) + \exp[i2\pi(-hx_j - lz_j + k/2 + l/2)]\}$$

In a general transform, h, k, and l could take any values. However, in a crystal they are integers, but in order to obtain a special condition, we must also consider the case that $h = l = 0$:

$$G(\mathbf{S})_{h=l=0} = 2\sum_{j=1}^{n/2} f_j\exp(i2\pi ky_j[\exp(i\pi k)])$$

Then, we have $G(S)_{h=l=0} = 0$ for $k = 2n + 1$, that is, the $0k0$ reflections are systematically absent when k is odd.

6.7. Figure S6.1 indicates the nodal lines for the P–S fringe system. Since the transform is chosen to be positive at the origin, $\pm$ regions can be allocated to the transform, as shown. Hence, the intense reflections can be allocated signs, as follow:

240−	250−	410 −	520 −
650+	710+	720 +	820 +
$\bar{1}30$ +	$\bar{1}40$ +	$\bar{2}30$ +	$\bar{2}40$ +
$\bar{3}70$ +	$\bar{4}40$ −	$\bar{4}70$ +	$\bar{5}30$ −
$\bar{5}40$ −	$\bar{6}70$ −	$\bar{7}10$ −	$\bar{7}60$ −
$\bar{9}10$ +	$\bar{9}20$ +	$\overline{10}, 00$ +	$\overline{10}, 10$ +
$\overline{10}, 20$ +			

6.8. In Fig. S6.2, the three points are plotted in (a). A transparency is made of the structure in (a), inverted in the origin. The structure (a) is then drawn three times on the transparency, with each of the atoms of the inversion, in turn, over the origin of (a), and in the same orientation. The completed diagram (b) is the required convolution: the six triangles outlined in (b) all produce the same set of nine vectors (three superimposed at the origin).

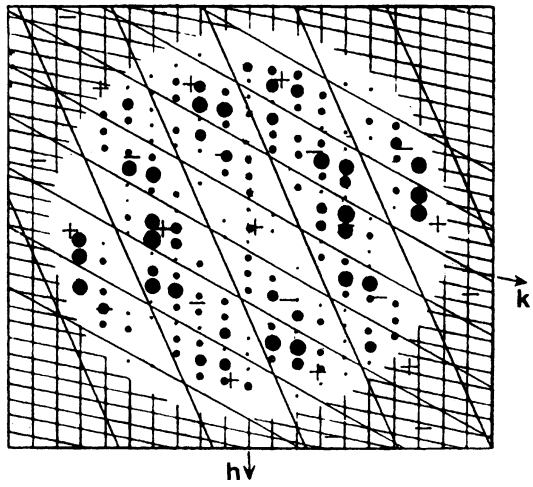

Fig. S6.1

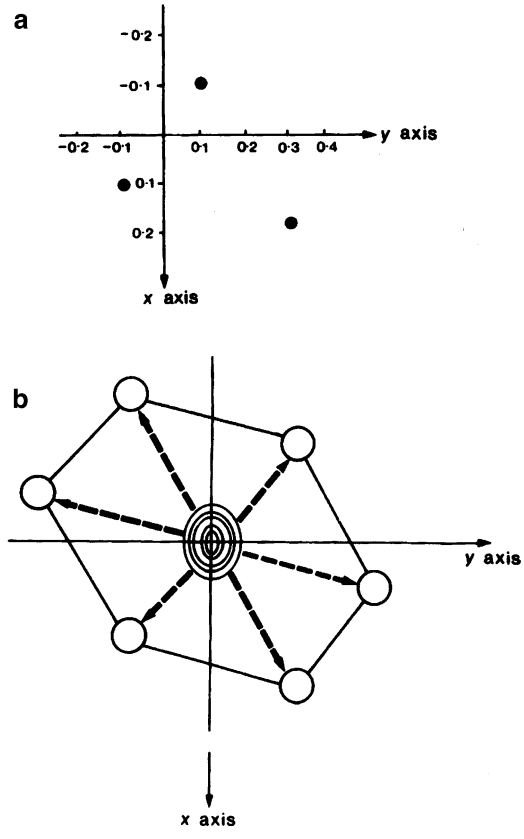

Fig. S6.2

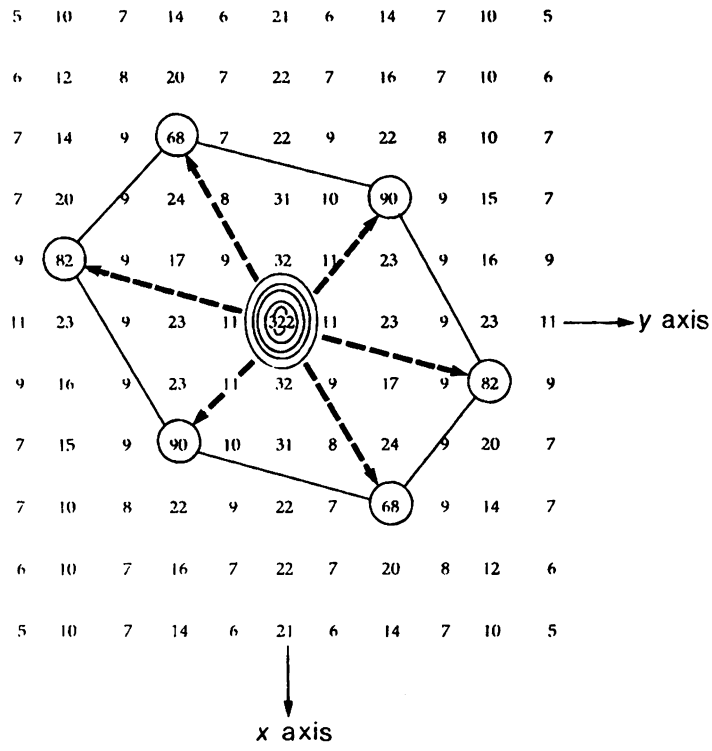

Fig. S6.3

6.9. Figure S6.3 shows the contoured figure field of Fig. S6.2. The same triangles are revealed, giving six sets of atom coordinates, as follow:

1	0.15, 0.10	−0.15,−0.10	−0.05, 0.30
2	0.05, 0.20	−0.05,−0.20	−0.20,−0.20
3	0.10,−0.10	−0.10, 0.10	−0.20,−0.30
4	0.05,−0.30	0.15, 0.10	−0.15,−0.10
5	0.25, 0.00	0.05, 0.20	−0.05,−0.20
6	0.10,−0.10	−0.10, 0.10	0.20, 0.30

6.10. The transform is positive in sign at the origin. Hence, by noting the succession of contours along the 00*l* row, we arrive at the following result:

001	002	003	004	005	006
+	−	+	+	−	−

6.11. The transform of $f(x)$ is given by

$$f_{\mathrm{T}}(x) = \frac{1}{\sqrt{2\pi}} \int_{-\infty}^{\infty} [\exp(-x^2/2) \exp(\mathrm{i}2\pi Sx)]\mathrm{d}x = \frac{2}{\sqrt{2\pi}} \int_{0}^{\infty} [\exp(-x^2/2) \cos(2\pi Sx)]\mathrm{d}x,$$

because $f_{\mathrm{T}}(x)$ is an even function. Hence, using standard tables of integrals,

$$f_T(x) = \frac{2}{\sqrt{2\pi}} \frac{\sqrt{\pi}}{2\sqrt{1/2}} \exp(-4\pi^2 S^2/2) = \exp(-2\pi^2 S^2).$$

The transform of $g(x)$, $g_T(x)$, is a δ-function with the origin at the point $x = 2$, so that $g_T(x) = \exp(i4\pi S)$, from Sect. 6.6.8. Hence, $c(x) = f_T(x)^* g_T(x) = \exp(i4\pi S - 2\pi^2 S^2)$.

6.12. (a) As h is increased, the form of $f(x)$ approaches a square more and more closely.
(b) m-lines occur at $\pm$¼, that is, at 15/60 and 45/60 in x
(c) At $x = 0$ and 2π the sine term in (6.15) is zero, so that $f(x) = \pi/2$. At $x = \pi$, the sine term is $\sin(2\pi h)30/60$, or $\sin(\pi h)$. Since h is an integer, then again $f(x) = \pi/2$.

Solutions 7

7.1. In $P2_1/c$, the general positions are $\pm(x, y, z; x, \frac{1}{2} - y, \frac{1}{2} + z)$, so that $A(hkl) = 2\{\cos 2\pi(hx + ky + lz) + \cos 2\pi(hx - ky + lz + k/2 + l/2)\} = 4\cos 2\pi(hx + lz + k/4 + l/4) \cos 2\pi(ky - k/4 - l/4)$. Introducing the y-coordinate of ¼, $A(hkl) = 4\cos 2\pi(hx + lz + k/4 + l/4)\cos 2\pi(l/4)$, so that the hkl reflections will be systematically absent for $l = 2n + 1$. The indication is that the c spacing should be halved, so that the true unit cell contains two species in space group $P2_1$ (see Fig. S7.1). This problem illustrates the consequences of sitting an atom on a glide plane: although we have considered here a hypothetical structure containing one atom in the asymmetric unit, in a multi-atom structure, an atom may, by chance, be situated on a translational symmetry element.

7.2. Refer to Chap. 2, Fig. 2.37, and Figs. S7.2 and S7.3.[13] There are eight rhodium atoms in the unit cell. If the atoms are in general positions, the minimum separation of atoms across any m plane is $\frac{1}{2} - 2y$. For any value of y, the distance would be too small to accommodate two rhodium atoms. Hence, they must occupy two sets of special positions. Positions on centers of symmetry may be excluded on the same grounds as above. Thus, the atoms are located on two sets of m planes as follow:

$$4\,\mathrm{Rh} \pm (x_1, 1/4, z_1; 1/2 - x_1, 3/4, 1/2 + z_1)$$
$$4\,\mathrm{Rh} \pm (x_2, 1/4, z_2; 1/2 - x_2, 3/4, 1/2 + z_2)$$

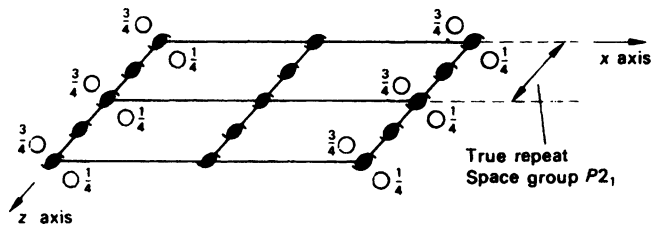

Fig. S7.1

[13] Mooney R, Welch AJE (1954) Acta Crystallogr 7:49.

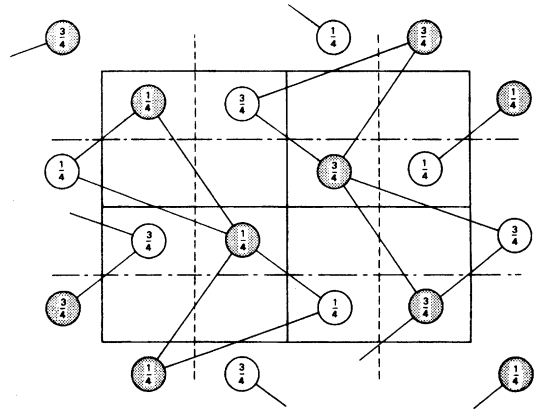

Fig. S7.2

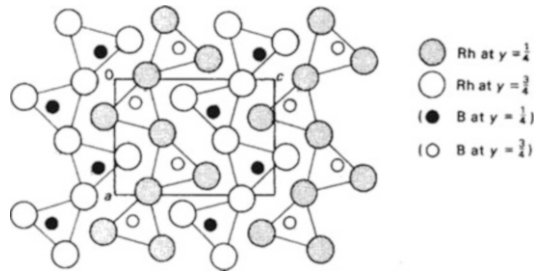

Fig. S7.3

7.3. The space group is $P2_1/m$. The molecular symmetry cannot be $\bar{1}$, but it can be m.
Hence, we can make the following assignments:
(a) Cl on m; (b) N on m; (c) two C on m, with four other C probably in general positions; (d) sixteen H in four sets of general positions, two H (in N–H groups) on m, and two H from CH_3 groups on m—those that have their C atoms on m. This arrangement is shown in Fig. S7.4a. The species CH_3, H_1 and H_2 lie above and below the m plane. The alternative space group $P2_1$ was considered, but the full structure analysis[14] confirmed $P2_1/m$. Figure S7.4b illustrates $P2_1/m$, and is reproduced from the *International Tables for X-ray Crystallography*, Vol. I, by kind permission of the International Union of Crystallography.

7.4. $A(hhh) = 4\{g_{Pt} + g_K[\cos\ 2\pi(3h/4) + \cos\ 2\pi(9h/4)] + 6g_{Cl}[3\cos\ 2\pi(hx)]\}$, where the factor 4 relates to an F unit cell (see Sect. 3.7.1). $B(hhh) = 0$, so that $F(hhh) = A(hhh)$, and $A(hhh)$

[14] Lindgren J, Olovsson I (1968) Acta Crystallogr B24:554.

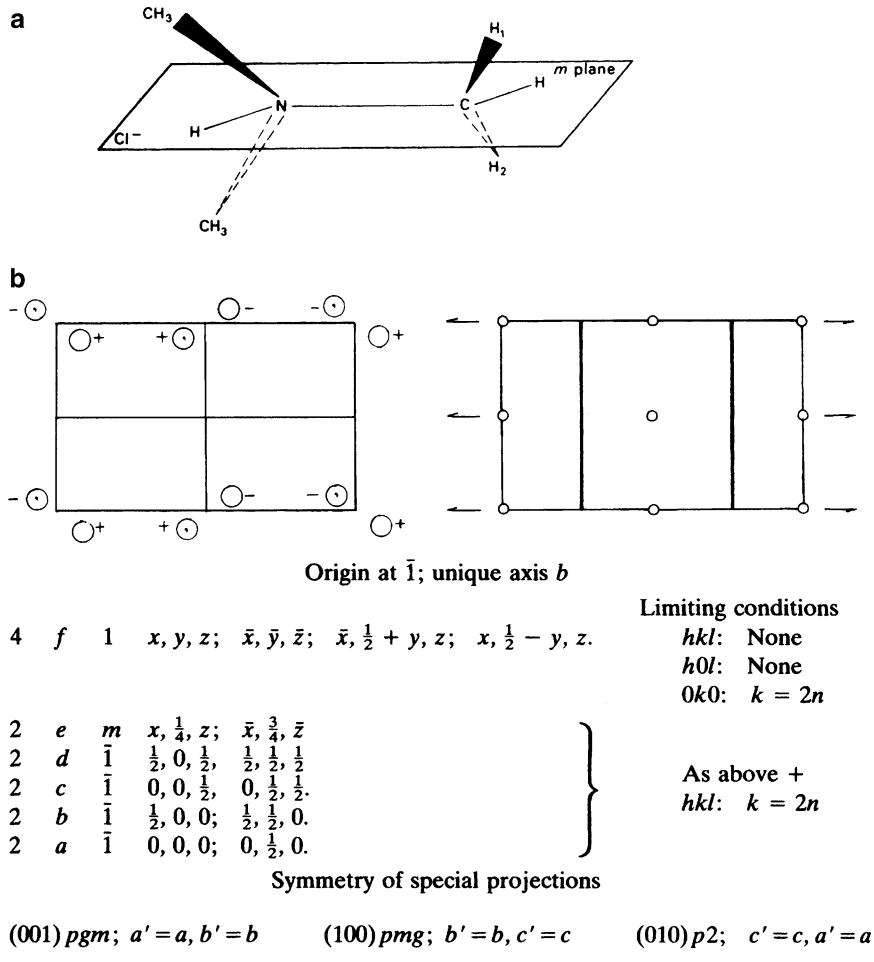

Fig. S7.4

simplifies to $4\{g_{Pt} + 2g_K \cos(3\pi h/2) + 6g_{Cl} \cos(2\pi hx)\}$. We can now calculate F(hhh) for the two values of x given:

		x = 0.23		x = 0.24	
hhh	F_o	$\|F_c\|$	K_1F_o	$\|F_c\|$	K_2F_o
111	491	340.6	314.7	317.4	329.5
222	223	152.2	142.9	159.5	149.6
333	281	145.2	180.1	190.8	188.6
K_1 = 0.641	R_1 = 0.11		K_2 = 0.671	R_2 = 0.036	

Clearly x = 0.24 is the preferred value. Pt–Cl = 2.34 Å. For a sketch and the point group, see Problem 1.11(c) and its solution.

7.5. $A_U(hkl) = 2\{\cos 2\pi(hx + ky + l/4) + \cos 2\pi(-hx + ky + l/4 + h/2 + k/2)\} = 4\{\cos 2\pi[ky + (h + k + l)/4] \cos 2\pi[hx - (h + k)/4]\}$. For (200), $A_U \propto |\cos 2\pi (2x - \frac{1}{2})|$ and, for this reflection to have zero intensity, $2\pi(2x - \frac{1}{2}) \approx (2n + 1)\pi/2$. For n = 1, $x \approx -1/8$ (by symmetry, the values 1/8, 5/8, and 7/8 are included). Conveniently, we choose the smallest of the

symmetry-related values, that is, 1/8. For (111), and using this value for x, $A_U \propto \cos 2\pi(y + 3/4)\ \cos 2\pi(1/8 - 1/2)$. For high intensity, $|\cos 2\pi(y + 3/4)| \approx 0$, $n\pi$. For $n = 0$, $y = 3/4$ (and 1/4 by symmetry). For $n = 1$, y is again $\frac{1}{4}$ and $\frac{3}{4}$. Proceeding in this manner with (231) leads to $y = 1/6$ (by symmetry, the values 1/3, 2/3, and 5/6 are included), and with (040) we find $y = 3/16$ (by symmetry, 5/16, 11/16, and 13/16 are included). The mean for the three value of y is (1/4 + 1/6 + 3/16)/3, or approximately 0.20.

7.6. Since there are two molecules per unit cell in $P2_1/m$ in this structure, and the molecules cannot have $\bar{1}$ symmetry, the special positions sets $\pm(x, \frac{1}{4}, z)$ are selected. The B, C, and N atoms lie on m. Since the shortest distance between m planes is 3.64 Å, the F_1, B, N, C, and H_1 atoms must lie on one and the same m plane (see Fig. S7.5a). Hence, the remaining two F and four H atoms must be placed symmetrically across the same m plane. These conclusions were borne out by the structure analysis.[15] Figure S7.5b is a stereoview of the packing diagram for $CH_3NH_2BF_3$, showing the H_1, C, N, B and three F atoms. The m plane is normal to the vertical direction in the diagram and the remaining two pairs of H atoms are disposed across the m plane as described above.

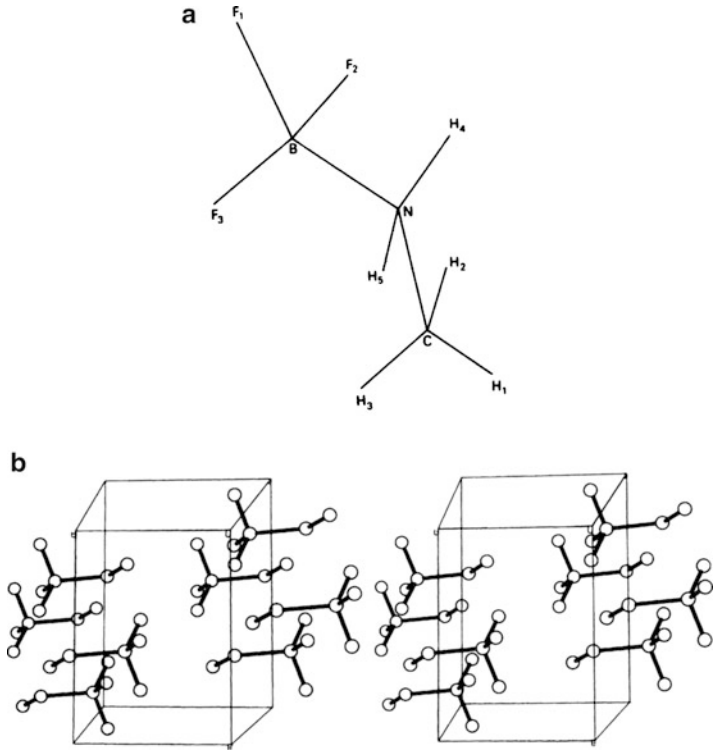

Fig. S7.5

7.7. (a) (i) $|F(hkl)| = |F(\bar{h}\,\bar{k}\,\bar{l})|$; (ii) $|F(0kl)| = |F(0\,\bar{k}\,\bar{l})|$; (iii) $|F(h0l)| = |F(\bar{h}\,0\,\bar{l})|$
(b) (i) $|F(hkl)| = |F(\bar{h}\,\bar{k}\,\bar{l})| = |F(h\,\bar{k}\,l)$;
(ii) $|F(0kl)| = F(0\,\bar{k}\,\bar{l})| = |F(0\,\bar{k}\,l)$
(iii) $|F(h0l)| = |F(\bar{h}\,0\,\bar{l})|$

[15] Geller S, Hoard JL (1950) Acta Crystallogr 3:121.

(c) (i) $|F(h\,k\,l)| = |F(\bar{h}\,\bar{k}\,\bar{l})| = |F(\bar{h}\,k\,l)| = |F(h\,\bar{k}\,l)| = |F(h\,k\,\bar{l})|$
(ii) $|F(0\,k\,l)| = |F(0\,\bar{k}\,\bar{l})| = |F(0\,\bar{k}\,l)|$;
(iii) $|F(h\,0\,l)| = |F(\bar{h}\,0\,\bar{l})| = |F(\bar{h}\,0\,l)|$

Any combination of $\pm hkl$ not listed follows the pattern of (a) (i). In (b), for example, $|F(\bar{h}\,0\,l)| = |F(h\,0\,\bar{l})|$

7.8. (a) In *Pa*, the symmetry element relates the sites *x, y, z* and $\frac{1}{2}+x,\ \bar{y},\ z$, so that the Harker line is $[\frac{1}{2}\,v\,0]$. In *P*2/*a*, the Harker section is (u 0 w) and the line $[\frac{1}{2}\,v\,0]$.
In $P222_1$, there are three Harker sections, (0 v w), (u 0 w), and ($u\,v\,\frac{1}{2}$).

(b) The Harker section (u 0 w) must arise through the symmetry-related sites *x, y, z* and $\bar{x}, y, \bar{z}$, which correspond to a two-fold axis along *y*. Similarly, the line [0*v*0] arises from a mirror plane in the Patterson normal to *y*. Since the crystal is non-centrosymmetric, the space group must be *P*2 or *Pm*. If it is *P*2, there must be, by chance, closely similar *y* coordinates for many of the atoms in the structure. If it is *Pm*, chance coincidences occur between the *x* and *z* coordinates. [These conditions are somewhat unlikely, especially when many atoms are present, so that Harker sections and lines can sometimes be used to distinguish between space groups that are not determined by diffraction symmetry alone.]

7.9. (a) $P2_1/n$, a non-standard setting of $P2_1/c$ (see also Chap. 2, Problem 2.12).

(b) The S–S vectors have the following Patterson coordinates:

(1)	$\pm(\frac{1}{2}, \frac{1}{2}+2y, \frac{1}{2})$	Double weight
(2)	$\pm(\frac{1}{2}+2x, \frac{1}{2}, \frac{1}{2}+2z)$	Double weight
(3)	$\pm(2x, 2y, 2z)$	Single weight
(4)	$\pm(2x, 2\bar{y}, 2z)$	Single weight
Section $v = \frac{1}{2}$	Type 2 vector	x = 0.182, z = 0.235
Section v = 0.092	Type 1 vector	y = 0.204
Section v = 0.408	Type 3 or 4 vector	x = 0.183, y = 0.204, z = 0.234

Thus we have four S–S vectors at: ±(0.183, 0.204, 0.235; 0.683, 0.296, 0.735). Any one of the other seven centers of symmetry, unique to the unit cell, may be chosen as the origin, whereupon the coordinates would be transformed accordingly. The sulfur atom positions are plotted in Fig. S7.6 [Small differences in the third decimal places of the coordinates determined from the maps in Problems 7.9 and 7.10 are not significant.]

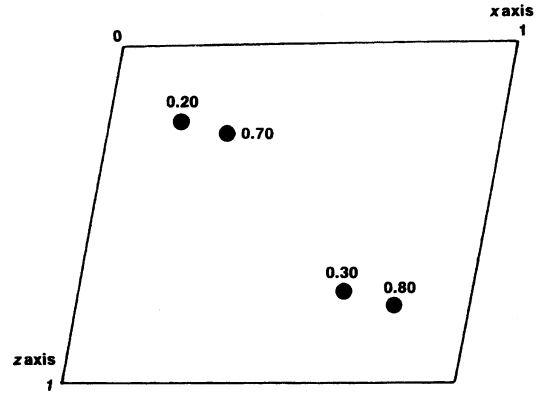

Fig. S7.6

7.10. (a) By direct measurement, the sulfur atom coordinates are S (0.266, 0.141) and S′ (−0.266, −0.141)

(b) Draw an outline of the unit cell on tracing paper, and plot the position of –S on it. Place the tracing over the idealized Patterson map (Fig. P7.2), in the same orientation, with the position of –*S* over the origin of the Patterson map, and copy the Patterson map on to the tracing (Fig. S7.7a). On another tracing, carry out the same procedure with respect to the position of −S′ (Fig. S7.7b). Superimpose the two tracings (Fig. S7.7c). Atomic positions correspond to positive regions of the two superimposed maps.

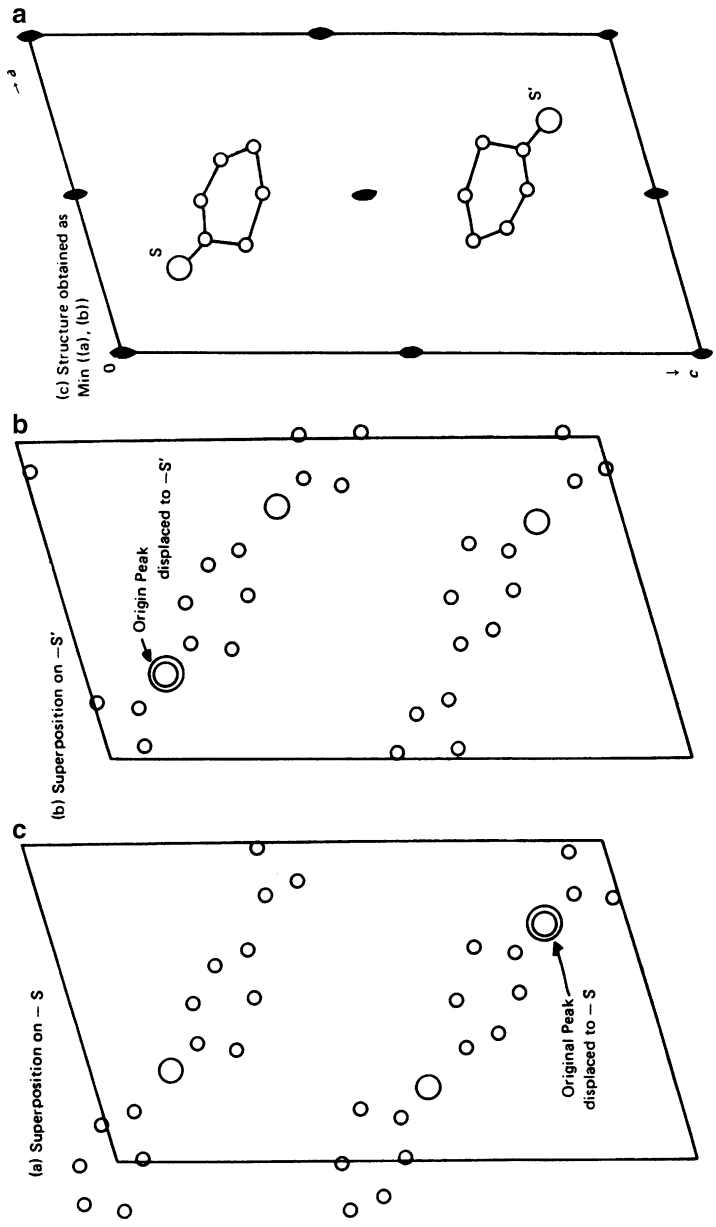

Fig. S7.7

7.11. (a) The summation to form $P(v)$ can be carried out with program FOUR1D. In using the program, each data line should contain k, $F_o(0k0)^2$, and 0.0, the zero datum representing the B coefficient of the Fourier series. $P(v)$ shows three non-origin peaks. If the highest of them is assumed to arise from the Hf–Hf vector, then $y_{Hf} = 0.105$; the smaller peaks are Hf–Si vectors, from which we could obtain approximate y parameters for the silicon atoms. Their difference in height arises mainly from the fact that one of them is, in projection, close to the origin peak. However, the simplified structure factor equation for $F_o(0k0)$, based on the hafnium atoms alone, is

$$F_o(0k0) \propto \cos(2\pi k y_{Hf})$$

so that the signs of the reflections, ignoring the weak reflections 012,0 and 016,0, are, in order, + − − + + −. (b) We can now calculate $\rho(y)$ with these signs attached to the $F_o(0k0)$ values. From the result, we obtain $y_{Hf} = 0.107$, $y_{Si_1} = 0.033$, and $y_{Si_2} = 0.25$. These values for y_{Si} lead to vectors which appear on $P(v)$. We conclude that the small peak on $\rho(y)$ at $y = 0.17$ is spurious, arising most probably from both the small number of data and experimental errors in them.

7.12. Since the sites of the replaceable atoms are the same in each derivative, and the space group is centrosymmetric, we can write $F(M_1) = F(M_2) + 4(f_{M1} - f_{M2})$, where f may be approximated by the corresponding atomic number, Z. Hence, we can draw up the following table:
(a)

	M			
h	NH_4	K	Rb	T1
1	−	−	+	+
2	a	+	+	+
3	+	+	+	+
4	−	a	+	+
5	+	+	+	+
6	−	−	a	+
7	a	+	+	+
8	a	+	+	+

a = Indeterminate, because F is small or zero.

(b) The peak at 0 represents K and Al, superimposed in projection. The peak at 0.35 would then be presumed to be due to the S atom.

(c) The effect of the isomorphous replacement of S by Se can be seen at once in the increases in $F_o(555)$ and $F_o(666)$ and decrease in $F_o(333)$. These changes are not in accord with the findings in (b). Comparison of the two electron density plots shows that $d_{S/Se}$ must be 0.19 (the x coordinate is $d/\sqrt{3}$). The peak at 0.35 arises from a superposition of oxygen atoms in projection, and is not appreciably altered by the isomorphous replacement.

7.13. $A = 100\cos 60 + (f_o + \Delta f')\cos\ 36 + 8\cos 126\ =\ 50 +\ 40.046 - 4.702 = 85.344$. $B = 100\ \sin 60 + (f_o + \Delta f')\ \sin 36 + 8\sin 126 = 86.603 + 29.095 + 6.472 = 122.17$. Hence, $|F(010)| = 149.0$, and $\phi\ (010) = 55.06°$. For the $0\bar{1}0$ reflection, we have $A = 100\cos 60 + (f_o + \Delta f')\cos 36 + 8\cos 54 = 50 + 40.046 + 4.702 = 94.748$. $B = 100\sin(-60) + (f_o + \Delta f')\ \sin(-36) + 8\sin 54 = -86.603 - 29.095 + 6.472 = -109.226$. Hence, $|F(0\bar{1}0)| =\ 144.6$, and $\phi(0\bar{1}0) = -49.06°$.

7.14. Draw a circle, at a suitable scale, to represent an amplitude $|F_P|$ of 858. From the center of this circle, set up a "vector" to represent $|F_{H1}|\exp(i\phi_1)$, where $|F_{H1}| = 141$ and $\phi_1 = (78 + 180)$ deg.

At the termination of this vector, draw a circle of radius 756 to represent $|F_{PH1}|$. Repeat this procedure for the other two derivatives (Fig. S7.8). The six intersections 1–1′, 2–2′, and 3–3′ are strongest in the region indicated by •- - -•. The required phase angle ϕ_M, calculated from (7.50), lies in this region. The centroid phase angle ϕ_B is biased slightly towards point 1.

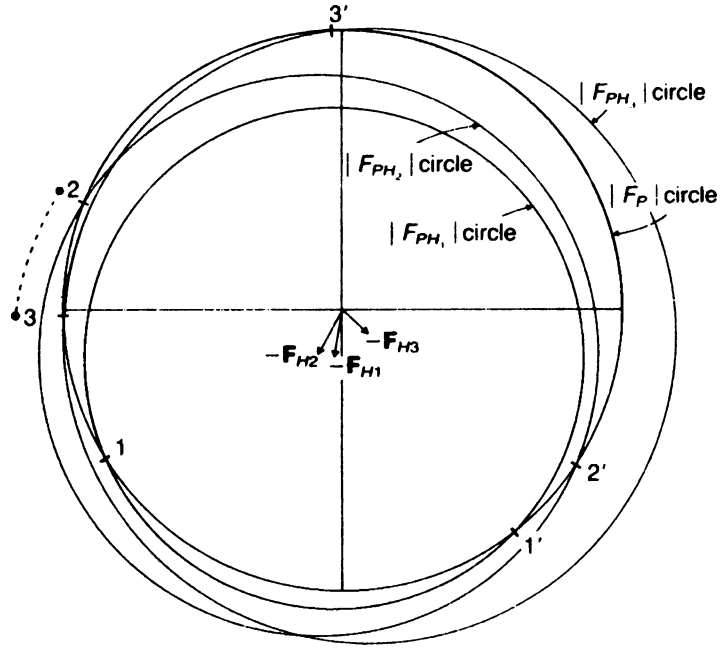

Fig. S7.8

7.15. Cos($hx - \phi$) expands to $\cos hx \cos\phi + \sin hx \sin\phi$ which, for $\phi = \pi/2$, reduces to $\sin hx$. Hence, $\psi(x) = \pi/2 + 2\sum_{h=1}^{\infty}(1/h)\sin hx = \pi/2 + 2\sum_{h=1}^{\infty}(1/h)\cos(hx - \phi)$. This equation resembles closely a Fourier series (see Sect. 6.2).

7.16. (a) The total mass of protein per unit cell is $18000Z \times 1.6605 \times 10^{-24}$ g, where Z is the number of protein molecules per unit cell. Since there is an equal mass of solvent water in the unit cell, $D/2Z = (18000 \times 1.6605 \times 10^{-24})/(40 \times 50 \times 60 \times 10^{-24} \sin 100^\circ) = 0.2529$ g cm^{-3}, so that $D = 0.5058Z$ g cm^{-3}. Sensible values for Z in $C2$ are 4 and 2. The former leads to a density that is much too large for a protein; $Z = 2$ gives $D = 1.012$ g cm^{-3}, which is an acceptable answer.

(b) In space group $C2$ there are four general equivalent positions (see Sect. 2.7.3). Since $Z = 2$, the protein molecule must occupy special positions on twofold axes, so that the molecule has symmetry 2.

7.17. In the notation of the text, we have for F(hkl)

$$\mathrm{F}_H(+) = \mathrm{F}'_H(+) + \mathrm{iF}''_H(+)$$
$$\text{and for } |\mathrm{F}(\bar{h}\,\bar{k}\,\bar{l})|$$
$$\mathrm{F}_H(-) = \mathrm{F}'_H(-) + \mathrm{iF}''_H(-)$$

where $\mathrm{F}'_H(+)$ and $\mathrm{F}'_H(-)$ are the structure factor components derived from the real part of (7.64) and (7.66), and $\mathrm{F}''_H(+)$ and $\mathrm{F}''_H(-)$ are its anomalous components. It is clear from Fig. S7.9 that

the moduli $|F_H(+)|$ and $|F_H(-)|$ are equal, but that $\phi_H(+) \neq \phi_H(-)$. In terms of the structure factor equations, we can write a single atom vector for **h** and $\bar{\mathbf{h}}$

$$F(\mathbf{h}) = (\mathbf{f}' + i\Delta\mathbf{f}'') \exp[i(\mathbf{2}\pi\mathbf{h} \cdot \mathbf{r} + \pi/\mathbf{2})]$$
$$F(\bar{\mathbf{h}}) = (f + i\Delta f'') \exp[-i(2\pi\mathbf{h} \cdot \mathbf{r} + \pi/2)]$$

from which we have $|F(\mathbf{h})| = F(\bar{\mathbf{h}})|$, but $\phi(\mathbf{h}) \neq \phi(\bar{\mathbf{h}})$; $\pi/2$ acts in the same sense (positive) in each case.

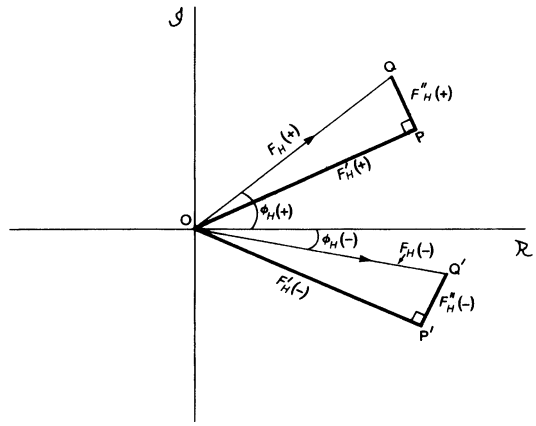

Fig. S7.9

7.18. In the notation of the text, and for a centrosymmetric structure, we have $F_{PH}(+) = A_P(+) + A'_H(+) + iA''_H(+)$ where

$$A_P(+) = \sum_{j=1}^{N_P} f_j \cos\, 2\pi(hx_j + ky_j + lz_j)$$
$$A'_H(+) = \sum_{j=1}^{N_H} f'_j \cos\, 2\pi(hx_j + ky_j + lz_j)$$
$$A''_H(+) = \sum_{j=1}^{N_H} \Delta f''_j \cos\, 2\pi(hx_j + ky_j + lz_j)$$

Clearly, $|F(h\,k\,l)| = |F(\bar{h}\,\bar{k}\,\bar{l})| = (A^2 + B^2)^{1/2}$, where $A = A_P(+) + A'_H(+)$ and $B = A''_H(+)$; $\phi(hkl) = \phi(\bar{h}\,\bar{k}\,\bar{l}) = \tan^{-1}(B/A)$, and cannot equal 0 or π because of the finite value of $A''_H(+)$.

7.19. If, for a crystal of a given space group, Friedel's Law breaks down, then the diffraction symmetry reverts to that of the corresponding point group. Thus, we have

	$\|F(hkl)\|$ equivalents	Bijvoet pairs
(a) $C2$ (2)	$hkl/\bar{h}\,k\,\bar{l}$	$hkl/\bar{h}\,k\,\bar{l}$with $h\,\bar{k}\,l/\bar{h}\,\bar{k}\,\bar{l}$

(continued)

(b) Pm (m)	$hkl/h\bar{k}l$	$hkl/h\bar{k}l$with $\bar{h}k\bar{l}/\bar{h}\bar{k}\bar{l}$
(c) $P2_12_12_1$ (222)	$hkl/h\bar{k}\bar{l}/\bar{h}k\bar{l}/\bar{h}\bar{k}l$	$hkl/h\bar{k}\bar{l}/\bar{h}k\bar{l}/\bar{h}\bar{k}l$ with $\bar{h}kl/h\bar{k}l/hk\bar{l}/\bar{h}\bar{k}\bar{l}$
(d) $P4$(4)	$hkl/\bar{k}hl/\bar{h}\bar{k}l/k\bar{h}l$	$hkl/\bar{k}hl/\bar{h}\bar{k}l/k\bar{h}l$ with $k\bar{h}\bar{l}/hk\bar{l}/\bar{k}h\bar{l}/\bar{h}\bar{k}\bar{l}$

Strictly, pairs related as hkl and $\bar{h}\bar{k}\bar{l}$ should be discounted, as they are, of course, Friedel pairs.

7.20. The number N of symmetry-independent reciprocal lattice points with a range $0 < \theta < \theta_{max}$ is $33.510\ V_c \sin^3\theta/(\lambda^3 Gm)$, from Chap. 7. The volume V_c of the unit cell is 6×10^4 Å^3, $G = 1$ for a P unit cell, and m, the number of symmetry-equivalent general reflections, is 8 for the Laue group mmm. Hence, $N = 74466.7 \sin^3\theta_{max}$.
(a) $0 < \theta < 10°$: $\sin^3\theta_{max} = 5.236 \times 10^{-3}$, so that $N = 389$ (779 if we consider the hkl and $\bar{h}\bar{k}l$ reflections).
(b) $10 < \theta < 20°$: $\sin^3\theta_{max} = 4.001 \times 10^{-2}$, so that $N = 2979 - 389$, or 2590.
(c) $20 < \theta < 25°$: $\sin^3\theta_{max} = 7.548 \times 10^{-3}$, so that $N = 5620 - 2979$, or 2641.
The resolution, defined in terms of d_{min}, is $d_{min} = \lambda/(2 \sin\theta_{max})$
(a) For $\theta_{max} = 10°$: $d_{min} = 4.32$ Å
(b) For $\theta_{max} = 20°$: $d_{min} = 2.19$ Å
(c) For $\theta_{max} = 25°$: $d_{min} = 1.77$ Å

Solutions 8

8.1. A possible set, with the larger |E| values, is 705, $6\,\bar{1}\,\bar{7}$, and $8\bar{1}\,\bar{4}$. Reflection $4\,2\,\bar{6}$ is a structure seminvariant, and 203 is linearly related to the pair $8\bar{1}\bar{4}$ and $6\bar{1}\bar{7}$. Reflection $4\bar{3}\,\bar{2}$ has a low |E| value, so that triple relationships involving it would not have a high probability. Alternative sets are 705, 203, $8\bar{1}\bar{4}$ and 705, 203, $6\,\bar{1}\,\bar{7}$. A vector triplet exists between $8\bar{1}\,\bar{4}$, $42\bar{6}$, and $4\bar{3}2$.

8.2. The equations for A and B lead to the following relationships:

$$|F(hkl)| = |F(\bar{h}\bar{k}\bar{l})| = |F(h\bar{k}l)| = |F(\bar{h}k\bar{l})| \neq |F(\bar{h}kl)|; |F(\bar{h}kl)| = |F(hk\bar{l})|$$

Because of the existence of the $k/4$ term, the phase relationships depend on the parity of k:

$$\begin{aligned} k = 2n : \phi(hkl) &= -\phi(\bar{h}\bar{k}\bar{l}) = -\phi(h\bar{k}l) = \phi(\bar{h}k\bar{l} \neq \phi(\bar{h}kl); \\ \phi(\bar{h}kl) &= \phi(hk\bar{l}) \\ k = 2n + 1 : \phi(hkl) &= -\phi(\bar{h}\bar{k}\bar{l}) = \pi - \phi(h\bar{k}l) = \pi + \phi(\bar{h}k\bar{l}) \neq \phi(\bar{h}kl; \\ \phi(\bar{h}kl) &= \pi + \phi(hk\bar{l}) \end{aligned}$$

8.3. Set (b) would be chosen: there is a redundancy in set (a) among 041, $\bar{1}62$, and $\bar{1}23$, because $|F(041)| = |F(0\,\bar{4}\,1)|$ in this space group. In space group $C2/c$, $h + k$ is even for reflections to occur, so that reflections 012, $\bar{1}23$, 162, and $\bar{1}62$ would not occur. The origin could be fixed by 223 and $13\bar{7}$: there are only four parity groups for a C-centered unit cell.

8.4. Following the procedure given in Chap. 4, Sect. 4.2, it will be found that $K = 4.0 \pm 0.4$, and $B = 6.6 \pm 0.3$ Å^2. Since $B = 8\pi^2\overline{U^2}$, the root mean square atomic displacement is $[6.6/(8\pi^2)]^{1/2}$, or 0.29 Å. (You were not expected to derive the standard errors in K and B; they are quoted in order to give an idea of the precision obtainable from a Wilson plot.)

8.5. A plot of the atomic positions in the unit cell and its environs shows that the shortest Cl. . .Cl contact distance is between atoms at ¼, y, z, and ¾, $\bar{y}$, z. Hence, d^2(Cl. . .Cl) $= a^2/4 + 4y^2b^2$,

so that d(Cl. . .Cl) = 4.639 Å. The superposition of errors (see Sect. 8.6) shows that the variance of d(Cl. . .Cl) is obtained from

$$[2d\sigma(d)]^2 = [2a\sigma(a)/4]^2 + [8y^2b\sigma(b)]^2 + [8b^2y\sigma(y)]^2$$

so that $\sigma(d)$ = 0.026 Å. (It may be noted that this answer calculates as 0.02637 Å to four significant figures. *Note*. If we use only the third term, that in $\sigma(y)$, then the result is 0.02626 Å. Thus, the error in a distance between atoms arises mostly from the errors in the corresponding atomic coordinates.)

8.6. In the first instance we average the sum of $\phi_{\mathbf{k}}$ and $\phi_{\mathbf{h-k}}$, namely, $(-37 - 3 - 54 + 38 + 13)/6$, or $-7.17°$. Applying the tangent expression leads to the better value of $-11.32°$.

8.7. Vectors of the type labeled P1- - - -P2 will not occur in the search Patterson as they involve atoms, in the region of P1, within the additional loop of the target molecule that are absent in the search molecule. Only the search molecule will be positioned by rotation and translation, and the missing parts of the structure, particularly in the loop, need to be located initially using Fourier and possibly least-squares methods, as in small-molecule analysis.

8.8. (a) It is not clear how the side chain comprising atoms 8–13 is oriented with respect to the rest of the molecule, which is predominantly flat. The facility in the PATSEE program for varying the linkage torsion angle could be used but was not necessary in practice because a sufficiently large independent search fragment was available.

(b) By chance the molecular graphics program oriented the search model, which is perfectly flat, to be in the XY plane. Hence all Z coordinates are zero in this plane.

(c) The CHEM-X (or ChemSketch) program allows a chemical model of the molecule to be constructed and provides coordinates for the atoms. These coordinates are given not as fractional coordinates but as Å values with respect to the internal orthogonal axis system of the program. To convert to fractional coordinates for the purpose of this problem, the X, Y, and Z values were each divided by 100 for all atoms. This set then belongs to an artificial unit cell with dimensions given in the question.

8.9. In Fig. S8.1, OP = 1.400 Å, OQ = 1.400 sin 60, and $Q1$ = 1.400 cos 60. Thus:

Coordinates in the unit cell are:		
Atom 1: X = 0.700	Y = 1.212	Z = 0.000
Atom 2: X = 1.400	Y = 0.000	Z = 0.000
Atom 3: X = 0.700	Y = −1.212	Z = 0.000
Atom 4: X = −0.700	Y = −1.212	Z = 0.000
Atom 5: X = −1.400	Y = 0.000	Z = 0.000
Atom 6: X = −0.700	Y = 1.212	Z = 0.000

Fractional coordinates in the given unit cell:		
Atom 1: X = 0.237	Y = 0.211	Z = 0.000
Atom 2: X = 0.473	Y = 0.000	Z = 0.000
Atom 3: X = 0.237	Y = −0.211	Z = 0.000
Atom 4: X = −0.237	Y = −0.211	Z = 0.000
Atom 5: X = −0.473	Y = 0.000	Z = 0.000
Atom 6: X = −0.237	Y = 0.211	Z = 0.000

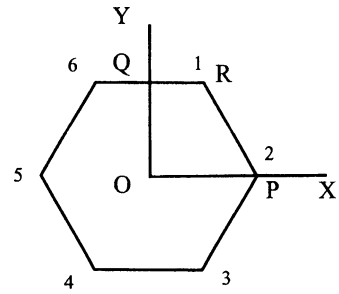

Fig. S8.1

8.10. From Chap. 4, (4.34) and Chap. 8, (8.1), with N atoms per unit cell, assuming scaled F_o values, dividing throughout by $\sum_{j=1}^{N} g_{j,\theta}^2$ (the ε factor is assumed to be unity), gives

$$|\mathrm{E}|^2 = 1 + \left(\left(1 \Big/ \sum_{j=1}^{N} g_{j,\theta}^2 \right) \sum_{j \neq k} g_{j,\theta} g_{k,\theta} \exp\left(\mathrm{i} 2\pi \mathbf{h} \cdot \mathbf{r}_{j,k} \right) \right)$$

The second term on the right-hand side represents sharpened $|\mathrm{F}|^2$ coefficients [see also Chap. 7, (7.19)]. The term in the Patterson function that creates the origin peak, $\sum_{j=1}^{N} g_{j,\theta}^2$, is now unity, so that a Patterson function with coefficients $(|\mathrm{E}|^2 - 1)$ produces a sharpened Patterson function with the origin peak removed.

8.11. (a) When using Molecular Replacement in macromolecular crystallography the search and target molecules should be compatible in size as well as in their three-dimensional structures. If this is not the case problems may be encountered in obtaining a dominant solution to MR. The more possible solutions which have to be inspected, using Fourier methods, the more laborious the process becomes, maybe to the point where the analysis becomes untenable.

(b) For small-molecule analysis it is more usual for the search "molecule" to be a fairly small fragment of the target molecule. In this case the search molecule must be as accurate as possible in bond lengths and angles because the data are at atomic resolution and the Patterson peaks similarly resolved. Programs such as PATSEE allow for more complex search molecules to be used which have one degree of torsional freedom, thus increasing the size of the whole search fragment.

8.12. The required determinant is $\begin{vmatrix} \mathrm{E}(0) & \mathrm{E}(\mathbf{h}) & \mathrm{E}(2\mathbf{h}) \\ \mathrm{E}(-\mathbf{h}) & \mathrm{E}(0) & \mathrm{E}(\mathbf{h}) \\ \mathrm{E}(-2\mathbf{h}) & \mathrm{E}(-\mathbf{h}) & \mathrm{E}(0) \end{vmatrix} \geq 0$, which evaluates as

$\mathrm{E}(0)^3 + \mathrm{E}(\mathbf{h})^2 \mathrm{E}(-2\mathbf{h}) + \mathrm{E}(2\mathbf{h})[\mathrm{E}(-\mathbf{h})]^2 - \mathrm{E}(0)|\mathrm{E}(2\mathbf{h})|^2 - \mathrm{E}(0)\mathrm{E}(\mathbf{h})|^2 - \mathrm{E}(0)|\mathrm{E}(\mathbf{h})|^2 \geq 0$ or $\mathrm{E}(0)$ $\{\mathrm{E}(0)^2 - |\mathrm{E}(2\mathbf{h})|^2 - 2|\mathrm{E}(\mathbf{h})|^2\} + 2\ |\mathrm{E}(\mathbf{h})|^2\ \mathrm{E}(2\mathbf{h}) \geq 0$. Inserting the given values for E(0), $|\mathrm{E}(\mathbf{h})|$, and $|\mathrm{E}(2\mathbf{h})|$, we obtain $3\{9 - 4 - 8\} + 8(\pm 2) \geq 0$, from which it is clear E($2\mathbf{h}$) is positive in sign in order to satisfy the determinant expression.

8.13. For the first triplet, $\mathbf{h} + \mathbf{k} + \mathbf{l} = 0\ 0\ 0$ modulo (2 2 2), where $\mathbf{h} = h_1 + h_2 + h_3$, and similarly for $\mathbf{k}$ and $\mathbf{l}$. Hence, the triplet is a structure seminvariant. The second triplet is also a structure seminvariant, for the same reason. In the third triplet, $\mathbf{h} + \mathbf{k} + \mathbf{l} = 0\ 0\ 0$ and is a structure invariant. None of these triplets is suitable for specifying an origin because their determinants are either zero or zero modulo 2 (see Appendix E).

8.14. Apply the structure factor (3.63). (a) In space group $P2_1$, the [010] zone is centric, plane group $p2$, so that $B' = 0$ and $A' = 2\cos 2\pi[(1 \times 0.3) + (3 \times 0.1)]$, so that $|\mathrm{F}| = 1.62$ and $\phi = 180°$.

(b) (i) Space group $P2_12_12_1$ in projection on to ($h0l$) becomes plane group $p2gg$, with coordinates $\pm(x, z; ½ - x, ½ + z)$. Proceeding as in (a), $|F| = 0.38$ and $\phi = 180°$. (ii) In the standard orientation, the coordinates are (see Fig. 2.35): $x, z; ½ - x, ½ + z; ½ + x, -z; -x, ½ - z$. Proceeding as before, $A' = 0$ and $B' = -1.18$, so that $|F| = 1.18$ and $\phi = -90°$. Alternatively, we recall from Appendix E that the phase change for an origin shift **r** is -2π**h.r**, which is $-2\pi(¾)$, so that $\phi = 180 - 270 = -90°$.

Solutions 9

9.1. (a) In space group $P2_1$, symmetry-related vectors have the coordinates $\pm(2x, {}^1/_2, 2z)$; the I–I vector in the half unit cell is easily discerned. By measurement on the map, $x_1 = 0.422$ and $z_I = 0.144$, with respect to the origin O.

(b) The contribution of the iodine atoms, F_I, to the structure factors is given by $2f_I \cos 2\pi(0.422x_I + 0.144z_I)$. Hence, the following table:

hkl	$(\sin\theta)/\lambda$	$2f_I$	f_I	F_o
001	0.026	105	65	40
0014	0.364	67	67	37
106	0.175	88	−20	33
300	0.207	84	−8	35

The signs of 001, 0014, and 106 are probably +, +, and −, respectively. The magnitude $|F_I(300)|$ is a small fraction of F_o, and could easily be outweighed by the contribution from the rest of the structure. Thus, its sign remains uncertain from the data given. Small variations in the values determined for f_I are acceptable; they derive, most probably, from small differences in the graphical interpolation of the f_I values.

(c) The shortest I–I vector is that between the positions listed above. Hence, $d_{I-I} = \{[2 \times 0.422 \times 7.26]^2 + [0.5 \times 11.55]^2 + [2 \times 0.144 \times 19.22]^2 + [2 \times 0.422 \times 0.144 \times 7.26 \times 19.22 \cos(94.07)]\}^{1/2} = 10.05$ Å.

9.2. A Σ_2 listing is prepared as follows:

h	**k**	**h** − **k**	$\lvert E(\mathbf{h})\rvert$	$\lvert E(\mathbf{k})\rvert$	$\lvert E(\mathbf{h}-\mathbf{k})\rvert$
0018	081	0817	9.5		
011	024	035	5.0		
	026	035	0.5		
021	038	059	0.4		
	0310	059	0.4		
024	035	059	9.6		
038	059	0817	7.2		
	081	011,7	6.0		
	081	011,9	10.2		
0310	059	081	7.9		
	081	011,9	9.2		

(Note the convention, that a two-figure Miller index takes a comma after it unless it is the third index.)

In space group $P2_1/a$, $s(hkl) = s(\bar{h}\,\bar{k}\,\bar{l}) = (-1)^{h+k}s(h\,\bar{k}\,l)$, and $s(h\,k\,\bar{l}) = (-1)^{h+k}\ s(\bar{h}\,k\,l)$. In using only two-dimensional reflections from the data set, we need just two reflections to

specify an origin, say, 0, 0. We take $s(081) = s(011,9) = +$ and proceed to the determination of signs, as follows:

h	k	h-k	Conclusions
$011,9(+)$	(Origin fixing)		
$081(+)$	(Origin fixing)		
$011,9(+)$	$081(+)$	038	$s(038) = +$
$011,9(+)$	$08\bar{1}(+)$	0310	$s(0310) = +$
$038(+)$	$0\bar{8}1(+)$	011,7	$s(011,7) = +$
$0310(+)$	$081(+)$	$0\bar{5}9$	$s(059) = -$
$059(-)$	$0\bar{3}\bar{8}(+)$	0817	$s(0817) = -$
$038(+)$	$059(-)$	$02\bar{1}$	$s(021) = -$
$0310(+)$	$059(-)$	$0\bar{2}1$	$s(021) = -$
$0817(-)$	$08\bar{1}(+)$	0018	$s(0018) = -$
		Let	$s(035) = a$
$059(-)$	$035(a)$	024	$s(024) = -a$
$035(a)$	$024(-a)$	011	$s(011) = -$
$035(a)$	$01\bar{1}(+)$	026	$s(026) = a$

The two indications for $s(021)$ and the single indication for $s(026)$ will have low probabilities, because of low |E| values, and must be regarded as unreliable at this stage. Within the data set, no conclusion can be reached about $s(a)$; both + and − signs are equally likely. Reflection 0312 does not interact within the data set.

9.3. The space group is $P2_1/c$, from Chap. 9, Table 9.4. Thus, $s|E(hkl)| = s|E(\bar{h}\,\bar{k}\,\bar{l})| = (-1)^{k+1}s|E(h\,\bar{k}\,l)|$; for the hk reflections, set $l = 0$ in these relationships. Figure S9.1 shows the completed chart. A Σ_2 listing follows; an N indicates that no new relationships were derivable with the reflection so marked; negative signs are represented by bars over the |E| values.

Σ_2 Listing				
Number	h	k	h − k	$\lvert E_{\mathbf{h}}\rvert$ $\lvert E_{\mathbf{k}}\rvert$ $\lvert E_{\mathbf{h-k}}\rvert$
1	300	040	$3\bar{4}0$	3.5
2		840	$\bar{5}\,\bar{4}0$	6.0
3		570	$\bar{2}\,\bar{7}0$	10.0
4	700	570	$2\bar{7}0$	13.0
5	800	670	$2\bar{7}0$	10.1
6		340	$5\bar{4}0$	7.7
7		411,0	$4\,\overline{11},0$	4.9
8		040	$8\bar{4}0$	4.2
9	730	$0\,\bar{4}\,0$	770	3.1
10		$5\,\bar{4}\,0$	270	6.9
11	040	N		
12	340	$7\bar{7}0$	$\bar{4}\,1\,1,0$	4.1

(continued)

13	540	*N*
14	840	*N*
15	270	*N*
16	570	*N*
17	670	*N*
18	770	*N*
19	411,0	*N*

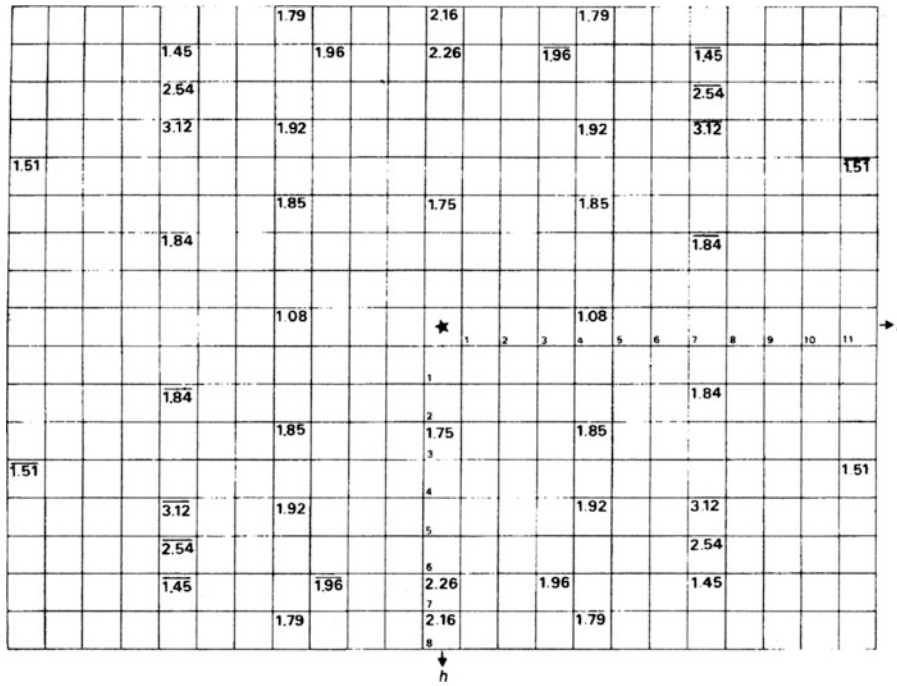

Fig. S9.1

An origin at 0, 0 may be chosen by specifying 270 (eoe, and occurring four times) and 540 (oee, and occurring three times), both as +. From the Σ_2 listing, we now have:

Number	Conclusion	Comments
10	$s(730) = +$	
7	$s(800) = -$	$s\,(411,\,0) = -s(4\,\overline{11},\,0)$
5	$s(670) = +$	
6	$s(340) = -$	Sign propagation has ended. Now let $s(040) = a$
1	$s(300) = -a$	
2	$s(840) = -a$	
3	$s(570) = -a$	
4	$s(700) = a$	
8	$s(840) = -a$	
9	$s(770) = a$	
11	$s(411,0) = -a$	

The symbol a would be determined by calculating electron density maps with both + and − values, and assessing the results in terms of sensible chemical entities. In a more extended, experimental data set, the sign of a may evolve. No Σ_2 relationship is noticeably weak, and the above solution to the problem may be regarded as acceptable.

9.4. (a) Use Chap. 8, Sect. 8.5.1, (8.105); since $\alpha = \gamma = 90$ deg, the fourth and sixth terms on the right-hand side are zero. Thus, the bond length is 2.119 Å. From Sect. 8.6, (8.114), the esd evaluates to 0.0001 Å. Thus, we write S(1)–S(2) = 2.119(1) Å.

(b) Writing down all Patterson vectors on the x,z projection of space group $P2_1$, we obtain:

A

$2x_1, 2z_1; 2x_2, 2z_2$

$-2x_1, -2z_1; -2x_2, -2z_2$

B

$x_1 - x_2, z_1 - z_2; -x_1 - x_2, -z_1 - z_2; -x_1 + x_2, -z_1 + z_2; x_1 + x_2, z_1 + z_2;$

$-x_1 - x_2, -z_1 + z_2; x_1 + x_2, z_1 + z_2; x_1 - x_2, z_1 - z_2; -x_1 - x_2, -z_1 - z_2$

Group A vectors are of single weight whereas group B vectors are of double weight. Hence the vectors around the origin would have the geometry shown in Fig. S9.2, and we expect the following arrangement, excluding the origin peak:

where $S_1D_1 = D_1S_2 = S_3D_3 = D_3S_4$ and $S_2D_2 = D_2S_3 = S_4D_4 = D_4S_1$.

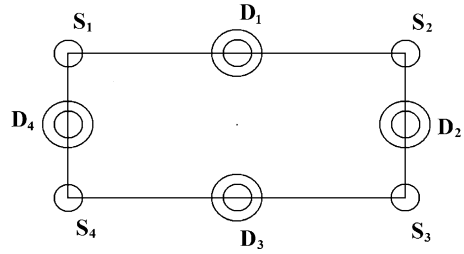

Fig. S9.2

Solutions 10

10.1. The number N of unit cells in a crystal is V(crystal)/V(unit cell). Both crystals have the volume V(crystal) = 2.4×10^{-2} mm^3. The protein unit-cell volume V(protein) = 60000 Å^3, or 60000×10^{-21} mm^3. The total number of protein unit cells N_P is therefore = 4×10^{14}. For the organic crystal unit cell, V(organic) = 1800 Å^3, or 1800×10^{-21} mm^3, so that the total number of organic unit cells N_0 is 1.333×10^{16}.

From Chap. 4, (4.1) and (4.2), we write

$$\mathcal{E}(hkl) = (I_0/\omega)(N^2\lambda^3)[e^4/m_e^2c^4]LpA|\mathrm{F}(hkl)|^2V(\mathrm{crystal}) \qquad \text{(S10.1)}$$

where N is the number of unit cells per unit volume of the crystal, L, p, and A are the Lorentz, polarization, and absorption correction factors, and the other symbols have their usual meanings.

Historically, this equation was derived in 1914[16] and confirmed by careful measurements on a crystal of sodium chloride in 1921[17]. In (S10.1), $\mathcal{E}$ (hkl) is the experimentally derived quantity and $|\mathrm{F}(hkl)|$ is the term required in X-ray analysis. For our purposes, we write

[16] Darwin CG (1914) Philosophical Magazine 27, 315.

[17] Bragg WL, James RW, Bosanquet CM (1921) Philosophical Magazine 42:1.

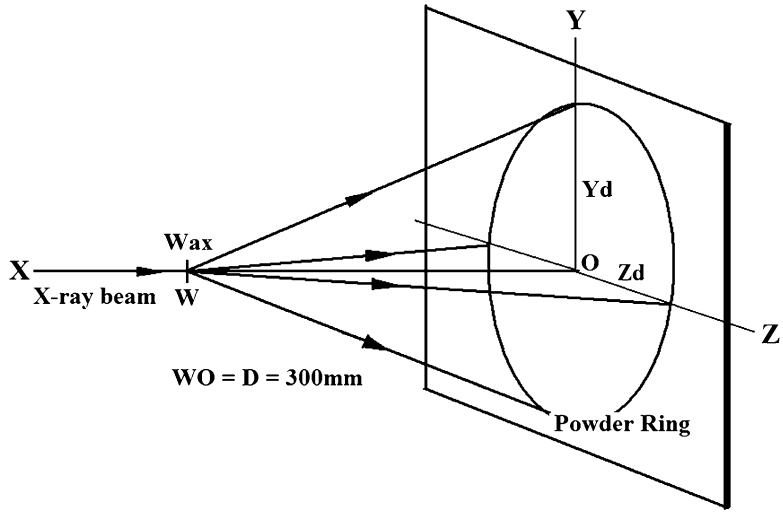

Fig. S10.2

$$\mathcal{E}(hkl) \propto N^2 = [N_{\text{cells}}/V(\text{crystal})]^2 \tag{S10.2}$$

where N_{cells} is the total number of unit cells in the crystal volume V(crystal). Since diffraction power D is proportional to energy, we have for the two cases under discussion:

$$\begin{aligned} D\,(\text{organic})/D\,(\text{protein}) &= [N_{\text{cells}}(\text{organic})/N_{\text{cells}}(\text{protein})]^2 = [(1.333 \times 10^{16})/(4 \times 10^{14})]^2 \\ &= 1110.6 \end{aligned}$$

Based on these considerations alone, the organic crystal will diffract over 1000 times more powerfully than the protein crystal. However, most protein data sets are now collected with synchrotron radiation, the intensity of which more than makes up for the deficiency in diffracting power calculated above. Other factors affect the intensity: in particular, it follows from Chap. 4, Sect. 4.2.1 that a local average value of $|\text{F}(hkl)|^2$ is proportional to $N_c f^2$ if, for simplicity, we assume an equal-atom structure, where N_c is here the number atoms per unit cell, which, to a first approximation, is proportional to the V (unit cell). Hence, the diffracting power of the crystal is directly proportional to V(unit cell), so that the above "squared effect" is somewhat diminished by the second factor.

10.2. The experimental arrangement and coordinate systems are shown in the diagram, Fig. S10.2. For the powder ring, the two coordinates Y_d and Z_d will be the same, that is, 70 mm, and the distance D is 300 mm. The angle subtended from O by the diffracted beam is 2θ so that $\tan 2\theta = 70/300$, or $\theta = 6.654°$. From the Bragg equation, $\lambda = 0.811$ Å.

10.3. (Following on from 10.2.) Let the separation of spots for the 300 Å spacing be ΔZ_d; then $\Delta Z_d/D = \tan 2\theta$ for a single diffraction order. Using the Bragg equation, we have $2 \times 300 \times \sin\theta = 0.811$ and $\theta = 0.0774$ deg. If $\Delta Z_d = 1$ mm then $D = 1/\tan 2\theta = 370$ mm. Using a value of D of 450 mm will be more than adequate. Note that the intensity falls off as the square of the distance, so that, in practice, moving the detector too far away will be costly in terms of lost data for a weakly diffracting protein crystal.

10.4. The information on limiting conditions indicates that there is either a 6_1 or a 6_5 screw axis in the crystal (Chap. 2, Table 10.2). As the Laue symmetry is $\frac{6}{m}mm$, it follows from Chap. 10, Table

10.1 that space group is either $P6_122$ or $P6_522$. Only the X-ray analysis can resolve this remaining ambiguity. Note that 6_1 and 6_5 screw operations are left-hand–right-hand opposites; only one can be correct for a given protein crystal.

10.5. The volume V_c is 3.280×10^6 Å^3. Substituting known values into the equation $D_c = \mu Z M_P m_u / V_c(1 - s)$ gives $0.383\ \mu/(1 - s)$ for D_c, where μ is the number of molecules per asymmetric unit, and s is the fractional solvent content to be found by trial and error. Assuming that μ is 1 molecule per asymmetric unit and s is 0.68, that is, the crystal contains 68% solvent by weight (the top value of the known range), then it follows that $D_c = 1.20$ g cm^{-3}, a reasonable result. Note that we could make $s = 0.70$, slightly higher than normal, and this would give $D_c = 1.28$ g cm^{-3}, which is again quite acceptable. The important result for the structure analysis is that $\mu = 1$ so that $Z = 12$.

As s from the above analysis is on the high side, we increase the number of molecules μ to 2. Then $D_c = 2 \times 0.383\ \mu/(1 - s)$, or $0.766/(1 - s)$ which, for $D_c = 1.4$ g cm^3 (see Chap. 10, Sect. 10.4.7), gives $s = 0.45$. This result is again reasonable, so that there is some ambiguity for this protein. All that can be done is to bear these results in mind during the X-ray analysis, and make use of any other facts which are known about the crystal. In the case of the protein MLI, it was known that the crystals diffracted X-rays only poorly, which is often a sign of high solvent content, and this fact is more consistent with $\mu = 1$.

10.6. The expected number of reflections $= 4.19 V_c / d_{\min}^3$, or 563450; this number includes all symmetry-related reflections. Since the Laue symmetry (Chap. 1, Table 1.6) is $\frac{6}{m}mm$, the number of unique data is 1/24 times the number in the complete sphere, namely, 23479. If only 21000 reflections are recorded, the data set would be approximately 89 % complete at the nominal resolution of 2.9 Å. This result corresponds more appropriately to 3.0 Å resolution (working backwards). Note that the above discussion is based on the number of reciprocal lattice points scanned in data collection and processing. Because protein crystals diffract poorly the number of reflections with significant intensities may well be as low as 50 %. These weak data do actually contain structural information and will usually be retained in the working data set.

10.7. The asymmetric unit is one protein molecule. About 10% of the 27000 Da is hydrogen leaving $27000 - 2700 = 24300$ Da, which is equivalent to 2025 carbon atoms (C = 12). For the atoms in the water molecules to be located (neglecting hydrogen atoms) we add a further 30 % of this number. The total number of non-hydrogen atoms to be located is then 2025 + 608, or 2633 (O = 16). The number of parameters required for isotropic refinement (3 positional and 1 temperature factor per non-hydrogen atom) is $(2633 \times 4) + 1$ (scale factor), or 10533. The unit-cell volume is $58.2 \times 38.3 \times 54.2$ sin (106.5), which equates to 115840 Å^3. Using the equation for the number N of reciprocal lattice points in the whole sphere at a given resolution limit, $4.19 V_c / d_{\min}^3$, and dividing by a factor 4 for (Laue group 2/m) we have the following results for the different resolutions:

	Reflections in 1 asymmetric unit	Data/parameter ratio
6 Å	$N = 2246/4 = 562$	0.053
2.5 Å	$N = 31066/4 = 7766$	0.74
1 Å	$N = 485400/4 = 121342$	11.7

Comments. The 6 Å structure is completely unrefinable. The 2.5 Å structure is refinable, but only if heavily restrained. The 1 Å isotropic model structure should refine provided the data quality is adequate.

10.8. From the general expression Web Appendix A4, (WA4.6), with $\gamma = 120°$ and $\phi = 120°$, we derive the matrix

$$\begin{bmatrix} 0 & \bar{1} & 0 \\ 1 & \bar{1} & 0 \\ 0 & 0 & 1 \end{bmatrix} \quad \text{which, together with the translation vector} \quad \begin{bmatrix} 0 \\ 0 \\ \frac{2}{3} \end{bmatrix}$$

for the 3_2 screw axis, leads to the general equivalent position set: x, y, z; $\bar{y}, x-y, \frac{2}{3}+z$; $y-x, \bar{x}, \frac{1}{3}+z$. The only condition limiting reflections is $000l$: $= 3n$.

10.9. If the protein belongs to a family, or group, of proteins having similar functions or biological or other properties in common, and the structure of one member of the family is known, either from an *ab initio* or other structure determination, molecular replacement can be attempted. The method usually requires the two proteins involved in MR to have amino acid sequences which correspond either identically or are of very similar types, that is, conserved for at least 30% of their total lengths (30% homology). Note that if the two proteins crystallize in the same space group and have very similar unit cells, they are very likely to be isomorphous, and the new structure should be determinable initially by Fourier methods alone. If the protein belongs to a new family for which no known structures exist, an *ab inito* method, MIR or MAD, has to be used for structure analysis. In the case of MAD, a tuneable source of synchrotron radiation is required.

Solutions 11

11.1. (a) From the Bragg equation, $1.25 = 2d(111)\ \sin\theta(111)$. Since $d(111) = a/\sqrt{3}$, $\theta(111) = 12.62°$. (b) Differentiating the Bragg equation with respect to θ, we obtain $\delta\lambda = 2d(111)\cos\theta(111)\,\delta\theta$. Remembering that $\delta\theta$ here is measured in radian, $\delta\lambda = 0.0243$ Å.

11.2. For the NaCl structure type, we can write $F(hkl) = 4[f_{Na^+} + (-1)^l f_{H^-/D^-}]$. Hence, the following results are obtained:

	(111)		(220)	
	NaH	NaD	NaH	NaD
X-rays	30.9	30.9	27.6	27.6
Neutrons	2.88	–1.28	–0.08	4.08

11.3. VIVALDI uses a white-beam Laue technique to record the diffraction data. Consequently each diffraction record (spot) will have a different wavelength associated with it which will have first to be determined in order for the spot to be assigned its *hkl* indices. This would usually require the unit cell of the crystal to be known, which would be easier to carry out first with monochromatic X-rays in the user's laboratory.

11.4. The spallation neutron beam at ORNL has been filtered in order to cover as small a wavelength range as is required in order to measure the data on a four-circle diffractometer. This would result in some loss of beam flux (power) which, in turn, would require the use of larger crystals in order to produce good quality diffraction data. VIVALDI uses a Laue white radiation technique which does not require the use of flux reducing filters.

11.5. Applying Chap. 11, (11.3) gives $\lambda = 1.865$ Å. [Work out the units of A in (11.3).]

11.6. The final picture should look something like Chap. 11, Fig. 11.12. It can be exported and saved in a variety of ways from the RASMOL menu.

Solutions 12

12.1. Since $R = 57.30$ mm, 1 mm on the film is equal to 1° in θ. Thus, 0.5 mm = 0.5° = 0.00873 rad. The mean Cu $K\alpha$ wavelength is 1.5418 Å. Differentiating the Bragg equation with respect to θ:

$$\delta\lambda = 2d \cos\theta \, \delta\theta = \lambda \cot\theta \, \delta\theta$$

Since $\delta\lambda = 0.0038$, we have $\cot\theta = 0.0038/(1.5418 \times 0.00873) = 0.2823$, so that $\theta \approx 74°$, the angle at which the $\alpha_1\alpha_2$ doublet would be resolved under the given conditions.

12.2. Perusal of the cubic unit-cell types leads us to expect that $(\sin^2\theta)/n$ for the first line (the low θ region) where $n = 1, 2, 3, \ldots$, would result in a factor that would divide into all other experimental values of $\sin^2\theta$ to give integer or near-integer results. By trial, we find that, for the first line, $(\sin^2\theta)/3$ leads to a sequence of values that correspond closely to those for a cubic F unit cell. Thus, dividing all other values of $\sin^2\theta$ by 0.0155 we obtain:

Line no.	$\sin^2\theta/0.0155$	N	a/Å	hkl	θ/o
1	3.00	3	6.192	111	12.45
2	4.10	4	6.118	200	14.60
3	11.08	11	6.170	311	24.48
4	16.04	16	6.185	400	29.91
5	23.95	24	6.199	422	37.54
6	26.90	27	6.203	333, 511	40.22
7	34.80	35	6.210	531	47.26
8	35.77	36	6.212	600, 442	48.12
9	42.64	43	6.218	533	54.39
10	47.54	48	6.222	444	59.13

Some accidental absences appear in this sequence of lines. Extrapolation of a *v.* $f(\theta)$ by the method of least squares (program LSLI) gives $a = 6.217$ Å. However, lines 1 and 2 produce significantly greater errors of fit than do the remaining eight lines. Since low-angle measurements tend to be less reliable, we can justifiably exclude lines 1 and 2. Least squares on lines 3 to 10 gives a probably better value, $a = 6.223$ Å.

12.3. The LEPAGE program gives the following results with the C-factor set at 1°:
Reduced Cell: P 4.693, 4.929, 5.679 Å; 90.12, 90.01, 90.72°
Conventional cell: Orthorhombic P 4.693, 4.929, 5.679 Å; 90.12, 90.01, 90.72°,
where all three angles are assumed to be 90° within experimental error. If we select the more stringent LEPAGE parameter $C = 0.5°$, we obtain
Reduced Cell: P 4.693, 4.929, 5.679 Å; 90.12, 90.01, 90.7°
Conventional cell: Monoclinic P 4.693, 5.679, 4.929 Å; 90.72, 89.99°
where α and γ may taken now to be 90° within experimental error. The parameters are reordered so that β is the unique angle.

12.4. From the program LEPAGE, we find:
Reduced Cell: P 6.021, 6.021, 8.515 Å; 110.70, 110.70, 90.01°
Conventional cell: Tetragonal I 6.021, 6.021, 14.75 Å; 90.00, 90.00, 90.00°
V(conventional unit cell)/V(given unit cell) = 2.

12.5. Let lines 1, 2, and 3 be 100, 010, and 001, respectively. Then, from multiples of their Q values, we have $a^* = 0.09118$ (average of 100, 200, 300, and 400; lines 1, 5, 17, and 33, respectively), $b^* = 0.09437$ (average of 010, 020, 030, and 040; lines 2, 6, 18, and 38, respectively), and $c^* = 0.1312$ (average of 002 and 003; lines 3 and 15, respectively). Consider next the possible $hk0$ lines. $Q_{110} = Q_{100} + Q_{010} = 172.2$; this line has been allocated to 001, which is probably erroneous. Continue with the [001] zone:

$hk0$	Q_{hk0}	Line number
110	172.2	3
120	439.5	9
130	885.0	20
210	421.5	8
220	688.8	15
230	1134.3	29
310	837.0	19
320	1104.3	27

This zone is well represented, and it follows that γ^* is 90°. If line 4 is now taken as 001, then line 25 could be 002. We check this assignment by forming expected Q_{0kl} values: $Q_{011} = 338.9$, but there is no line at this Q value, nor a pair of lines equidistant above and below this value, as there would be if the assignment is correct and $\alpha^* \neq 90°$. $Q_{021} = 606.2$, but this line fails the above test. It seems probable that line 4 is not 001. However, it must involve the l index and one of the indices h or k. If it is 101, then, for $\beta^* = 90°$, $Q_{001} = 249.8 - 83.1 = 166.7$, and if it is 011, then, for $\alpha^* = 90°$, $Q_{001} = 249.8 - 89.1 = 160.7$. For the second of these assignments, although a line at 160.7 is not present, there are the multiples 002 and 003 at lines 12 (642.8) and 39 (1446.3), respectively. With this assumption, line 4 is 011, line 12 is 002, and line 39 is 003.

Confirmation arises from 012, 021, and 022 at lines 16 (731.9), line 10 (517.1), and line 25 (999.2). Thus, an average $c^* = 0.1267$ and $\alpha^* = 90°$. We now search for $h0l$ lines. For $\beta^* = 90°$, $Q_{101} = 243.8$; this line cannot be fitted into the pattern. $Q_{102} = 725.9$: there is no line at this value, but lines 11 and 21 are very nearly equidistant (166.1 and 166.5) from 725.9. Hence, the difference, 332.6 is 10^4 ($8c^* a^* \cos \beta^*$), so that $\beta^* = 68.91°$. We have now a set of reciprocal unit-cell parameters from which, since two angles are 90°, the direct unit cell is calculated as $\beta = 111.09°$, $a = 1/(a^* \sin \beta) = 11.755$, $b = 1/b^* = 10.597$, $c = 1/(c^* \sin \beta) = 8.459$ Å. We make the conventional interchange of a and c, so that β is the unique angle, and $c > b > a$, and now apply the further check of calculating the Q values for this unit cell, using the program QVALS, with the results listed in Table S12.1.

In using this program, we remember that the unit cell appears to be monoclinic, so that we need to consider hkl and $h\,k\,\bar{l}$ reflections. From Table S12.1, it is evident that several reflections overlap, within the given experimental error. The unit cell type is P. The $h0l$ reflections are present only when h is an even integer. The reflections $30\bar{3}$ and 300, at the Q values 1444.8 and 1444.9, respectively are probably not present and overlapped by the $23\bar{2}$ and 230. Hence, the space group is probably Pa (non-standard form of Pc) or $P2/a$ (non-standard form of $P2/c$). To consider if the symmetry is actually higher than monoclinic, the unit cell is reduced, using

the program LEPAGE. We find that the first unit cell is reduced, but the conventional unit cell is orthorhombic B ($\equiv C$ or A), with a high degree of precision:

$$a = 8.459,\ b = 10.597,\ c = 21.935\ \text{A};\ \alpha = \beta = \gamma = 90.00^{\circ}$$

Since Miller indices transform as unit-cell vectors, we find from the transformation matrix given by the program LEPAGE that $h_B = -h$, $k_B = -k$, and $l_B = h + 2l$; the transformed indices are listed in Table S12.2. We note that the indices are listed as directly transformed. If we were dealing with structure factors, we could negate all the negative indices, because $|\mathrm{F(hkl)}| = |\mathrm{F(h\,k\,1)} = |\mathrm{F(h\,k\,1)}| = |F(h\,\bar{k}\,l)| = |F(h\,k\,\bar{l})|$ in the orthorhombic system.

Table S12.1 Observed and calculated Q values for substance X and the hkl indices of the lines referred to the first unit cell

Q(obs)	hkl	Q(calc)
83.1	0 0 1	83.1
89.1	0 1 0	89.1
172.2	0 1 1	172.2
249.8	1 1 0	249.6
	$1\,1\,\bar{1}$	249.6
332.6	0 0 2	332.5
356.1	0 2 0	356.2
416.0	$1\,1\,\bar{2}$	415.8
	1 1 1	415.9
421.5	0 1 2	421.6
439.3	0 2 1	439.3
516.9	$1\,2\,\bar{1}$	516.7
	1 2 0	516.7
559.8	$2\,0\,\bar{1}$	559.0
642.9	$2\,0\,\bar{2}$	642.1
	2 0 0	642.2
648.6	$2\,1\,\bar{1}$	648.1
683.3	$1\,2\,\bar{2}$	683.0
	1 2 1	683.0
688.8	0 2 2	688.7
732.1	$2\,1\,\bar{2}$	731.2
	2 1 0	731.2
748.4	0 0 3	748.2
	$1\,1\,\bar{3}$	748.4
	1 1 2	748.4
801.5	0 3 0	801.5
837.2	0 1 3	837.3
884.5	0 3 1	884.6
892.4	$2\,0\,\bar{3}$	891.5
	2 0 1	891.6
916.0	$2\,2\,\bar{1}$	915.2
962.3	$1\,3\,\bar{1}$	962.0
	1 3 0	962.0

(continued)

Table S12.1 (continued)

981.7	2 1 $\bar{3}$	980.6
	2 1 1	980.6
999.1	2 2 $\bar{2}$	998.3
	2 2 0	998.4
1016.	1 2 $\bar{3}$	1015.5
	1 2 2	1015.6
1015.	0 2 3	1104.4
1129.	1 3 $\bar{2}$	1128.2
	1 3 1	1128.3
1134.	0 3 2	1134.0
1248.	1 1 $\bar{4}$	1247.2
	1 1 3	1247.2
1249.	2 2 $\bar{3}$	1247.7
	2 2 1	1247.8
1308.	2 0 $\bar{4}$	1307.2
	2 0 2	1307.3
1330.	0 0 4	1330.1
1361.	2 3 $\bar{1}$	1360.5
1369.	3 1 $\bar{2}$	1367.6
	3 1 $\bar{1}$	1367.6
1397.	2 1 $\bar{4}$	1396.2
	2 1 2	1396.3
1419.	0 1 4	1419.2
1425.	0 4 0	1424.8
1444.	2 3 $\bar{2}$	1443.6
	2 3 0	1443.6
1461.	1 3 $\bar{3}$	1460.8
	1 3 2	1460.8

From an inspection of the *hkl* indices in Table S12.2 for the transformed unit cell, we find

hkl:	$h + l = 2n$
0*kl*:	None
*h*0*l*:	$h = 2n$; $(l = 2n)$
*hk*0:	$(h = 2n)$

Table S12.2 Transformation of the *hkl* indices from the monoclinic (first) unit cell to the orthorhombic *B* unit cell

h	k	l		h_B	k_B	l_B	h	k	l		h_B	k_B	l_B
0	0	1	→	0	0	2	1	3	$\bar{1}$	→	$\bar{1}$	$\bar{3}$	$\bar{1}$
0	1	0	→	0	$\bar{1}$	0	1	3	0	→	$\bar{1}$	$\bar{3}$	1
0	1	1	→	0	$\bar{1}$	2	2	1	$\bar{3}$	→	$\bar{2}$	$\bar{1}$	$\bar{4}$
1	1	0	→	$\bar{1}$	$\bar{1}$	1	2	1	1	→	$\bar{2}$	$\bar{1}$	4
1	1	$\bar{1}$	→	$\bar{1}$	$\bar{1}$	$\bar{1}$	2	2	$\bar{2}$	→	$\bar{2}$	$\bar{2}$	$\bar{2}$

(continued)

Table S12.2 (continued)

h	k	l		h_B	k_B	l_B	h	k	l		h_B	k_B	l_B
0	0	2	→	0	0	4	2	2	0	→	$\bar{2}$	$\bar{2}$	2
0	2	0	→	0	$\bar{2}$	0	1	2	$\bar{3}$	→	$\bar{1}$	$\bar{2}$	$\bar{5}$
1	1	$\bar{2}$	→	$\bar{1}$	$\bar{1}$	$\bar{3}$	1	2	2	→	$\bar{1}$	$\bar{2}$	5
1	1	1	→	$\bar{1}$	$\bar{1}$	3	0	2	3	→	0	$\bar{2}$	6
0	1	2	→	0	$\bar{1}$	4	1	3	$\bar{2}$	→	$\bar{1}$	$\bar{3}$	$\bar{3}$
0	2	1	→	0	$\bar{2}$	2	1	3	1	→	$\bar{1}$	$\bar{3}$	3
1	2	$\bar{1}$	→	$\bar{1}$	$\bar{2}$	$\bar{1}$	0	3	2	→	0	$\bar{3}$	4
1	2	0	→	$\bar{1}$	$\bar{2}$	1	1	1	$\bar{4}$	→	$\bar{1}$	$\bar{1}$	$\bar{7}$
2	0	$\bar{1}$	→	$\bar{2}$	0	0	1	1	3	→	$\bar{1}$	$\bar{1}$	7
2	0	$\bar{2}$	→	$\bar{2}$	0	$\bar{2}$	2	2	$\bar{3}$	→	$\bar{2}$	$\bar{2}$	$\bar{4}$
2	0	0	→	$\bar{2}$	0	2	2	2	1	→	$\bar{2}$	$\bar{2}$	4
2	1	$\bar{1}$	→	$\bar{2}$	$\bar{1}$	0	2	0	$\bar{4}$	→	$\bar{2}$	0	$\bar{6}$
1	2	$\bar{2}$	→	$\bar{1}$	$\bar{2}$	$\bar{3}$	2	0	2	→	$\bar{2}$	0	6
1	2	1	→	$\bar{1}$	$\bar{2}$	3	0	0	4	→	0	0	8
0	2	2	→	0	$\bar{2}$	4	2	3	$\bar{1}$	→	$\bar{2}$	$\bar{3}$	0
2	1	$\bar{2}$	→	$\bar{2}$	$\bar{1}$	$\bar{2}$	3	1	$\bar{2}$	→	$\bar{3}$	$\bar{1}$	$\bar{1}$
2	1	0	→	$\bar{2}$	$\bar{1}$	2	3	1	$\bar{1}$	→	$\bar{3}$	$\bar{1}$	1
0	0	3	→	0	0	6	2	1	$\bar{4}$	→	$\bar{2}$	$\bar{1}$	$\bar{6}$
1	1	$\bar{3}$	→	$\bar{1}$	$\bar{1}$	$\bar{5}$	2	1	2	→	$\bar{2}$	$\bar{1}$	6
1	1	2	→	$\bar{1}$	$\bar{1}$	5	0	1	4	→	0	$\bar{1}$	8
0	3	0	→	0	$\bar{3}$	0	0	4	0	→	0	$\bar{4}$	0
0	1	3	→	0	$\bar{1}$	6	2	3	$\bar{2}$	→	$\bar{2}$	$\bar{3}$	$\bar{2}$
0	3	1	→	0	$\bar{3}$	2	2	3	0	→	$\bar{2}$	$\bar{3}$	2
2	0	$\bar{3}$	→	$\bar{2}$	0	$\bar{4}$	1	3	$\bar{3}$	→	$\bar{1}$	$\bar{3}$	$\bar{5}$
2	0	1	→	$\bar{2}$	0	4	1	3	2	→	$\bar{1}$	$\bar{3}$	5
2	2	$\bar{1}$	→	$\bar{2}$	$\bar{2}$	0							

giving the diffraction symbol as $B\ .\ a\ .$ which, under the transformation $\mathbf{a}' = \mathbf{a}$, $\mathbf{b}' = \mathbf{c}$, $\mathbf{c}' = -\mathbf{c}$, becomes $C * * a$. Hence, the space group is either $Cmma$ or $C2ma$ ($\equiv Abm2$).

12.6. Crystal *XL*1: $a = 6.425$, $b = 9.171$, $c = 5.418$ Å, $\alpha = 90$, $\beta = 90$, $\gamma = 90°$. The unit cell is orthorhombic. The systematic absences indicate the diffraction symbol as $mmm\ P\ n\ a\ * *$, which corresponds to either $Pna2_1$ or $Pnam$. The latter is the $\mathbf{a\bar{c}\,b}$ setting of $Pnma$. [Reported: KNO_3; 9.1079, 6.4255, 5.4175 Å; $Pbnm$, which is the **cab** setting of $Pnma$.] The LEPAGE reduction confirms the above cell as reduced and conventional, under reordering, such that $a < b < c$. What is the space group now?

12.7. Crystal *XL*2: $a = 10.482$, $b = 11.332$, $c = 3.757$ Å, $\alpha = 90$, $\beta = 90$, $\gamma = 90°$. The unit cell is orthorhombic, with space group $Pbca$. The LEPAGE reduction confirms the above cell as reduced and conventional, under reordering such that $a < b < c$.

12.8. Crystal *XL*3: $a = 6.114$, $b = 10.722$, $c = 5.960$ Å, $\alpha = 97.59$, $\beta = 107.25$, $\gamma = 77.42°$. The unit cell is triclinic, space group $P1$ or $P\bar{1}$. The LEPAGE reduction gives $a = 5.960$, $b = 6.114$, $c = 10.722$ Å, $\alpha = 77.42$, $\beta = 82.41$, $\gamma = 72.75°$. [Reported: $CuSO_4.5H_2O$: 6.1130, 10.7121, 5.9576 Å, 82.30, 107.29, 102.57°; $P\bar{1}$.]

Solutions 13

The solutions given here apply to the structure determinations of (1) the nickel *o*-phenanthroline complex (NIOP) and (2) 2-*S*-methylthiouracil (SMTX & SMTY). The correctness of the other XRAY structure examples should be judged by both the state of the refinement achieved and the chemical plausibility of the structure, as discussed in Sect. 8.7.

13.1. NIOP

Table S13.1 lists the refined x, y and B parameters for the atoms in the Ni *o*-phenanthroline complex; two-dimensional refinement by XRAY to $R \approx 9.8$ %.

Table S13.1

Atom	x	y	Pop.	B/Å^2
Ni	0.23511	0.17804	1.000	2.02
S1	0.31780	0.10370	1.000	2.10
S2	0.15409	0.10022	1.000	2.21
C1	0.46164	0.15015	1.000	2.05
C2	0.39174	0.22786	1.000	2.22
C3	0.32252	0.24182	1.000	3.55
C4	0.14559	0.23252	1.000	1.14
C5	0.08009	0.21567	1.000	2.83
C6	0.00165	0.13681	1.000	2.08
C7	0.00321	0.95462	1.000	5.63
C8	0.27653	0.44349	1.000	2.91
C9	0.47796	0.08704	1.000	0.85
C10	0.39398	0.16063	1.000	2.09
C11	0.33069	0.30042	1.000	3.47
C12	0.27678	0.33480	1.000	2.85
C13	0.31090	0.39206	1.000	2.40
C14	0.18671	0.44236	1.000	4.71
C15	0.15426	0.37717	1.000	3.69
C16	0.19049	0.33477	1.000	1.65
C17	0.14168	0.29263	1.000	1.35
C18	0.07108	0.16047	1.000	3.90

Note: The total number of non-hydrogen atoms in the molecule is 21. The ID numbers refer to atoms as follow: 1 Ni, 2 S, 3 N, 4 C.

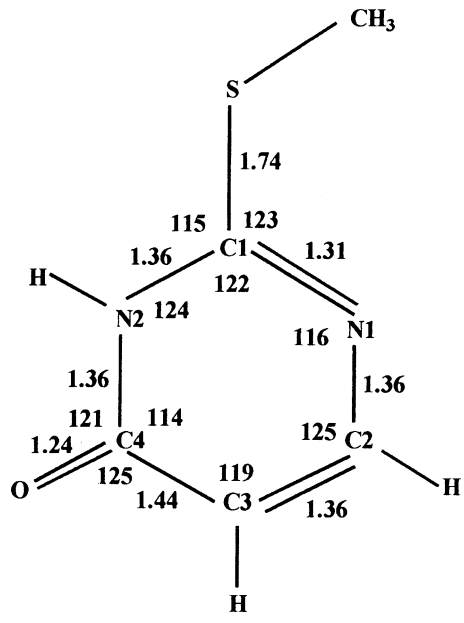

Fig. S13.1

13.2. SMTX and SMTY

Figure S13.1 shows the molecular structure of 2-*S*-methylthiouracil. Not all angles have been listed; the values for S–CH_3 and C(l)–S–CH_3 will evolve from your result for the position of the –CH_3 group.

Index

M. Ladd and R. Palmer, *Structure Determination by X-ray Crystallography: Analysis by X-rays and Neutrons*, DOI 10.1007/978-1-4614-3954-7,